Bio-inspired silica: development for drug delivery applications and biocompatibility

Scott Davidson

PhD Thesis, 2016

University of Strathclyde
Department of Chemical and Process Engineering

Declaration of Authenticity and Author's Rights

The thesis, dissertation, design or report shall include, on the page immediately subsequent to the title-page, the following declarations of authenticity and author's rights: ‘This thesis is the result of the author’s original research. It has been composed by the author and has not been previously submitted for examination which has led to the award of a degree.’ 'The copyright of this thesis belongs to the author under the terms of the United Kingdom Copyright Acts as qualified by University of Strathclyde Regulation 3.50. Due acknowledgement must always be made of the use of any material contained in, or derived from, this thesis.’

Signed:

Date:

Acknowledgements

I would like to thank my supervisors, Dr Siddharth V. Patwardhan, Prof. M. Helen Grant, Dr Dimitrios A. Lamprou and Dr Andrew Urquhart, for their guidance, advice and help throughout the whole PhD. This project would not have been completed if it were not for their (sometimes tough) encouragement and mentoring. I would also like to thank Catherine "Katie" Henderson for her help with all my experiments in the bioengineering labs, especially with the unpleasant task of removing the guts of rats.

Thanks also to the other members of my group (Joe, Thomas, Colin and Eleni) for advice and good chat. For funding of the PhD I would like to thank EPSRC-DTG. Thanks also to Dr. Keiji Numata (RIKEN) and the Japanese New Energy and Industrial Technology Development Organization (NEDO) for funding drug delivery research.

Thanks to all the technical staff in chemical engineering and SIPBS who helped at various points in the project and thanks to the administration staff in chemical engineering (especially Caroline and Laura) who have been of great help throughout the PhD.

I would like to thank all the friends I have made throughout my PhD, who all helped make the past 3 and a half years fun and enjoyable. From chemical engineering, David, Paul, Joy, Javier, Mark, Carlotta, Alessia, Dorin, Evan, Calum Stewart, Craig, Rab, Chris and Hrvojka/Hrvinator, and from SIPBS; Rachel, David K, Ivan, Lauren, Stewart, Monika, Olivia and David M. Thanks also to my friends outside of university who have also had to listen to me talk about the PhD for 3 and half years. Finally I would like to thank my family for their support and guidance throughout the years.

Contents

Declaration of Authenticity and Author's Rights 2

Acknowledgements 3

List of Figures 6

List of Tables 10

List of abbreviations 11

Publications and Conference presentations 12

Abstract 13

1. Chapter 1: Introduction 15

1.1 An introduction to nanomedicines 16

1.2 An introduction to drug delivery systems 17

1.3 A brief introduction to silica 21

1.4 The chemistry of silica synthesis in solution 24

1.5 Synthesis and properties of mesoporous silica nanoparticles 27

1.6 Mesoporous silica nanoparticles (MSN) as a drug delivery system 30

1.7 An introduction to bio-inspired silica (BIS) 36

1.8 The potential for "bio-inspired" silica (BIS) as a drug delivery system 42

1.9 Aims 45

2. Chapter 2: Materials and Methods 46

2.1. Chemicals 47

2.2. *In situ* drug loading into BIS and drug release 48

2.3. Synthesis of MCM-41 and post-synthesis drug loading 49

2.4. Drug detection via high pressure liquid chromatography (HPLC) 50

2.5. Porosity analysis 54

2.6. Molybdic acid colorimetric assay 54

2.7. Movement of silica across rat intestine 56

2.8. Imaging rat gut sections 59

2.9. Haemolytic activity of silica 59

2.10. Scanning electron microscopy (SEM) 60

3) Chapter 3: Investigating the bio-inspired silica system for drug delivery applications using ibuprofen as a model drug molecule 62

3.1 The effect of the amine additive on the loading and release of ibuprofen 64

3.2. Altering reactant concentrations to understand the silica-drug system 76
3.3. Understanding additive-drug interactions to control DDS formulation 81
3.4. Investigating the release of ibuprofen from BIS under different pH 90
3.5. Conclusions 93
4) Chapter 4: Investigating the use of bio-inspired silica to improve adrenocorticoid insufficiency treatment with hydrocortisone 95
4.1. An introduction to hydrocortisone 96
4.1.1. Adrenocortical insufficiency 98
4.1.2. Issues with the treatment of adrenocortical insufficiency 100
4.2. Potential hydrocortisone delivery systems 102
4.3. Stability of Hydrocortisone during *in situ* loading into BIS 104
4.4. Effect of different amines in the loading and release of hydrocortisone into BIS 111
4.5. The effect of maturation time on the *In situ* loading onto and release of hydrocortisone from BIS-PAH 118
4.6. Conclusions 124
5) Chapter 5: Determining the biocompatibility of bio-inspired silica 125
5.1. An introduction to biocompatibility 126
5.2. Effects of silica in the GI tract 130
5.3. Haemolytic activity of silica 135
5.4. Potential bioaccumulation of silica 137
5.5. Conclusions 139
6) Chapter 6: Conclusions and Future Work 141
References 153
Appendix 164
Appendix 1 – Nitrogen adsoption theory 164
Appendix 2 – Example adsorption isotherms 170
Appendix 3 - HPLC traces of hydrocortisone 172

List of Figures

Figure 1-1 - A summary of the methods of synthesising silica and the types of particles that are produced 22
Figure 1-2 - Number of papers published per year according to a search on Web of Science with the topics "mesoporous silica" and "drug delivery". 24
Figure 1-3 - The polymerisation of silica; starting as silicic acid monomers which condense to dimers then cyclic trimers and tetramers before becoming particles, Figure reproduced from ref [47] 25
Figure 1-4 - Sol-gel formation. Where acidic pH results in particles aggregating together into chains and forming a gel and basic pH prevents this, so Ostwald ripening occurs leading to larger particles and the formation of a sol. Figure reproduced from ref [47] 26
Figure 1-5 - Scheme showing the synthesis of MCM-41 with CTAB surfactant micelles as a template, Figure reproduced from ref [33] 28
Figure 1-6 - Pore structures of MCM-41 and MCM-48 [51] 29
Figure 1-7 - Schematic of the "stimuli-responsive" polymers entrapping drug molecules into MSN, only releasing cargo upon an external stimulus [72] 33
Figure 1-8 - Electron micrographs of silica structures produced from several species of diatom. Figure reproduced from ref [80] 37
Figure 1-9 - The mechanism by which amines (in this case pentaethylenehexamine (PEHA)) catalyse the condensation of silica [77] 39
Figure 1-10 - A schematic of micro-emulsions of amine forming and resulting in the formation of hollow silica particles, Figure reproduced from ref [87] 41
Figure 1-11 - Silica precipitation with synthetic R5-cargo conjugates and release of cargo under a stimulus responsive cleaving of R5-cargo bond [93] 43
Figure 2-1 - (A) An example HPLC trace of ibuprofen in 70:30 ethanol:PBS. Peak is observed at 4.7 Minutes. (B) Standard curve for ibuprofen run on HPLC. Equation of the line is y = 649 X, r2 is 0.95 52
Figure 2-2 -A) An example HPLC trace of hydrocortisone in 70:30 ethanol: water. Peak is observed at 7.1 Minutes. (B) Standard curve for hydrocortisone run on HPLC. Equation of the line is y= 1321X and r2 is 0.99 53
Figure 2-4 - Standard curve of sodium metasilicate measured using the molybdic acid colorimetric assay. Equation of the line is y= 0.0756X and r^2 is 0.99 56
Figure 2-5 - Standard curve to calculate the concentration of glucose (using a gluc-pap assay kit). Equation of the line is y = 1.178X + 0.1384 and r^2 is 0.99 58
Figure 2-6 - Standard curve to calculate the concentration of fluorescent silica particles by measuring fluorescence. Equation of the line is y = 503.3X and r^2 is 0.99 59
Figure 3-1 - BIS Synthesised with Different Amines, (A) % loading efficiency and % drug content (wt/wt) of ibuprofen into four different BIS and MCM-41 n=3, error bars represent one standard deviation 65
Figure 3-2 - BIS Synthesised with Different Amines (A) The % release of loaded ibuprofen from four different BIS and MCM-41 (data fitted using equation 2.1), (B) Total mass of ibuprofen (mg) released from 10mg of silica sample, (C) Release of loaded ibuprofen

expressed as a % of final concentration released from BIS synthesised with different amines and MCM-41. n=3, error bars represent one standard deviation. 67
Figure 3-3 – (A) Pore size distribution of four different BIS and MCM-41, (B) Surface area, pore volume and pore size figures for four different BIS and MCM-41 (* due to broad pore size distributions, specific pore sizes are not applicable) n=1 73
Figure 3-4 SEM images of (A) BIS-PAH, (B) Ibuprofen loaded BIS-PAH, and (C) MCM-41 74
Figure 3-5 - Average size of different BIS-PAH particles (empty and ibuprofen loaded) and MCM-41 measured via SEM images. Average and standard deviation error bars were calculated from one image (Figure 3-4)..... 74
Figure 3-6 :- Schematic of the effect of amine on BIS aggregation. Where short amines result in a tight silica aggregate which traps drug molecules and longer amines result in a more open silica aggregate structure, allowing for increased drug release..... 75
Figure 3-7- Effect of reactant concentrations on the % loading efficiency and % drug content (wt/wt) of ibuprofen into BIS synthesised with different reactant ratios and MCM-41 , n=3, error bars represent one standard deviation. 77
Figure 3-8 - Effect of reactant ratios on the release of ibuprofen (A) The % release of loaded ibuprofen from BIS synthesised with different reactant ratios, and MCM-1, data fitted using equation 2.1 ,(B) Total mass of ibuprofen (mg) released from 10mg of silica sample, (C) Release of loaded ibuprofen expressed as a % of final concentration released from BIS synthesised with different reactant ratios, and MCM-41. n=3, error bars represent one standard deviation. 79
Figure 3-9 – (A) Pore size distribution of BIS synthesised with different reactant concentrations and MCM-41, n=1 (B) Surface area, pore volume and pore size figures for BIS synthesised with different reactant concentrations, and MCM-41 80
Figure 3-10 - Effect of reaction pH on the % loading efficiency and % drug content (wt/wt) of ibuprofen into BIS synthesised at different pH, and MCM-41 n=3, error bars represent one standard deviation 82
Figure 3-11 – Effect of reaction pH on the release of ibuprofen (A) The % release of loaded ibuprofen from BIS synthesised at different pH and MCM-1, data fitted using equation 2.1, (B) Total mass of ibuprofen (mg) released from 10mg of silica sample, (C) Release of loaded ibuprofen expressed as a % of final concentration released from BIS synthesised at different pH and MCM-41. n=3, error bars represent one standard deviation..... 84
Figure 3-12 - (A) SEM image of BIS-PAH synthesised at pH 7 (B) SEM images of BIS-PAH synthesised at pH 5 (C) Average size of different BIS-PAH particles (synthesised at pH 7 or pH 5) measured via SEM images. Average and standard deviation error bars were calculated from one image (Figure 3-4)..... 87
Figure 3-13 - (A) Pore size distribution of BIS synthesised at different pH and MCM-41, n=1 (B) Surface area, pore volume and pore size figures for BIS synthesised at different pH and MCM-41..... 88
Figure 3-14 - Scheme to illustrate the differences in charge of silica, amine and ibuprofen during synthesis at pH ranging from 9 to 5..... 89
Figure 3-15 – Effect (A) The % release of loaded ibuprofen at different pH values from BIS-PAH 2:2, data fitted using equation 2.1 ,(B) Total mass of ibuprofen (mg) released at different pH values from 10mg of silica sample, (C) Release of loaded ibuprofen expressed

as a % of final concentration released at different pH from BIS-PAH 2:2. n=3, error bars represent one standard deviation. 91
Figure 4-1 - The hormonal responses which induce the production and release of glucocorticoids (i.e. cortisol) (figure created using images from [130,131]) 97
Figure 4-2- The measurement of blood cortisol levels in normal individuals over the course of a day. Figure reproduced from reference [132] 98
Figure 4-3 - A simulated profile of patient's blood cortisol levels. Solid line represents a healthy patient. Dotted line represents an Addison's disease patient taking three doses of hydrocortisone [140,147]. 101
Figure 4-4– Hydrocortisone detected using an isocratic reverse phase HPLC method, with 40 µl injection volume and a mobile phase of acetonitrile: water (7:3) at a flow rate of 1ml min^{-1} through a ACE 5 C-18 column (150X4.6 nm with 5 µm particle size). , Hydrocortisone retention time is approximately 7.1 minutes and was detected using UV absorbance at the wavelength 246 nm. (A) HPLC trace of hydrocortisone in 70% ethanol, where the drug is not degrading and peak at ~7.1 minutes is visible (B) HPLC trace of hydrocortisone exposed to BIS synthesis conditions, , where the normal hydrocortisone peak can be seen at 7.1 minutes along with an additional peak at 2.2 minutes, associated with a degradation product 105
Figure 4-5 - The % degradation of hydrocortisone when exposed to various conditions (A) 70:30 - EtOH:H2O (pH 7.4), (B) 70:30 - EtOH:PBS (pH 7.2), (C) 1M HCl (pH 1), (D) 30mM Sodium metasilicate (pH 12), (E) 30mM Sodium metasilicate (pH 7), (F) 1mg/ml PAH (pH5), (G) 1M NaOH (pH 14), (H) Heated at 85ºC for 1 hour 106
Figure 4-6 - The structure of hydrocortisone with the two main sites of degradation (C17 side chain and ring A) labelled [157] 107
Figure 4-7 - Degradation products of HC under basic conditions. The following is a list of the names of molecules shown in this Figure, it should be noted that since the paper this Figure was taken from is from 1980, some of the nomenclature may be out of date. I (hydrocortisone), II (corticosterone), , VI (11β,20-dihydroxy-3-oxo-4-pregene-21-oic acid), VII (11β,17α-dihydroxy-3-oxo-4-androsten-17β-carboxylic acid) ,VIII (11β-hydroxy-4-androsteb-3,17-dione and X are D-homosteroids [156] 108
Figure 4-8 - Degradation of betamethasone to betamethasone 17-acid under basic conditions. A reaction which also occurs in HC [158]. 109
Figure 4-9 – The degradation of HC at various temperatures over time as calculated using the published HC degradation rate equation $ci/ct = 10^{t(K/2.303)}$, where ci is the initial concentration, ct is the concentration at time t, t is the time and K is the rate constant [159].. 110
Figure 4-10 - Products from the degradation of ring A in the hydrocortisone molecules. Figure reproduced with permission from reference [159]. 110
Figure 4-11 - Effect of amine additive on (A) % loading efficiency of hydrocortisone into BIS synthesised with different amine additives and MCM-41, (B) hydrocortisone content per mg of silica into four different BIS and MCM-41. n=3, error bars represent one standard deviations 113
Figure 4-12 - (A) Pore size distribution of BIS synthesised with amines and MCM-41, (B) Surface area, pore volume and pore size figures for BIS synthesised with amines and MCM-41 (* due to broad pore size distributions, specific pore sizes are not applicable), n =1 115

Figure 4-13 - (A) The % release of loaded hydrocortisone from four different BIS and MCM-41, data fitted using equation 2.1, (B) Release of loaded hydrocortisone expressed as a % of final concentration released from four different BIS and MCM-41. F n=3, error bars represent one standard deviations 117
Figure 4-14 - Effect of drug loading time (A) % loading efficiency of hydrocortisone into BIS with various drug loading times and MCM-41, (B) Average hydrocortisone content per mg of silica into BIS with various drug loading times and MCM-41, n=3, error bars represent one standard deviations 120
Figure 4-15 - (A) Surface area, pore volume and pore size figures for BIS with various drug loading times and MCM-41, (B) The % release of loaded hydrocortisone from BIS with various drug loading times and MCM-41, n=1 122
Figure 4-16 - (A) The % release of loaded hydrocortisone from BIS with various drug loading times and MCM-41, data fitted using equation 2.1,(B) Release of loaded hydrocortisone expressed as a % of final concentration released from BIS with various drug loading times and MCM-41. n=3, error bars represent one standard deviation. 123
Figure 5-1 - mM of Glucose transported across the inverted gut wall of a rat over an hour in the absence or presence of DNP. Details on method can be found in chapter 2.7, n=3 and error bars are one standard deviation. 132
Figure 5-2 - Average percentage of FITC-BIS-PAH passing through a section of rat gut over an hour at 37^{o}C, with and without the presence of DNP (an active transport inhibitor), n=3 and error bars represent one standard deviation. 133
Figure 5-3 - Light and FITC microscopy images of the inside and outside surfaces of rat gut with the addition of no silica (Control), fluorescent silica or fluorescent silica and DNP ... 134
Figure 5-4 - Percentage haemolysis induced by varying concentrations of BIS-PAH and MCM-41. n=3, error bars represent one standard deviation. 136
Figure 5-5 – Dissolution of silica (A) mM of silicic acid released from 10mg of BIS or MCM-41 when incubated for 30 days at 37^{o}C in 1.5ml of dH_2O, (B) % of silica dissolved under these conditions n=3, error bars represent one standard deviation. 138

List of Tables

Table 1-1 -Non-exhaustive list of potential medicinal uses for nanoparticles [5] 17
Table 1-2 - The limitations of free drug molecules which drug delivery systems aim to remove [11] 18
Table 1-3- Different types of DDS being currently researched [18] 20
Table 1-4 - Examples of reaction conditions of three types of MSN [52] 29
Table 3-1 - : Results of silica yield and of mathematical fitting (using equation 2.1) of release data presented in Figure 3-2 68
Table 3-2: - Results of silica yield and of mathematical fitting (using equation 2.1) of release data presented in Figure 3.6 78
Table 3-3 - Results of silica yield and of mathematical fitting (using equation 2.1) of release data presented in Figure 3-10 85
Table 3-4 - Percentage ionisation of the three relevant species involved during the synthesis of BIS at various pH 89
Table 3-5 - Results of silica yield and of mathematical fitting (using equation 2.1) of release data presented in Figure 3-14 92
Table 3-6 - Percentage ionisation of the three relevant species during drug release at various pH 92
Table 4-1 - Results of mathematical fitting (using equation 2.1) of release data presented in Figure 4.13 114
Table 4-2 - Results of mathematical fitting (using equation 2.1) of release data presented in Figure 4.16 121
Table A1-1 - Description of adsorption isotherms (Figure 2.3) [97] 166

List of abbreviations

BIS	Bio-inspired silica
AIDS	acquired immune deficiency syndrome
BIS-PAH	bio-inspired silica synthesised with poly(allylamine hydrochloride)
CAH	Congenital adrenal hyperlasia
DETA	diethylenetriamine
DNP	dinitrophenol
DDS	drug delivery system
D-PBS	Dulbecco's phosphate buffered saline
FDA	Food and Drug Administration
CTAB	hexadecyltrimethylammonium bromide
HPLC	high pressure liquid chromatography
HC	Hydrocortisone
MSN	Mesoporous Silica Nanoparticle
MCM	Mobil Composition of Matter
NP	nanoparticle
PEHA	pentaethylenehexamine
PBS	phosphate buffered saline
PAH	poly(allylamine hydrochloride)
PAH-FITC	poly(fluorescein isothiocyanate allyamine hydrochloride)
PEG	Poly-ethylene glycol
RBC	Red Blood Cell
SBA	Santa Barbara Amorphous type material
SEM	scanning electron microscope
TEPA	tetraehylenepentamine
TEOS	tetraethoxysilane
UV	ultraviolet

Publications and Conference presentations

Publications

- Davidson, S., Lamprou, D. A., Urquhart, A. J., Grant, M. H. & Patwardhand, S. V., Bioinspired Silica Offers a Novel, Green, and Biocompatable Alternative to traditional Drug Delivery Systems. *ACS Biomaterial Science and Engineering* **2**, 1493-1503 (2016)[1]

Conference poster presentations

- Davidson S, Urquhart, A., Grant M. H., Patwardhan S.V., Bio-inspired Silica Nanoparticles: Optimisation for Delivery Applications. 11th International Conference on Materials Chemistry (MC11) (University of Warwick) 2013
- Davidson S, Urquhart, A., Grant M. H., Patwardhan S.V, Bio-inspired Silica nanoparticles: Optimisation for Delivery Applications and Understanding Biological Safety. Northern Post-Graduate Chemical engineering conference (University of Newcastle) 2013
- Davidson S, Lamprou D.A., Grant M. H., Patwardhan S.V., Controllable bio-inspired silica for drug delivery applications. UK and Ireland Controlled Release Society Meeting, April 2015, Nottingham.
- Davidson S, Lamprou D.A., Grant M. H., Patwardhan S.V., Bio-inspired silica nanoparticles as drug delivery vehicles, 2015 Controlled Release Society Annual Meeting, 2015, Edinburgh
- Davidson S, Lamprou D.A., Grant M. H., Patwardhan S.V, Controllable bio-inspired silica as a drug delivery system (DDS), 10th world meeting on pharmaceutics, bio-pharmaceutics and pharmaceutical technology, 2016, Glasgow

Abstract

The development of a drug delivery system (DDS) is essential to remedy the limitations of free drug molecules. The use of silica as a DDS over other systems (for example, liposomes) can be attributed to it being more robust and versatile. This thesis investigates bio-inspired silica (BIS) and compares it to mesoporous silica nanoparticles (MSN), which have received much attention for drug delivery applications. The BIS synthesis utilised amines to condense silica quicker than MSN, under benign conditions and without the use of hazardous chemicals. With this synthesis method drugs can be loaded *in situ* and there is potential for amines to have dual function of condensing silica and acting as functionalisation. BIS has also been shown to be more biocompatible than MSN. Due to these reasons it can be argued that BIS has the potential to be a more desirable silica DDS than MSN.

Using ibuprofen as a model drug, reaction conditions (e.g. choice of amine additive, synthesis pH and maturation time) were systematically investigated to elucidate their effects upon drug loading and release. BIS synthesised with the amine poly(allylamine hydrochloride) (PAH) (which will henceforth referred to as BIS-PAH) was focused on, as this was the only amine system which released a significant proportion of loaded drug and achieved comparable or improved ibuprofen loading when compared to MCM-41. PAH plays an important role in facilitating the loading of ibuprofen, however if too much is present, release is inhibited greatly. The condensation rate of silica is also an important factor; when condensation rate was increased more drug was able to be released. This is likely due to less of the drug being entrapped within the silica particle and more being phys-adsorbed to the silica surface.

Next the use of BIS to deliver hydrocortisone (HC) was investigated. Current treatments for adrenocorticoid insufficiency using hydrocortisone do no mimic the natural circadian variation in levels of blood cortisol. Firstly, the stability of HC during the *in situ* loading process was measured and data are presented that show that HC must be loaded post-synthesis, to avoid degradation in the reaction mixture. The efficiency of loading was largely unaffected by amine, however, only BIS-PAH allowed for drug release. Longer BIS-PAH maturation times gave lowered loading but the release was improved.

Finally, biocompatibility of BIS was also investigated and it was found that, BIS was able to pass through the gut wall into the blood stream, and it was non-haemolytic when compared to MCM-41. There is a potential for bioaccumulation due to silica's chemical stability.

Although the use of BIS for delivery of hydrocortisone was unsuccessful, BIS does have several advantages over MCM-41 (such as quicker synthesis route, involving a one-pot synthesis and drug loading method, simple controllability, lack of hazardous chemicals and superior biocompatibility) and the results presented here show that BIS has similar or improved drug loading and release profiles to MCM-41 when using ibuprofen. With further drug and biocompatibility experiments, these benefits give BIS real potential as a viable DDS to be further investigated.

Chapter 1: Introduction

1.1 An introduction to nanomedicines

Nanoparticles (defined as particles with diameters between 1-100 nanometres) have been applied to a huge range of applications including use as catalysts, high-performance batteries, cosmetics, and as food additives [2,3]. One exciting application of nanoparticles (NP) is in medicine. The idea of using nanoparticles in medicine has been around for many years. An early example comes from a paper published in 1976 which describes an investigation into the potential use of organic nanoparticles in a vaccination against Clostridium tetani (the bacterial agent causing tetanus in humans) [4]. Despite nearly four decades of research, there is currently no universally accepted classification for nanomedicines (although the national cancer institute (NCI) and the FDA (Food and Drug Administration) are trying to develop one) which has led to some reviewers of the field to create their own criteria. One such reviewer described nanomedicine as the "use of nanoscale or nanostructured materials in medicine, engineered to have unique medicinal effects based on their structures, including structures with at least one characteristic dimension up to 300 nm" [5].

Nanomedicines can have several advantages over conventional medicines and as such are seen as potential solutions for many medical problems [5,6]. Nanomedicines can have higher cellular uptake [7,8] and can stay longer in the blood stream, increasing the efficacy of the loaded drug [9] and are also able to target tumours by accumulating within cancerous cells more than in healthy cells [10]. A comprehensive study of the literature by Etheridge et al. in 2013 yielded significant information on the types of nanomedicine being studied or commercially available [5].

The majority of nanomedicines under investigation or on the market were 200nm or smaller in diameter, to be administered intravenously and the vast majority of them were for cancer treatments. Other applications for nanoparticles in nanomedicine are shown in Table 1.1.

Clearly nanomedicines have great potential to be extensively used in the future and one area which is attracting more and more interest is in drug delivery.

Table 1-1 -Non-exhaustive list of potential medicinal uses for nanoparticles [5]

• Cancer Treatment	• Treatment of infectious diseases
• Drug delivery	• Bone substitutes
• Anaesthetics	• Surgical devices
• In vivo imaging	• Dentistry
• Tissue engineering	• Treatment of inflammatory/ immune disorders

1.2 An introduction to drug delivery systems

The development of drug delivery systems (DDS) is a wide field, of which nanotechnology and nanomedicine are only a part. DDS are formulations which are able to release a drug molecule at a defined site or rate [11] and are being heavily investigated and developed due to the many limitations of free drug molecules, which are summarised in Table 1.2.

Table 1-2 - The limitations of free drug molecules which drug delivery systems aim to remove [11]

• Poor solubility
• High toxicity
• Requirement of high doses
• Aggregation of drug due to poor solubility
• Non-specific delivery
• In vivo degradation
• Short half-life (i.e. removed from the body quickly)

The main aims of any DDS are threefold; 1) to improve the bioavailability of one's drug molecules, either by reducing its degradation or by increasing its uptake into the target site, 2) to control the rate the drug is released so that the concentration of drug remains within its therapeutic window (i.e. ideal concentration for activity) for longer, and 3) to reduce any side effects caused by the free drug molecules by specifically targeting the drug to its point of activity [12].

Aside from the obvious medicinal benefits DDS potentially have, there are also large economic benefits to be gained. Firstly developing DDS to solve the problems of drugs (seen in Table 1) is far more cost effective than developing completely new drugs from the start. New DDS cost approximately $20-50 million and take around 3-4 years to develop. On the other hand, the development of a new drug molecule can cost around $500 million and take 10-12 years [13]. Once on the market there is big money to be made, with a predicted 1.5 trillion US Dollar value for the drug delivery technology market by 2020 [14]

Despite nearly four decades of research and the huge economic potential, there are currently very few DDS available on the market. Most of these fall into two categories: Liposomal or lipid-based systems and PEGylated systems (i.e. where the drug is stabilised via the attachment of polyethylene glycol (PEG)) [12,15]. The majority of nanoparticle drug delivery systems approved by the FDA (Food and Drug Administration) have been designed for the delivery of anti-cancer agents or for treating dangerous chronic infections. This is likely due to the greater acceptance of some side-effects caused by the treatments for these diseases, than for treatments for much milder diseases. Some interesting examples include Doxil, which was approved for use in 1995. This consists of PEG-stabilised liposomal doxorubicin and was approved to fight Kaposi's sarcoma (a tumour caused by a type of herpes virus, which is highly common and dangerous in AIDS patients) [16]. Another example, here of a system developed to tackle a chronic infection, is PEG-intron (a pegylated interferon α-2B molecule). This was approved in 2000 and is used to treat patients with chronic hepatitis C infections [17].

Since the types of DDS available on the market are limited, there is continued research into other potential materials. Some of the most common systems being researched and their advantages and disadvantages are reviewed in table 1.3.

Table 1-3- Different types of DDS being currently researched [18]

DDS	Description	Advantages	Disadvantages	Ref.
Liposomes	Vesicles consisting of a lipid bilayer	Self-assembly; hydrophobic drugs can be passively loaded; slow degradation; deliver drug into cells; biocompatible	Relatively low drug loading and sustained release; require functionalisation to provide stability; can be degraded by enzymes leading to premature release.	18-22
Dendrimers	Branched and globular macromolecules.	Selectively host biomaterials; multiple targeting.	Toxicity; can have side effects when degraded.	23-25
Carbon Nanotubes	Tubes of a single or multiple layers of a graphene sheet.	Can be applied to many different therapeutic agents.	Insolubility can lead to health problems; long term *in vivo* clinical trials lacking.	26-28
Gold Nanoparticles	Nanoparticles of gold.	Controlled release via temperature or kinetic energy possible; reduces therapeutic dose of cytotoxic drugs required.	Accumulation and excretion not fully understood; high cost.	29,30
Mesoporous Silica nanoparticles	Nanoparticles of silica.	High surface area for drug loading; controllable pore size and structure to control release.	Long synthesis time; hazardous chemicals used; potential for aggregation; uncontrolled release; potentially cytotoxic.	28,31-35

The focus of this project is on the use of silica nanoparticles as a drug delivery system. In recent years the number of papers published on mesoporous silica nanoparticles for drug delivery applications has risen exponentially, making silica an important material for the future of drug delivery systems [36]. The successful use of silica DDS over other systems (such as polymer nanoparticles or liposomes) can be partially attributed to silicas thermal and chemical stability. Silica is also thought to be more robust and versatile than many conventional DDS [36,37]. While there are currently no silica-based drug delivery systems on the market, there is a gold coated silica (Auroshell) which is in the first stage of development to be sold as an anti-cancer agent [38].

1.3 A brief introduction to silica

Silica (SiO_2) is a major component of the earth's crust and is found in many different forms from crystalline quartz in rocks and sand to amorphous silica found in many living organisms [39]. Different forms of silica exhibit different properties and behaviours and can be synthesised in a large variety of ways (summarised in Figure 1.1).

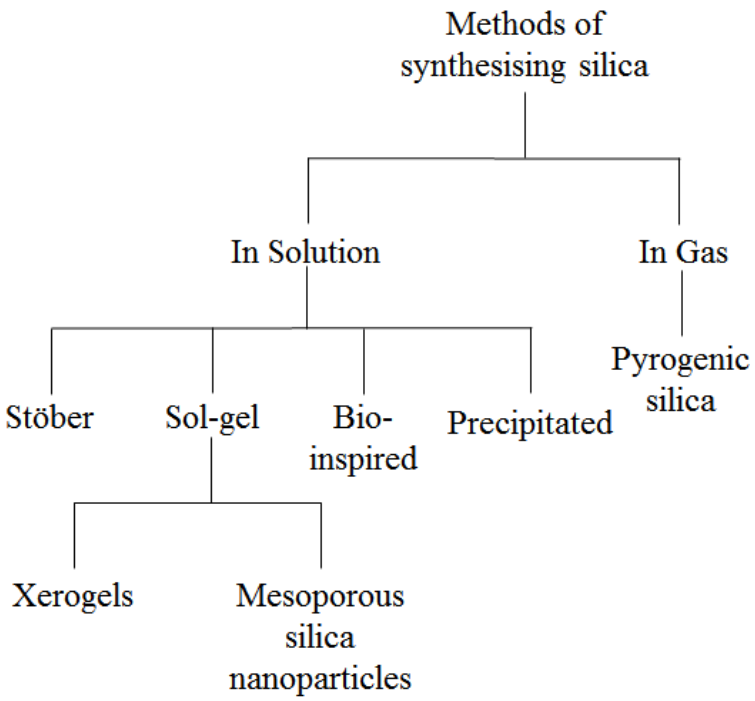

Figure 1-1 - A summary of the methods of synthesising silica and the types of particles that are produced

For drug delivery applications not all of these synthesis methods are suitable. For example precipitated and pyrogenic/fumed silica are both powders and form a "smoke" when shaken in the air which can be harmful if breathed in and so will not be discussed here [40].

The Stöber process was first developed in an attempt to produce monodispersed suspensions of silica particles. These particles are normally non-porous with a diameter in the colloidal range (1-1000 nm) and, since their initial construction in 1968, have been put to a wide range of applications, from being used in hard drives to use in biotechnology [41,42]. To create Stöber silica, the catalyst ammonia (dissolved in alcohol) is mixed with alkoxy silicate and continuously stirred to keep the forming particles in suspension. The silica condenses very quickly, with the solution becoming opaque after 10 minutes. In the original paper,

the particles were left to form for 2 hours before the reaction was stopped [43]. While there has been some research into using Stöber silica for drug delivery, the particles are non-porous which decreases the loading capacity for drug molecules and makes them largely unfavourable for drug delivery applications.

The sol-gel process can produce two different types of silica; xerogels and mesoporous silica. Xerogels can be synthesised by first forming a silica network (gel) in an aqueous environment. This gel is then dried which leaves behind glassy SiO_2 nanoparticles (known as xerogels) [40]. These silica xerogels are largely non-toxic and can have very versatile properties since both their chemical and physical properties can be easily influenced by temperature, pH and even the drying process [44]. The xerogels have received some attention for drug delivery applications [45]; however, their dependence on pH and slow growth rates make them unfavourable for this application.

Mesoporous silica nanoparticles (MSNs) are synthesised using the sol-gel method with the addition of surfactants which act as the template, directing silica condensation. This template is then removed to leave behind silica with large surface areas (> 800 m^2g^{-1}) and a tunable pore size of between 2 and 15 nm [33,34]. For loading and controlling the release of drug molecules, surface area and porosity are greatly important and so, MSN are at the forefront of research into silica's use for drug delivery and (as shown in Figure 1.2) papers on this topic have risen exponentially over the past 10 years.

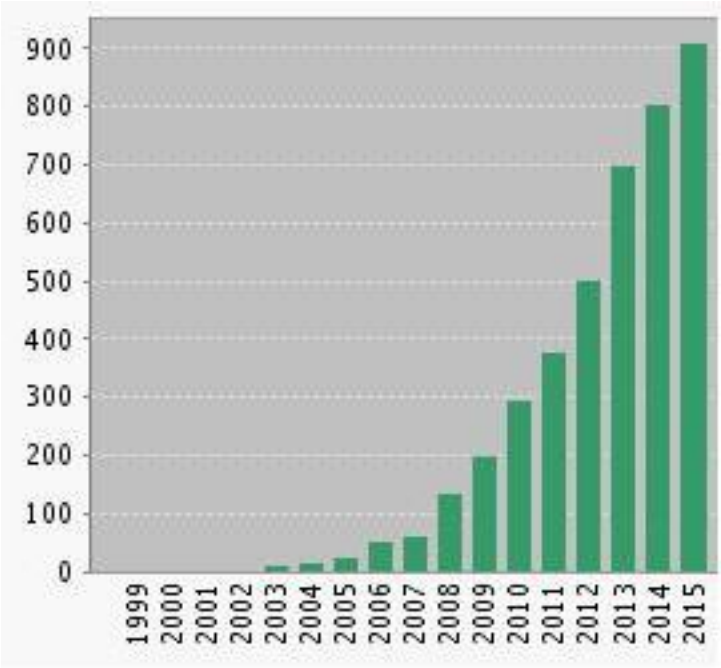

Figure 1-2 - Number of papers published per year according to a search on Web of Science with the topics "mesoporous silica" and "drug delivery".

Due to the attention MSN are receiving for drug delivery applications they will act as the benchmark with which to compare bio-inspired silica (BIS) (BIS will be discussed in section 1.6). However, before more details on MSN and BIS are given it is important to understand the chemistry of silica synthesis in solution.

1.4 The chemistry of silica synthesis in solution

The synthesis of silica is a condensation reaction from silicic acid to silica and occurs in 3 steps; 1) polymerisation of monomer to form particles, 2) growth of particles and 3) the aggregation of particles to form chains and networks which result in the liquid thickening into a gel [46].

Silicic acid can be easily made by dissolving a soluble silicate (such as sodium metasilicate) in water. Higher concentrations of silicic acid ([Si] > 100 ppm) result in the formation of silica dimers in a nucleophilic substitution (SN2) reaction

(Reaction 1) of an oxygen atom onto another silicon atom, leading to the formation of a siloxane bond (Si-O-Si) [46,47].

$$(OH)_3\text{-SiOH} + HOSi\text{-}(OH)_3 \rightarrow (OH)_3\text{-Si-O-Si-}(OH)_3 + H_2O \qquad \text{[Reaction 1]}$$

As shown in Figure 1.3, polymerisation continues in such a way to give the highest number of Si-O-Si bonds and to keep Si-OH groups to a minimum. Due to this, further condensation of the dimer leads to cyclic molecules, which then form into three-dimensional structures and eventually resulting in "spherical units". These spheres of SiO_2 (usually between 2-3 nm) act as nuclei from where the particles can grow (Figure 1.3) [46].

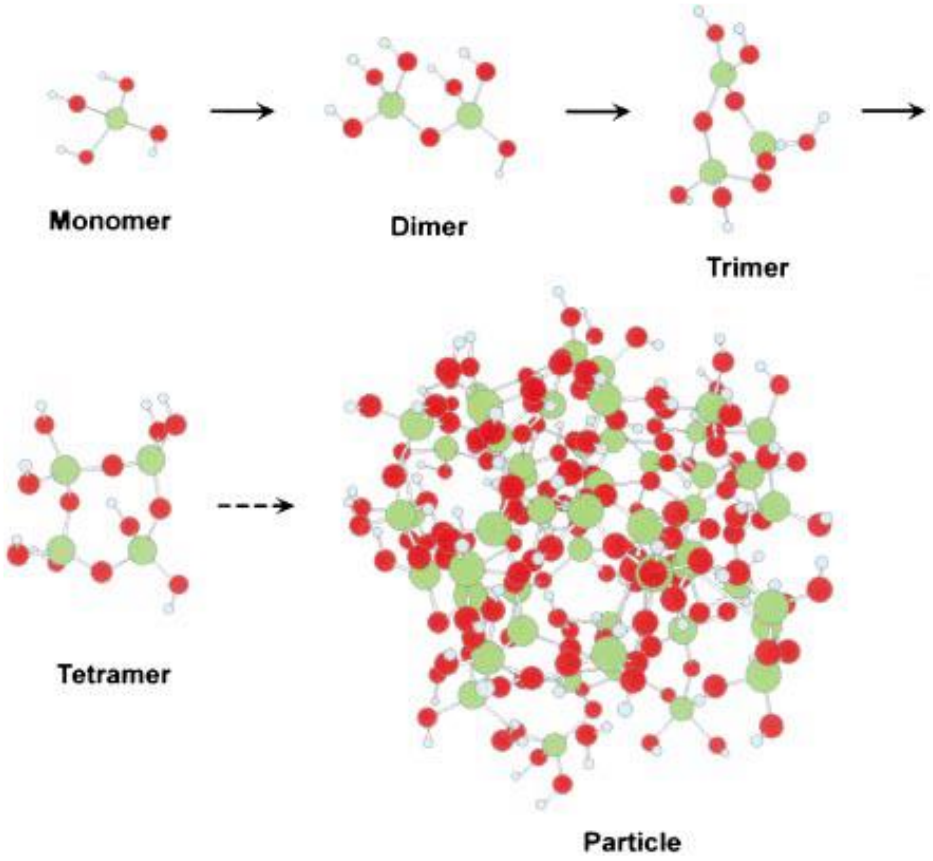

Figure 1-3 - The polymerisation of silica; starting as silicic acid monomers which condense to dimers then cyclic trimers and tetramers before becoming particles, Figure reproduced from ref [47]

The rate of polymerisation and how the particles grow are greatly influenced by pH and the presence of salts. Under acidic conditions, hydroxyl groups are protonated and the silica nuclei are neutral and so do not repel each other. This allows for the linking of particles via free silanol groups on different silica nuclei forming new siloxane bonds. As shown in Figure 1.4 this results in the particles forming chains and eventually a 3D open network with large water filled cavities and is known as a gel. Gel time increases as the pH lowers due to increasing protonation of the silanol group making condensation reactions rarer. Quickest gel times occur at pH 6 (when there are no salts in the reaction) or pH 7 (when salts are present since salts lower the ionic charge of particles) [46,47].

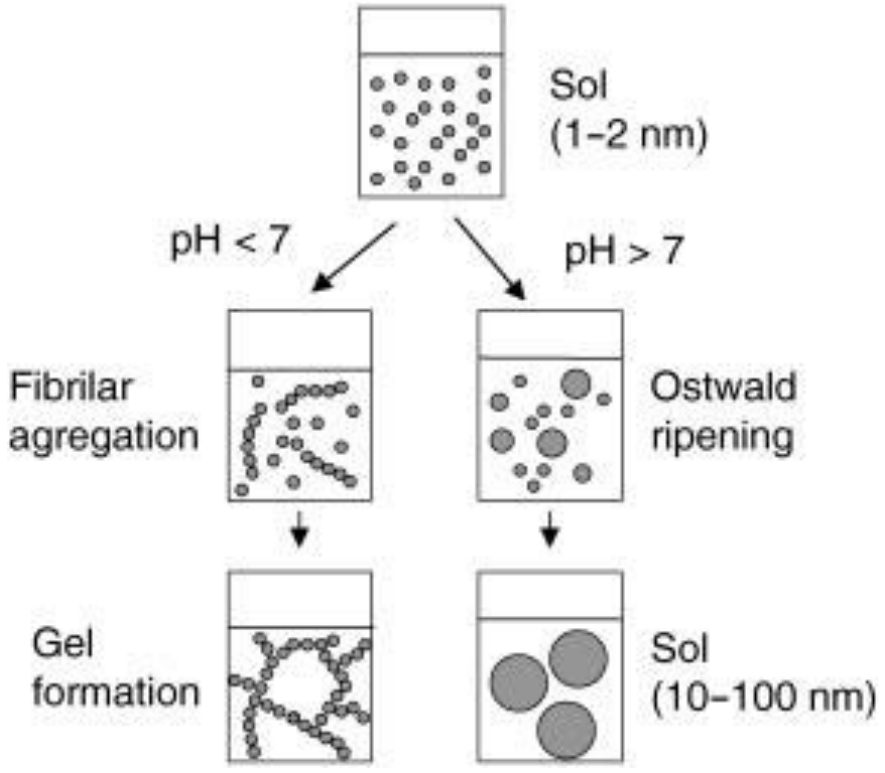

Figure 1-4 - Sol-gel formation. Where acidic pH results in particles aggregating together into chains and forming a gel and basic pH prevents this, so Ostwald ripening occurs leading to larger particles and the formation of a sol. Figure reproduced from ref [47]

Under basic conditions, the particles are all negatively charged and will repel each other. This means that gels generally cannot be formed. However; particle growth can occur through a process called Ostwald ripening (Figure 1.4). Ostwald ripening is where small particles are in a constant state of dissolving and then re-depositing onto any larger particles until the particles reach a size where they can no longer dissolve [46]. Once all the particles are too big to re-dissolve, growth stops and the resulting structure is known as a Sol.

1.5 Synthesis and properties of mesoporous silica nanoparticles

As stated previously, the focus of the use of silica for drug delivery applications is upon mesoporous silica nanoparticles (MSNs). These particles are characterised by their large surface areas (> 800 m^2 g^{-1}) and their tunable pore sizes of between 2 and 15 nm [33,34]. A wide variety of MSN have been created, but the focus here will be on three types which have received most attention into their use as drug delivery systems: MCM-41, MCM-48 (MCM: Mobil Crystalline Materials) and SBA-15 (SBA: Santa Barba Amorphous).

To create the high surface area and tunable pore sizes, surfactants are employed as structure-directing agents. In the example shown in Figure 1.5, CTAB (cetyltrimethyl-ammonium bromide) is used as a surfactant which self-assembles into rod-shaped micelles. When a silica precursor is added, the silica condenses around the micelles, taking their shape. The surfactant can then be removed (either through calcination or acid solvent extraction) which leaves behind a silica structure with the desired surface area and pore sizes [36]. Table 1.4 gives example synthesis methods for three different types of MSN.

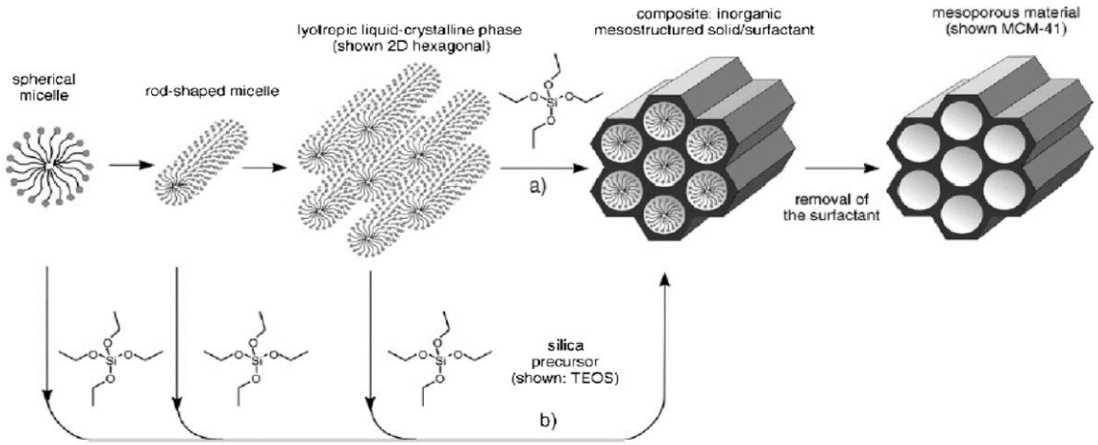

Figure 1-5 - Scheme showing the synthesis of MCM-41 with CTAB surfactant micelles as a template, Figure reproduced from ref [33]

The choice of surfactant can change the pore structure dramatically. MCM-41 and SBA-15 both have a 2D hexagonal channel pore structure, where SBA-15 generally has thinner pore walls and wider pore sizes than MCM-41 (5-30 nm compared to 1.6-10 nm). This could be useful for the loading of larger molecules onto the silica. MCM-48 has an interesting porous structure, where two interpenetrating continuous networks of channels form within these particles. It is thought that this provides very easy access for any guest molecule and also prevents pore blockage [48-50]. The hexagonal pore structure of MCM-41 and the bi-continuous pore structure of MCM-48 can be visualised in Figure 1.6.

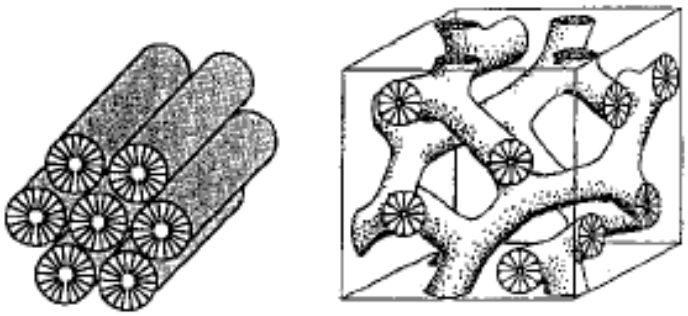

MCM-41 MCM-48

Figure 1-6 - Pore structures of MCM-41 and MCM-48 [51]

Table 1-4 - Examples of reaction conditions of three types of MSN [52]

MSN	Reaction conditions	Ref.
MCM-41	Cetyltrimethylammonium bromide (CTAB) (surfactant) is dissolved in a solution of water and tetramethyl ammonium hydroxide (TMAOH). Solution is heated to 35 ^{O}C with constant stirring for 30 minutes before tetraethyl orthosilicate (TEOS) is added drop wise. Mixture is stirred for an hour at 38 ^{O}C and then stirred for 2 hours without heat. Solution is autoclaved at 100 ^{O}C for 24 hours. Surfactant is removed via acid solvent extraction. Silicate is finally recovered via gravity filtration.	48
MCM-48	CTAB (surfactant) and F127 (tri-block coploymer) are dissolved in a solution of water, ethanol and ammonium hydroxide. TEOS is then added and mixture left stationary at room temperature for 24 hours. Solid is recovered via ultrahigh speed centrifugation and washed in water. Sample is then dried at 70 ^{O}C. Surfactant removed via calcination at 550 ^{O}C.	53
SBA-15	TEOS (a silica precursor), PEO20PPO70PEO20 (tri-block coploymer) and hydrochloric acid are dissolved in water and heated at 30^{O}C for 20 hours and then 95 ^{O}C for 24 hours before being washed, dried (at 70 ^{O}C) and calcinated at 550 ^{O}C (to remove the surfactant).	54

While MSNs have huge potential as and have been heavily investigated for drug delivery applications, they do have some drawbacks. Synthesis of these particles requires several hours of work can take between 10 and 146 hours[55-58] and requires hydrothermal conditions (the use of high temperature during synthesis and calcination) as well as using and producing hazardous chemicals (such as TEOS) [55-58]. This increases the cost of production, creates issues for scale up (i.e. high energy cost and large volumes of hazardous chemicals), along with potential negative environmental impacts. Therefore, a method of synthesising silica under benign conditions and in a much shorter time scale would be much more favourable, and this is the case for bio-inspired silica. Before discussing bio-inspired silica, the literature regarding the use of MSN for drug delivery applications will be reviewed.

1.6 Mesoporous silica nanoparticles (MSN) as a drug delivery system

As discussed in section 1.2, there are currently very few drug delivery nanoparticles on the market. This is likely due to both safety issues and the lack of optimisation of drug delivery system properties (i.e. lack of good drug loading, release profiles and specific targeting). This means that there is a huge potential market for a nanoparticle drug delivery system with controlled release of several potential drugs [59]. As yet silica nanoparticles have not been fully utilised as DDS and investigations into this potential have mainly focussed on more fundamental properties of a DDS (i.e. the ability to hold and have controlled release of drugs and also to have low cytotoxicity).

MSN were first shown to have potential as a drug delivery system in 2001, where a study reported the effective loading of ibuprofen onto the MCM-41 and also

showed a prolonged diffusion of the drug out of the nanoparticles over 80 hours when immersed in simulated body fluid [60] . Since then MSN have come to the forefront of silica research for drug delivery applications due to their large surface area (> 800 m^2 g^{-1}) (which allows for a huge capacity to hold drug molecules) and the ability to have fine control over MSNs properties. Size and shape of nanoparticle and the size and geometry of the pores can be altered, which allows for the potential for a wide range of drugs (with different sizes and properties) to be loaded onto the silica [36,61]. MSNs are also generally regarded as being more robust and versatile than more conventional drug delivery systems and can also be produced reliably, making them advantageous to the pharmaceutical industry [36].

A major advantage of using any DDS is the ability to control the release of drug molecules. This allows one to alter the dosage of drug being released which can result in increased activity time, decreased toxicity and increased patient compliance (due to fewer tablets being administered) [12,62]. Drug release from MSN can be easily controlled, simply by utilising the controllability of MSN porosity. Some studies have shown that a decrease in pore size results in the reduction of the release rate of ibuprofen and erythromycin (an antibiotic) [63,64]. Altering the surface area can also increase drug loading, which will affect the dose of drug being released [65].

However, an important issue for all types of MSN is the host–guest interaction (i.e. the interaction between the MSN and the drug). If the MSNs are made from pure silica then the only binding sites available are between the free Si-OH groups and the functional groups of the guest molecule (likely forming only weak intermolecular hydrogen bonds) [36,66]. This issue can be easily remedied via the addition of different functional groups on the mesopore walls, a process known as

"functionalisation". A study in 2003 hypothesised that as ibuprofen contains an acid group, then if the silica pore walls were functionalised with basic groups, the "host/guest" interaction would be strengthened. This study functionalised MCM-41 with amino-propyl groups and observed a longer release profile in functionalised MCM-41 when compared to unfunctionalised silica [67]. Another study functionalised SBA-15 with alkyl groups of varying lengths, in an attempt to load L-tryptophan (a hydrophobic amino acid) which is impossible to do with unfunctionalised MSNs. This study observed that an increase in the length of the alkyl group resulted in a higher loading of L-tryptophan. This was due to the long hydrocarbon chains creating a hydrophobic environment where L-tryptophan is able to reside [68].

The guest molecule ultimately determines the type of functionality required to improve loading and release and MSN can be functionalised with many other groups including –CN, -Cl, -SH, -F and phenol groups [69]. Along with pore size, functionalisation is an important tool for controlling drug loading and the rate of drug release; however, it does not offer any target specificity.

The ability to control the release of drugs and target this release to a specific site in the patient's body is one of the key roles of a drug delivery system. This characteristic ensures that the drug is released at the site of drug action, thus increasing the efficacy of the drug and reducing toxicity (especially significant for anti-cancer drugs). One of the most common methods of controlling drug release is through the use of "stimuli-responsive" polymers (often called "smart materials"). As shown schematically in Figure 1.7, these polymers can be manipulated by external stimulation and so can be used to "plug" the pores of MSNs under one condition, but then be removed and allow the drug to be released under a different

condition (Figure 1.7). There are a whole range of external stimuli which can be used to manipulate these "smart materials", ranging from magnetism, ultrasound and light, to the more conventional, temperature and pH [70,71].

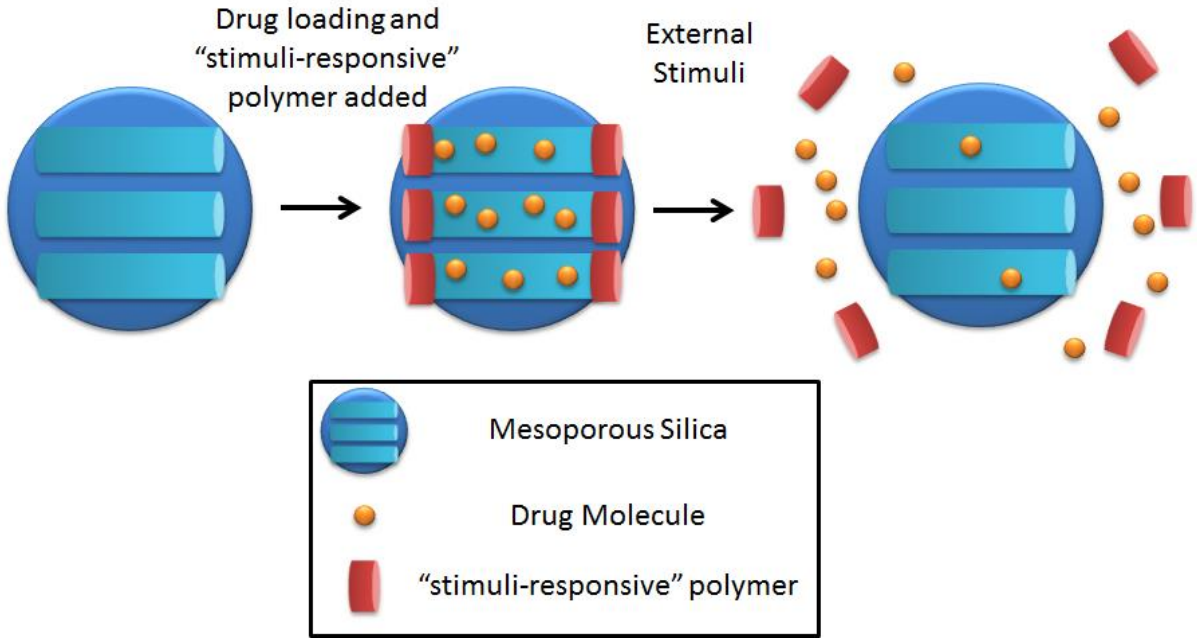

Figure 1-7 - Schematic of the "stimuli-responsive" polymers entrapping drug molecules into MSN, only releasing cargo upon an external stimulus [72]

Zhou, *et al.* (2007) investigated the use of poly(N-isopropylacrylamide) (PNIPA) as a stimuli-responsive polymer for controlling the release of ibuprofen from mesostructured cellular foam (MCF) (this was used rather than MCM-41 due to its larger pore sizes and therefore it was better suited for holding larger molecules). This study observed a temperature transition of PNIPA between 30-40^{o}C. This proved hopeful as the core temperature of the human body (where one usually desires the drug to be released) is 37 ^{o}C. While this study observed a higher percentage of drug release at higher temperatures (80-90% at 50 ^{o}C), there was still a promising percentage of drug released at 37 ^{o}C (around 50%) which allowed to

authors to conclude that this type of release control has some potential for drug delivery applications [71].

Perhaps a more useful method of controlling drug release is through pH. By far the most preferred route of administering drugs is orally. But the use of this route of administration comes with the varying environments of the gastrointestinal tract. A drug must first survive the low pH of the stomach (around pH 1.2) before reaching the more neutral small intestine, where it can then be absorbed into the blood. A study in 2007 by Song, *et al*., showed some promising results using pH to control drug release. This study loaded SBA-15 with bovine serum albumin (BSA). The SBA-15 used was functionalised with amine groups which allowed for the coating of the particle with poly(acrylic acid) (PAA). PAA would remain attached to the particle under acidic conditions (and so entrap the BSA), but releases from the silica at neutral pH (and so releasing the drug). PAA has the additional advantage of being able to attach to the mucosal lining of the upper small intestine, which will allow for the drug to be released in close proximity to the intestinal wall. With this system, very promising results were seen. Without the protective coating, BSA was released from SBA-15 at similar efficiencies regardless of pH (45% at pH 7.4 and 50% at pH 1.2). However, when the SBA-15 is coated with PAA, only 10% of BSA is released under acidic conditions, but around 40% is released at pH 7.4 [73].

While oral administration of drugs is the preferred route, it is not always the best route. Sometimes intravenous administration is the preferred route to administer drugs, but how to target its release? Some types of tissues to which many drugs are targeted are actually slightly more acidic than normal blood and tissue, such as some tumours and inflammatory tissues. It is this slight difference which allows for

specific drug targeting. Yang, *et al.* (2005) investigated a method of releasing drugs from MSN under acidic conditions. Here they coated carboxylic acid functionalised SBA-15 (which has been loaded with vancomycin) with poly(dimethyldiallylammonium chloride (PDDA) and observed a slow and prolonged release of the vancomycin at pH 4.5. This release pattern is very useful in drug delivery as it ensures a prolonged maintenance of the optimum concentration of drug at the site of action [74].

MSN are clearly a useful material for drug delivery applications since they have the ability to load a high amount of drug (due to its high surface area) and can control the release by altering the porosity. There is also the opportunity to improve these characteristics by employing functionalisation and stimuli-responsive materials. However, they do have some major issues. These nanoparticles are produced using harsh chemicals (such as TEOS and CTAB) and require an energy intensive calcination step (which increases the cost of production). Functionalisation and drug loading add a further step each in the manufacturing process, increasing the timescale. There is also evidence that functionalisation could lead to biocompatibility issues. Functionalised MSN were seen to be significantly more cytotoxic than unfunctionalised Stöber particles, this is greatly detrimental to the argument for using MSN for drug delivery applications [35]. Therefore the one-step synthesis and drug loading process which occurs under benign conditions will be clearly more favourable as this is more compatible with drugs and biomolecules [75].

The bio-inspired method of silica synthesis offers these benefits (as discussed in sections 1.5 and 1.6), however, a recent paper has been published which describes a one-pot *in situ* loading of drugs into mesoporous silica [76]. This paper mixed drug

molecules (either ibuprofen or heparin) with P123 (the surfactant which produces micelles for silica condensation) before adding TEOS and allowing silica to form (over the course of ~10 hours). The temperature is kept at 37ºC to avoid drug degradation [76]. This is an interesting synthesis route, and favourable drug loading and release were observed. Drug release profiles were attributed to the dissolution of P123, since no calculation step occurred to remove the surfactant and create a true mesoporous material. The authors argue that the lack of calcination decreases CO_2 emissions and since no organic solvents are used, the process is environmentally friendly. This method has many of the same advantages as BIS and could be a potential rival system; however more work on the system and its biocompatibility is required.

1.7 An introduction to bio-inspired silica (BIS)

The "biomineralisation" of silica has mostly been observed in species of aquatic unicellular organisms, such as diatoms (a class of algae). But several more complex organisms also possess this ability, such as some sponge species and even some plants [77]. Diatoms are a widespread group of eukaryotic algae and a major component of ocean phytoplankton (contributing up to 40% of the total ocean's primary energy production [78]). Diatoms have rigid cell walls which are constructed out of amorphous, hydrated silica and are intricately and beautifully structured. Examples of which are shown in Figure 1.8 [79,80].

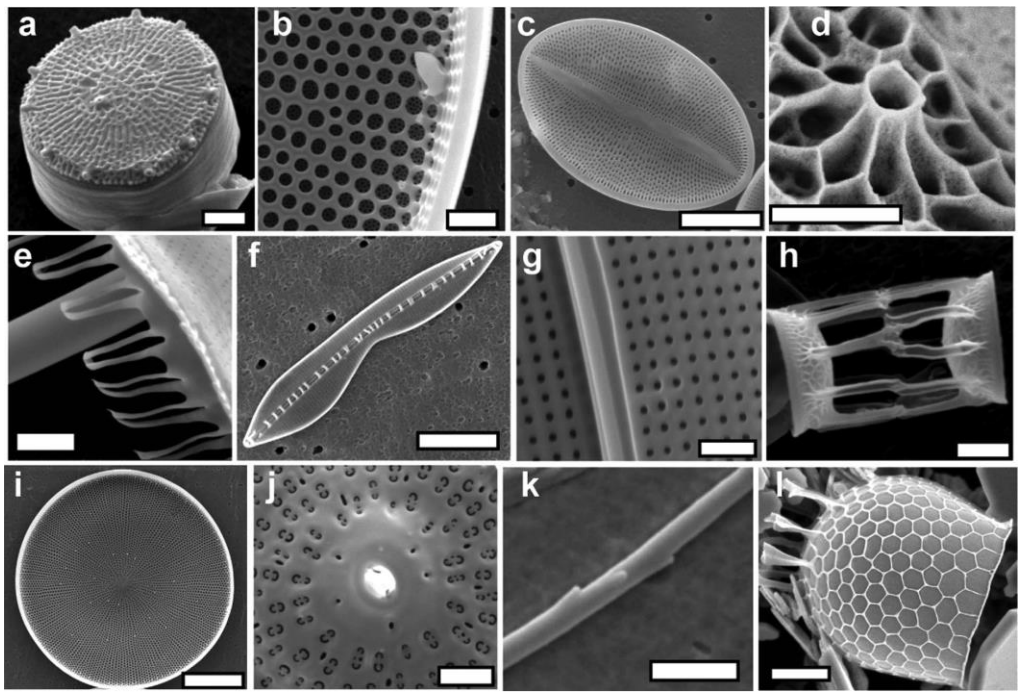

Figure 1-8 - Electron micrographs of silica structures produced from several species of diatom. Figure reproduced from ref [80]

It has been observed that the structure of the silica cell wall is species dependent and did not vary through generations, suggesting the genetic control, and also the involvement of proteins in the bio-mineralisation of silica [79-81]. Long-chain polyamines allow living organisms to condense silica and several proteins have been identified [80-82]. Such proteins include silicatein (found in some sponge species [83]) and silaffins (so named due to their affinity to silica), which are a group of proteins found in diatoms [84]. It is the synthesis conditions which makes biologically condensed silica interesting. During bio-mineralisation, silica is condensed under mild pH, ambient temperatures and in an aqueous environment. By studying and understanding the chemistry of the bio-mineralisation of silica in nature, a method inspired by this has been devised and is known as the bio-inspired method of synthesising silica.

Initially polyamines found in nature (e.g. silaffins) were used to synthesise bio-inspired silica (BIS); however there were issues with their availability and purity [85] Therefore, analogues were investigated and a large range of poly-peptides, small molecules and synthetic polymers have been discovered with the ability to condense silica, and these are summarised in the literature [85]. The bio-inspired mechanism is similar to the sol-gel chemistry (as described in chapter 1.4) but utilises amines to enhance proton transfer during silica condensation. Since silica condensation is fastest at pH 7, this is the mechanism shown in Figure 1.9 [46,47,77].

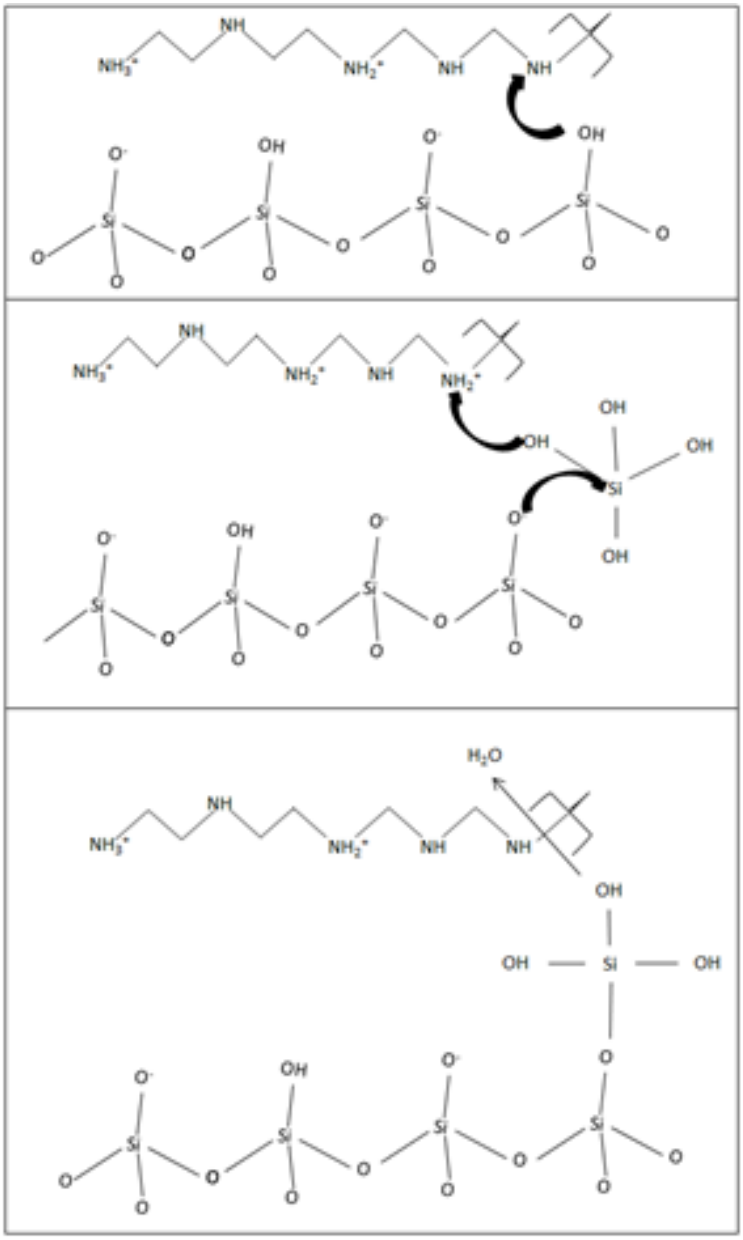

Figure 1-9 - The mechanism by which amines (in this case pentaethylenehexamine (PEHA)) catalyse the condensation of silica [77]

Figure 1.9 shows that initially the positively charged amines are attracted to deprotonated silanol groups on the surface of the silica. This brings the amine and the silica into close proximity, allowing the non-charged amine groups to carry out their catalytic activity. While classed as uncharged, these amine groups do have some basic characteristics (due to the presence of a lone pair of electrons). This property allows for the deprotonation of a surface silanol group, which in turn allows

the now negative oxygen to nucleophillically attack a silicon atom in a free silicic acid molecule ($Si(OH)_4$) via an S_N2 reaction. The complete binding of the silicic acid to the silica occurs due to the weakly protonated amine group acting as a bronsted acid and donating the proton onto the silicic acid, resulting in the removal of water (as a leaving group). When anime is not present in the reaction mixture, free silicic acid molecules must directly attack charged silanol groups. This results in a hydroxyl ion acting as the leaving group. This ion is a much less favourable leaving group than water, which is why this reaction is normally so slow [77].

The choice of amine additive can have a great effect on the resulting silica's properties. The number of amine groups per molecule and the level of methylation of the polyamine used both have significant effects on the size, porosity and shape of the silica product. Belton, *et al.* (2005) investigated if the length of the polyamine used (i.e. the number of amine groups per molecule) had had any effect on the resulting silica product. It was observed that the resulting silica became more granular in structure with increasing length of polyamines. With more amine groups per molecule, the condensation of silica was more efficient and resulting particles were less porous and so had reduced surface areas. This study observed a clear cut off where, if the numbers of amines per molecule exceed four, only non-porous silica nanoparticles formed. Whereas when smaller polyamines were added porous silica nanoparticles were formed. [77].

Whether the polyamine remains in solution or forms into droplets also impacts the structure of the silica nanoparticles. If the amine comes out of solution and creates a micro-emulsion, then a hydrophobic environment is formed, which is ideal for the removal of water molecules produced in the condensation of silica.

When micro-emulsions form, the silica condenses around the droplet and so hollow nanoparticles are yielded (Figure 1.10). Hollow nanoparticles are important in biomedicine (with their potential use in dental implant materials and for drug delivery systems) as well as in other areas, such as use in thermal insulators [86].

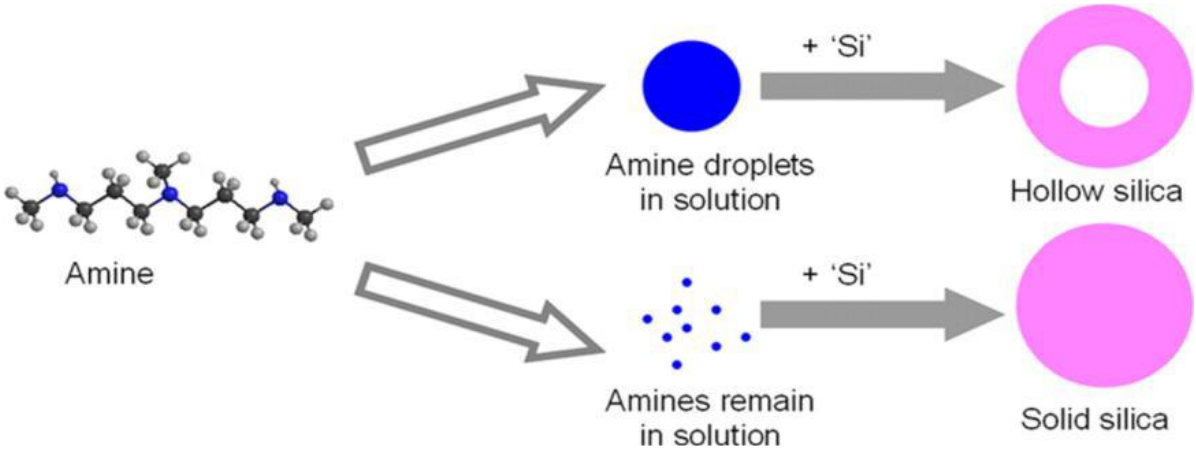

Figure 1-10 - A schematic of micro-emulsions of amine forming and resulting in the formation of hollow silica particles, Figure reproduced from ref [87]

Longer polyamines and polyamines with more methyl groups are more hydrophobic and so are more likely to come out of solution. Interestingly, it has been observed that if amine groups are separated by more than three methyl groups, micro-emulsions are not formed due to an increase in the ease of amine groups becoming charged, which will also impact on the polyamine's catalytic activity [87]. The production of a micro-emulsion is not essential for the catalytic effect of polyamines on silica condensation; however, it is critical in the production of hollow silica nanoparticles. If the amines remain in solution, only solid silica nanoparticles will form (Figure 1.10).

Along with drug delivery applications, other applications for BIS have been well studied within the Patwardhan group. BIS has been immobilised with enzyme for use as a biocatalyst, and it was found that using BIS resulted in better enzyme

activity over a wider range of temperatures and pH conditions than using free enzyme [88]. Carbon capture is also a potential application for BIS and it has been shown that enzyme immobilised BIS can sequester similar amounts of carbon dioxide to free enzyme, and BIS improved the thermal stability of the enzyme, allowing for excellent reuse potential and had good storage properties [89]. Finally, a feasibility study on the large scale and continuous production of BIS has been carried out and found that the manufacture of BIS is more economically favourable and resulted in lower CO_2 emission than the manufacture of other types of silica. This shows that BIS has great potential for manufacture at an industrial scale [90].

1.8 The potential for "bio-inspired" silica (BIS) as a drug delivery system

As yet, there have only been four papers discussing the potential use of specifically bio-inspired silica (BIS) for drug delivery.

A 2012 paper investigated the use of BIS for the delivery of ibuprofen. Here a surfactant (CTAB) was used in order to create mesoporosity within the nanoparticles [91]. It is important to note that while the use of BIS is a greener process; the method reported here takes 15 hours to synthesise the particles and also requires three steps (synthesis, calcination and drug loading), therefore this method does not solve the problems of MSN.

Sano, *et al.* in 2010 presented a method where a dual-function protein (called #284) was loaded onto the silica nanoparticles [75]. This protein had been previously shown to be able to penetrate cell membranes and induce apoptosis (controlled cell death) as well as the ability to induce the precipitation of silica [92]. While this study

showed promising release profiles of the protein, not all proteins or drugs will have the dual properties of pharmaceutical activity and facilitate silica precipitation.

Another study utilised a synthetic silaffin variant (R5 peptide) which can trigger the condensation of silica. Here the R5 peptide was covalently linked with a cargo molecule (CG12AB) via a disulphide bond which could be cleaved under reducing conditions, thus releasing the cargo molecule. A scheme of this is shown in Figure 1.11 [93].

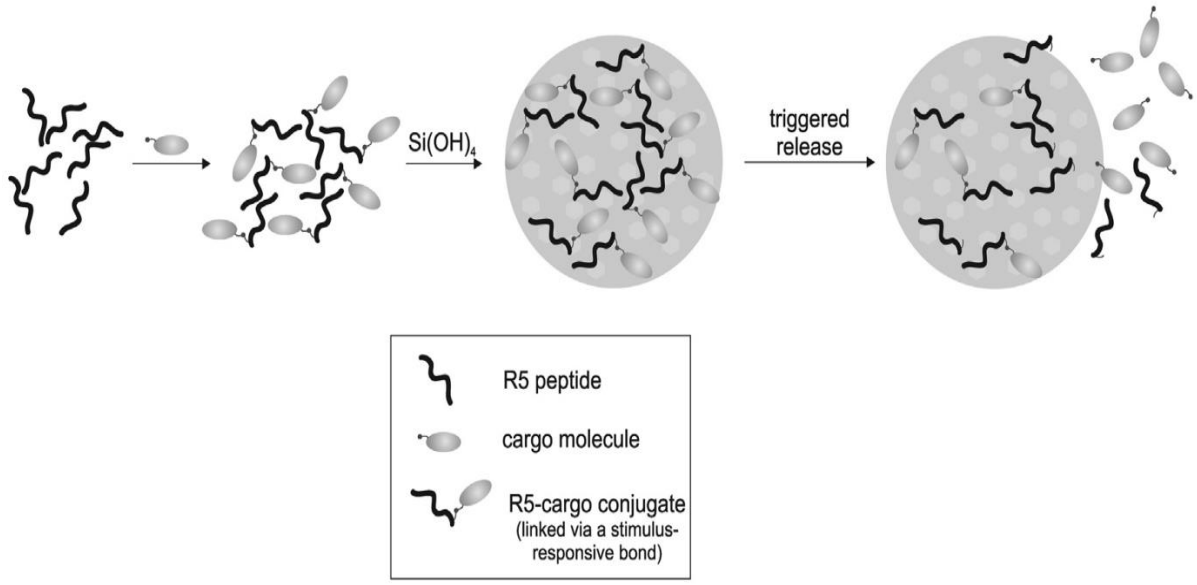

Figure 1-11 - Silica precipitation with synthetic R5-cargo conjugates and release of cargo under a stimulus responsive cleaving of R5-cargo bond [93]

This study had the goal of controlled drug release, however, in the absence of TCEP (tris(2-carboxyethyl)phosphine) (which would cleave the di-sulphide bonds) only 18% of the R5-cargo conjugate was burst released (i.e. uncontrolled release). A higher rate of uncontrolled release (48% of R5-cargo conjugate was released) was observed under acidic conditions and so the authors argued that this characteristic may be of interest for releasing cargo in acidic environments (e.g. in some cellular compartments, such as lysosomes, or in and around tumour cells).

Finally, preliminary work from our group reported the green synthesis of silica with in situ drug loading of calcein (a hydrophilic drug-like molecule) [35]. Steven, *et al*., also observed that release of calcein from BIS occurred in a two stage process with the initial burst release (attributed to the drug being phys-adsorbed to the silica surface) followed by a slower, more prolonged release (attributed to the diffusion of drug out of the internal porosity of the silica or to drug interactions with the amines). The level of burst release could be controlled by changing the amines used, with longer amines (such as PAH) having lower burst release than from BIS synthesised with smaller amines (such as DETA). The advantages of this synthesis route are that it requires no calcination or use of hazardous chemicals and the amine additive was separate from drug molecule (making the system more versatile).

It is clear then that while BIS do have several advantages over MSN in their synthesis (e.g. quicker and under benign conditions) there is still a lot of work to be done to improve the loading and release of drugs from these silica particles.

1.9 Aims

The main aim of this research is to primarily understand *in situ* drug loading into the BIS system. Specifically, we plan to determine predictive rules, investigate the effects of amine additive, drug interactions and silica chemistry on DDS performance (drug loading and release profiles). Ibuprofen will be utilised as a model drug to determine these predictive rules which then can be applied to a drug in need of an effective DDS; hydrocortisone. Further, in order to make BIS a viable DDS, it should exhibit similar or improved loading and release profiles for ibuprofen when compared to the competitor MCM-41 based DDS. Finally, for any DDS to be viable it must be fully biocompatible and the biocompatibility of BIS will be investigated using gut and blood models.

Chapter 2: Materials and Methods

2.1. Chemicals

All reagents were purchased from Sigma unless otherwise stated, and used without further purification.

Chemicals used in this project include: - Acetronitrile (HPLC Plus, ≥99.9%), ammonia (NH_3, anhydrous, ≥99.98%) , anhydrous sodium sulphite (97%), ammonium molybdate $\cdot 4H_2O$ (USP testing specifications), calcium chloride hexahydrate (98%) , concentrated hydrochloric acid, diethylenetriamine (DETA) (99%), dinitrophenol (≥98.0%) (DNP), Dulbecco's PBS, formic acid (≥95%), glucose (≥99.5%), heparin, hexadecyltrimethylammonium bromide (CTAB) (United States Pharmacopeia (USP) Reference Standard), hydrocortisone (BioReagent, suitable for cell culture), hydrochloric acid solution 1M (HCl, Fisher), ibuprofen (≥98%), magnesium sulphate heptahydrate (≥99.5%), oxalic acid $\cdot 2H_2O$ (≥99%), pentaethylenehexamine (PEHA) (technical grade), p-methylaminophenolsulphate (99%) (Metol), potassium chloride (≥99.0%), phosphate buffered saline (PBS) (tablets pH 7.4), poly(allylamine hydrochloride) average M_w ~17,500 (PAH), poly(fluorescein isothiocyanate allyamine hydrochloride) (Poly(allylamine hydrochloride) : Fluorescein isothiocyanate 50:1), potassium phosphate monobasic, sodium chloride (≥99.5%), sodium metasilicate pentahydrate (technical) (Fisher), sulphuric acid (98%), tetraehylenepentamine (TEPA) (Acros organics), tetraethoxysilane (99.999% trace metals basis) (TEOS), Triton X-100 (laboratory grade).

2.2. *In situ* drug loading into BIS and drug release

To a solution of sodium metasilicate in deionised water (dH_2O) a solution of amine additive (in dH_2O) was added, followed by a 1 mg/ml drug (ibuprofen or hydrocortisone) solution (in 70:30 ethanol: water). Then a known volume of 1M HCl (the volume of HCl required varied depending on the amine additive used) was added to reduce the pH of the solution to the desired pH (pH 7, unless otherwise stated). The concentrations of the reactants in the final solution were 30mM of sodium metasilicate, 1 mg ml^{-1} PAH and 1 mg ml^{-1} drug, this ratio was termed 1:1:1 Despite different levels of hydrophobicity, the same concentrations of ibuprofen and hydrocortisone were used to eliminate this variable. For a 50ml batch of 1:1:1, 0.3182g sodium silicate, 0.05ml of PAH and 0.05g of ibuprofen were used. When synthesising BIS with other amines (DETA, TEPA and PEHA), a molar ratio of [Si]:[N] of 1:1 was used. This equates to 0.05155g of DETA, 0.05678g of TEPA and 0.05809g of PEHA for a 50ml batch. Once acid was added, silica precipitated within seconds and the solution was left for 5 minutes (longer maturation times did not affect drug loading efficiency or silica yield) before being centrifuged at 8000 rpm for 15 minutes in order to stop the reaction. The supernatant was stored at 4^{o}C in order to determine the drug loading efficiency (% of drug which was loaded into the silica) and drug content (% weight of drug in the silica-drug complex) via the HPLC method described in section 2.4. The silica pellet was resuspended, washed in deionized water and centrifuged, twice more (no detectable drug was observed in these supernatants , however due to the sensitivity of the HPLC, there is a potential loss of 0.005 m/ml of ibuprofen or hydrocortisone which was not detectable.) and finally dried at 45 ^{o}C for at least 5 hours.

Once dried, 10 mg of the silica was suspended in 1.4 ml of PBS (pH 7.4) and incubated at 37 ^{o}C to measure the drug release. This method of measuring drug release was set up to create a very simple system to preliminary investigate the BIS system. At each time point (1, 3, 5, 7 and 24 hour time points), samples were centrifuged at 8000 rpm for 15 minutes and 1 ml of the supernatant was taken for HPLC analysis and replaced with fresh PBS. Release is expressed as the % of the drug loaded into the silica which has been released from 10mg of silica during the experiment. Each sample was measured in triplicate and release profiles were obtained from each sample in triplicate.

2.3. Synthesis of MCM-41 and post-synthesis drug loading

MCM-41 was synthesised by first dissolving CTAB in 300 ml of 25 % ammonia at 35 ^{o}C. While stirring, 20 ml of TEOS was slowly added. This solution was then stirred for 3 hours and then aged for 24 hours at room temperature in a closed container to allow silica to form. The product was then vacuum filtered and washed with 1 litre of distilled water and finally dried overnight at 85 ^{o}C. To remove the surfactant (CTAB), MCM-41 was calcinated at 500^{o}C for 5 hours. This was based on previously published methods [94]. MCM-41 used in this investigation was synthesised with the help of Abdunaser M. Ewlad-Ahmed.

To load drug, 10mg of MCM-41 was immersed in a 1 mg ml^{-1} solution of drug (in 70:30 ethanol: water) at 37 ^{o}C for 24 hours. Samples were centrifuged at 8000 rpm for 15 minutes and the supernatant removed for HPLC analysis to determine the drug loading efficiency (chapter 2.4). Supernatant was replaced with fresh PBS for a release experiment. At each time point, samples were centrifuged at 8000 rpm for 15

minutes and 1ml of the supernatant was taken for HPLC analysis and replaced with fresh PBS.

2.4. Drug detection via high pressure liquid chromatography (HPLC)

Drug loading and release were determined via an HPLC analysis method. HPLC is a widely used separation and analytical technique. HPLC involved injecting a liquid sample through a tube which contains porous particles of 3-10 µm diameters (known as the stationary phase) at high pressure. Components in the mobile phase are separated in the column based on chemical and/or physical interactions with the stationary phase. This means that some components stay in the column longer than others and so the mixture is separated. On leaving the column, elutants are detected and measured as a function of time [95].

The property of the mixture to be separated dictates the choices of the mobile and stationary phases. The most common HPLC method is known as reversed phase. Here, the stationary phase is non-polar (such as C-18) and the mobile phase is water and a water-misable organic solvent (e.g. methanol or acetonitrile). This method is so commonly used due to its versatility, being used for polar, non-polar, ionisable and ionic materials. Other methods include normal phase (stationary phase is polar and mobile phase is non-polar) which is used for water sensitive compounds and chiral compounds, ion exchange (stationary phase contains ionic groups and the mobile phase is an aqueous buffer) which is used for inorganic and organic cations and anions and finally size exclusion (where molecules are separated because smaller molecules can diffuse into pores and larger ones cannot) which is used for

polymer characterisation and for proteins. Once eluted, samples must then be detected with spectroscopic detection being favoured (either with UV absorbance or mass spectroscopy). Refractive index detection and fluorescence can also be employed [95].

For this project, an auto-sampler (GINA50) with a pump (P580) and variable wavelength detector (UVD170S) was used along with an ACE 5 C-18 column (150X4.6 nm with 5 µm particle size) at room temperature. To measure ibuprofen an isocratic (i.e. mobile phase remains constant) reversed phase HPLC method was used with 30 µl injection volume and a mobile phase of acetonitrile: 0.1% formic acid (70:30) at a flow rate of 1ml min^{-1}. Ibuprofen retention time was approximately 4.7 minutes and was detected using UV absorbance at a wavelength of 220 nm (λ_{max} wavelength of ibuprofen). The area under the curve of the ibuprofen peak can be found and a standard curve can be constructed (Figure 2.1). Detection is limited to a range between 1mg/ml (above which the detector is bleached) and 0.005 mg/ml (below which peaks are too small to integrate).

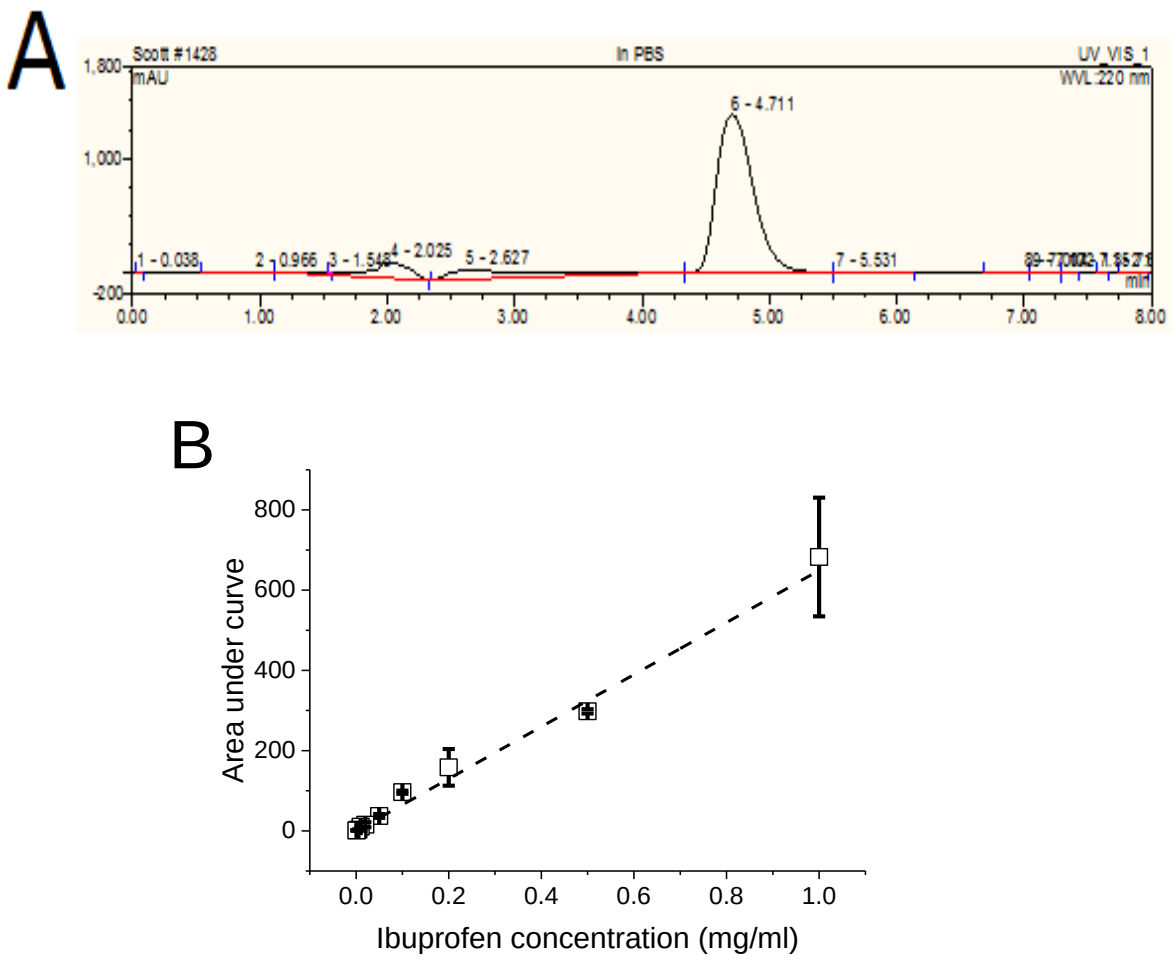

Figure 2-1 - (A) An example HPLC trace of ibuprofen in 70:30 ethanol:PBS. Peak is observed at 4.7 Minutes. (B) Standard curve for ibuprofen run on HPLC. Equation of the line is y = 649 X, r2 is 0.95

To measure hydrocortisone, an isocratic reverse phase HPLC method was used with 40 µl injection volume and a mobile phase of acetonitrile: water (7:3) at a flow rate of 1ml min^{-1}. Hydrocortisone retention time is approximately 7.1 minutes and was detected using UV absorbance at the wavelength 246 nm (λ_{max} wavelength of hydrocortisone) [96]. The area under the curve of the hydrocortisone peak was found and a standard curve can be constructed (Figure 2.2). Detection is limited to a range between 0.5 mg/ml and 0.005 mg/ml.

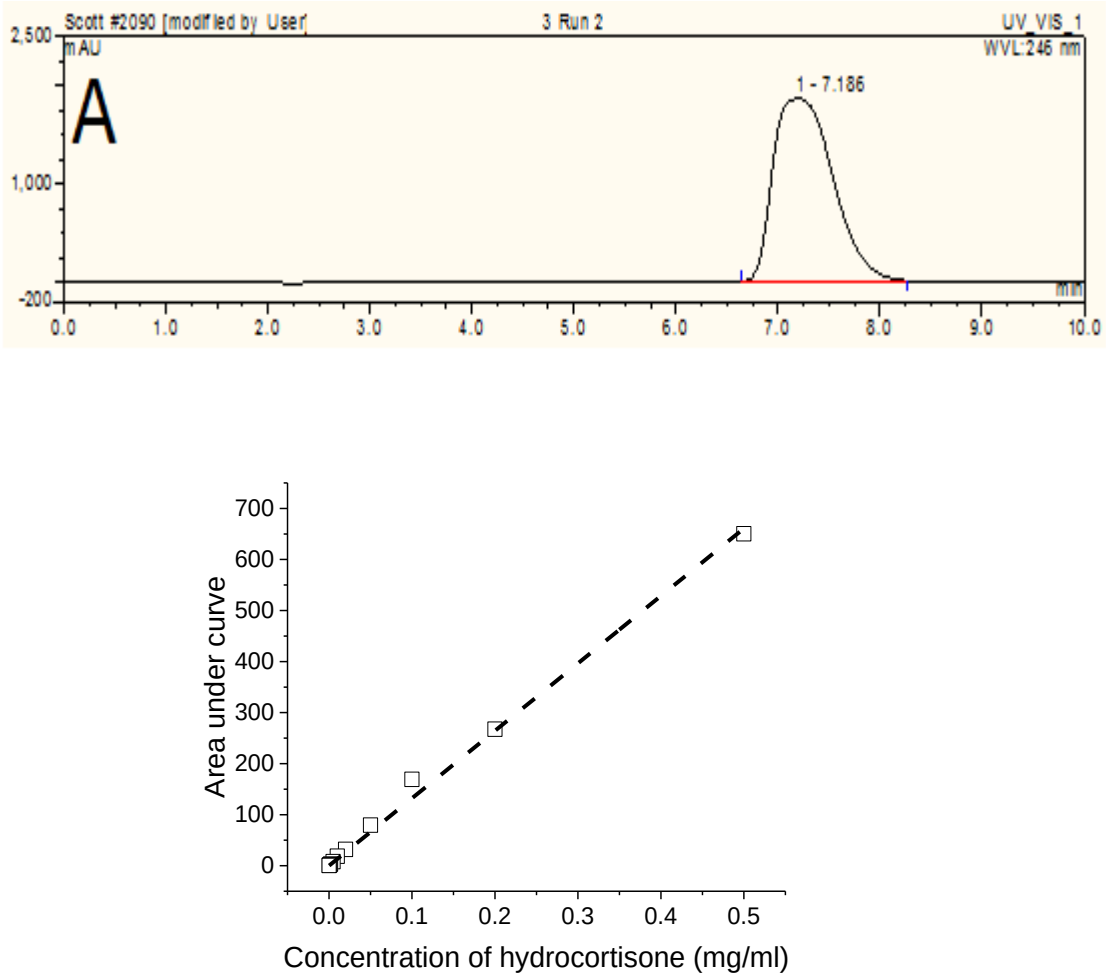

Figure 2-2 -A) An example HPLC trace of hydrocortisone in 70:30 ethanol: water. Peak is observed at 7.1 Minutes. (B) Standard curve for hydrocortisone run on HPLC. Equation of the line is y= 1321X and r2 is 0.99

Release data were plotted and fitted with a single exponential equation (Equation 2.1) where Y_0 is the final % release, R_0 is the slope at each point, X is time (hours. One would expect A to equal Y_0 but due to the time resolution it is left as a free parameter within the fitting equation. By multiplying A and R_0 the maximum rate of release (% release per hour) was deduced.

$$y = Y_0 - A\, e^{-R_0 X} \qquad \textbf{Equation 2-1}$$

2.5. Porosity analysis

Gas adsorption is an important technique often used in materials science to elucidate several surface characteristics of a sample, including surface area, porosity and pore size distribution. This is achieved by monitoring the way a gas (normally nitrogen) is adsorbed (via physisorption) on the surface of a material at its boiling point over a range of pressures [97].

In this investigation silica nanoparticles were characterised using a micromeritics ASAP 2420 System. Analysis occurred in two steps. The first step, de-gasing, was carried out for at least 120 minutes at 120^{o}C, in order to remove any adsorbed impurities which may be on the surface of the silica particles, prior to nitrogen adsorption. Sample tubes were then evacuated and held at the boiling point of nitrogen (-198.5^{o}C) by immersing in liquid nitrogen and allowing for nitrogen gas to enter the sample tubes and adsorb into the silica sample. The apparatus monitors the pressure of the vessel and the levels of nitrogen adsorption.

Analysis of the data monitored by the micromeritics instrument included BET (Brunauer, Emmett, Teller [98]) theory, used to characterise the surface areas of the silica particles, and the BJH (Barrett, Joyner, Halenda[99]) theory which allowed for the characterisation of the silica pore size distributions. These two theories are discussed in more detail in appendix 1.

2.6. Molybdic acid colorimetric assay

The molybdic acid colorimetric assay is employed to measure the concentration of silica monomers in solution. This method is often used to measure kinetics of

silica polymerisation, however, in this study it is employed to determine the degradation/dissolution of condensed silica back to monomeric silica [46]. This assay is highly sensitive and can detect silicic acid as low as 0.02 ppm ($3.32X10^{-4}$ mM) [46].

This assay works by first binding monomeric $Si(OH)_4$ with acidified ammonium heptamolybdate to form the yellow silicomolybdic acid (Reaction 2.1). This reaction is exclusive to monomeric silica and not polymeric silica since silicomolybdic acid contains only one silicon atom [46].

$$7\ Si(OH)_4 + 12\ H_6Mo_7O_{24}\cdot 4H_2O + 174\ H_2O = 7\ H_8Si(Mo_2O_7)_6\cdot 28\ H_2O \quad \text{[Reaction 2.1]}$$

When concentrations of silicic acid are too low (only a few parts per million), then the yellow colour of the silicomolybdic acid complex may be too weak to be detected and so the complex is reduced to molybdenum blue [46].

Molybdic acid is made with 10g ammonium molybdate, 500ml dH_2O and 60ml concentrated hydrochloric acid and adjusted to a final volume of 1L. The reducing agent is made with 10g oxalic acid, 3.35g metol, 2g sodium sulphide, 250ml dH_2O and 50ml concentrated sulphuric acid; this solution is then diluted to 500ml upon cooling.

10mg of silica sample was immersed in 1.5 ml of dH_2O and incubated at 37^oC for 23 hours or 30 days, to determine the level of dissolution with would occur *in vivo*. At each time point, samples were centrifuged at 8000 rpm for 15 minutes. The supernatant was then stored at 4^oC for measurement. To measure silica monomer concentration, 100 µl of silicic acid solution is added to a solution containing 15ml dH_2O and 1.5 ml molybdic acid. This was allowed to stand at room temperature for exactly 15 minutes. This allowed silicic acid monomers to react with molybdic acid

and form a yellow complex. 8ml of reducing agent was then added, whereupon the solution was reduced and changed to a blue colour. The absorbance of the solution was then measured at 810nm after 2hours but before 24 hours. A standard curve is made by measuring known concentrations of sodium metasilicate solutions (Figure 2.4). Detection range was between 15mM and 0.015mM.

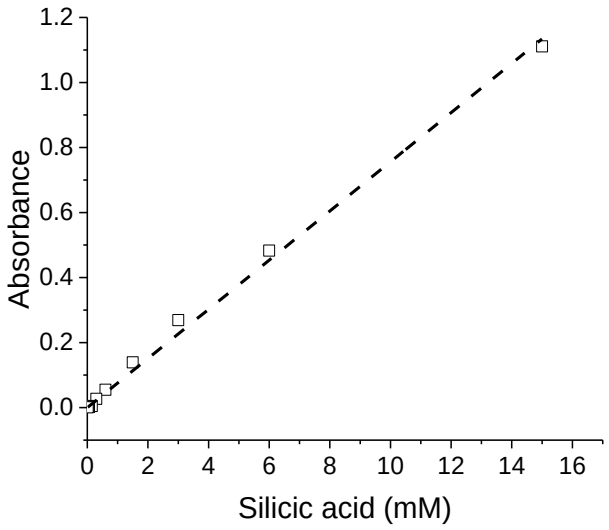

Figure 2-3 - Standard curve of sodium metasilicate measured using the molybdic acid colorimetric assay. Equation of the line is y= 0.0756X and r^2 is 0.99

2.7. Movement of silica across rat intestine

Rats (200-250g, male, Sprague Dawley) were anesthetised via intraperitoneal injection with pentobarbitone (60mg/kg) and sacrificed for the experiment. All experiments using animals were carried out under Home Office licence PPL 60/4341 valid until May 2017 and held by Professor M. Helen Grant. The small intestine was removed and washed through with 37^{o}C Krebs solution (made from distilled H_2O, 16.09% (w/v) NaCl, 1.1% (w/v) KCl, 0.22M KH_2PO_4, 2.74% (w/v)

$MgSO_4.7H_2O$, 0.12M $CaCl_2.6H_2O$). Intestines were then inverted and bathed in Krebs solution, ensuring 37°C temperature was kept constant. Small sections of gut (~5-6 cm) were cut and tied closed firmly at one end with thread, filled with 1ml of fresh Krebs solution, and then the open end was also tied closed. Rat aesthesis and dissection was carried out by Catherine Henderson.

In order to verify the health of the sections of gut, a control experiment was set up which measured the active passage of glucose across the gut wall. Sections of gut were either immersed in 6ml of 1mM glucose solution or in 1mM DNP (dinitrophenol) solution (to inhibit the active transport of glucose [100]) for 15 minutes at 37°C before a glucose solution (to make a final concentration of 1mM) was added. DNP inhibits all energy requiring cellular processes (including the active transport of glucose) by preventing the uptake of phosphates into the mitochondria thus inhibiting the production of adenosine triphosphate (ATP) during the oxidative phosphorylation process [100-102]. Sections of gut were then incubated at 37°C for an hour, before being cut open and their contents removed. Glucose concentrations were measured using a Glucose (gluc-pap) assay kit purchased from Randox.

In this assay kit glucose is enzymatically oxidised by glucose oxidase which forms hydrogen peroxide and gluconic acid. The hydrogen peroxide is reacted with phenol (using the catalysts peroxide and 4-aminophenazone) to form quinoneimine which is a violet dye. This violet colour was then be measured using an anthos 2020 plate reader at 500nm and a standard curve was be constructed (Figure 2.5). Detection was limited to a range between 0mMol/L and 1.3mMol/L of glucose.

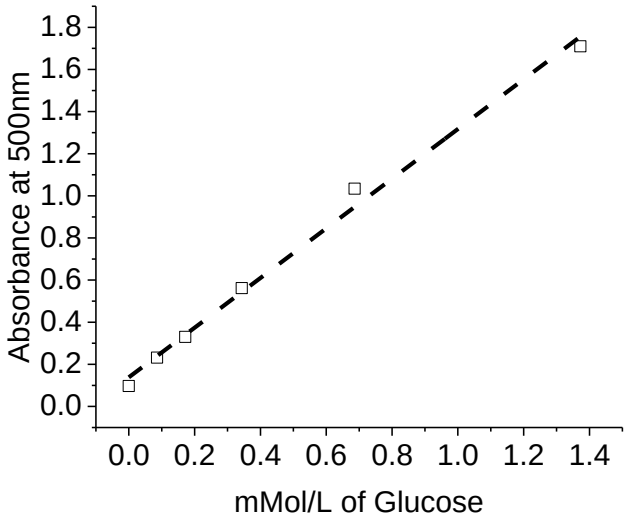

Figure 2-4 - Standard curve to calculate the concentration of glucose (using a gluc-pap assay kit). Equation of the line is y = 1.178X + 0.1384 and r^2 is 0.99

To measure the passage of silica through the gut wall, fluorescent silica was synthesised using the same method in section 2.2 except that PAH-FITC was used as the amine additive, thus creating fluorescent silica. Fluorescence was measured on a RF-530IPC fluorometer at the excitation wavelength of 495nm, and the emission wavelength of 515nm. A standard curve was constructed (Figure 2.6) so that fluorescence could be related to the concentration of silica. Detection was limited to a range between 0.001mg and 0.5mg of fluorescent silica. Tubes of inverted rat guts were incubated in 1 mg/ml silica solution (in Krebs) or 1mg/ml silica solution and 1mM DNP for an hour at 37^{o}C. Guts sections were then cut open and contents removed and the fluorescence measured.

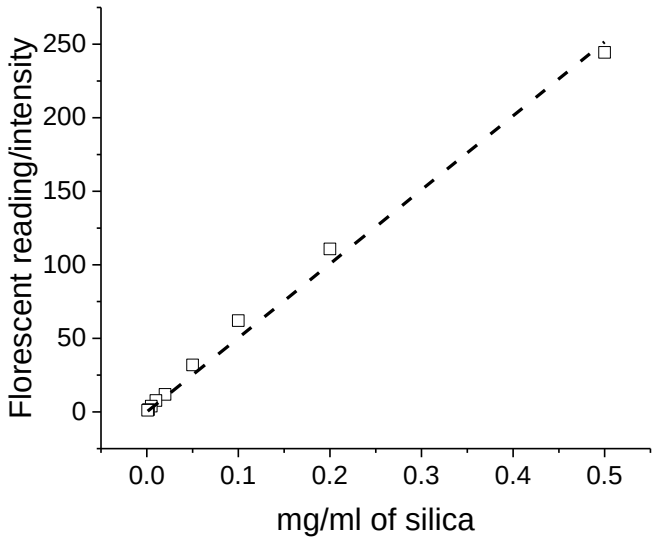

Figure 2-5 - Standard curve to calculate the concentration of fluorescent silica particles by measuring fluorescence. Equation of the line is y = 503.3X and r^2 is 0.99

2.8. Imaging rat gut sections

Sections of rat guts were preserved for imaging by submersion in a formalin solution (neutral buffered 10%) for half an hour followed by two PBS washes. The inside and outside surface of the gut sections were then imaged using a Carl Zeiss Axio Imager Z1 with 10x/0.30 lens. This further confirmed the movement of silica across the gut wall. Gut sections were mounted using two methods; either by stretching the gut and pinning the edges or by compressing gut sections under Immu-mount and a coverslip.

2.9. Haemolytic activity of silica

To measure the haemolytic activity of silica, male rats (Sprague Dawley) were bled and the blood was stabilised with heparin (100 µl of 1000 units ml^{-1}). 4ml of heparin

stabilised blood was diluted with 9ml of Dulbecco's PBS (D-PBS) and centrifuged at 2250g for 5 minutes. The supernatant was carefully removed and the blood washed five times with D-PBS. After the last wash, the red blood cells (RBC) were diluted with 40ml of D-PBS. 0.2ml of diluted RBC was then added to 0.8ml of silica suspension at the desired concentration to make a final silica suspension. Suspensions of BIS-PAH in D-PBS were made at concentrations of 12.5, 62.5, 125, 312.5 or 625 µg/ml to make final concentrations of 10, 50, 100, 252 or 500 µg/ml once mixed with RBC. Positive and negatives controls were set up by adding 0.2ml of RBS to either 0.8ml D-PBS (negative control) or 0.8ml of 0.2% Triton X-100 (positive control). All samples were prepared in triplicate and briefly vortexed before being left static at room temperature for 4 hours. Samples were then mixed gently again and centrifuged at 10,000g for 2 minutes. 10µl of supernatant was used to measure the absorbance of haemoglobin using an anthos2020 plate reader at 577nm with a reference wavelength of 655nm. Haemolysis was calculated as % haemolysis = [(sample absorbance – negative control)/(positive control – negative control)] X 100 [103].

2.10. Scanning electron microscopy (SEM)

Scanning electron microscopy (SEM) is a useful technique for imaging surfaces and particles with a resolution of ~10nm. Before imaging, the sample must be correctly prepared. Metals require no preparation since they already have the ability to conduct electricity. Non-metals are required to be sputter-coated (normally with gold) to create a thin layer of conductivity. The SEM works by firing a beam of highly concentrated electrons down the microscope and through a series of lenses to

direct the electrons towards the sample and maximise efficiency. With more electrons, a higher magnification can be achieved. This must all be carried out in a vacuum to avoid obstruction of the electron beam and impairment of the results. Once the electron beam (known as the incident beam) hits the sample, x-rays and three kinds of electrons are emitted from the sample; primary backscattered electrons, secondary back scattered electrons and Auger electrons. An electron recorder detects the deflected primary and secondary backscatter electrons and is able to translate the scattering into an image (micrograph) [104].

To image silica samples SEM was carried out using a Hitachi SU6600 field electron-SEM. Samples were mounted on sample holders using sticky carbon tape and then gold splutter coated under vacuum to prevent the charging of the sample. Micrographs were taken using a 20kV potential difference and a working distance of 8.7mm.

Chapter 3: Investigating the bio-inspired silica system for drug delivery applications using ibuprofen as a model drug molecule

The main aim of this research is to primarily understand *in situ* drug loading into BIS system. Specifically, we plan to determine predictive rules, investigate the effects of amine additive and drug interactions and silica chemistry on DDS performance (drug loading and release profiles). Further, in order to make BIS a viable DDS, it should exhibit similar or improved loading and release profiles for ibuprofen when compared to the competitor MCM-41 based DDS.

Ibuprofen was chosen since it is a commonly used model drug for DDS development due to its small molecular size (1.0 x 0.6 nm^2) [60], its stability [105], ease of detection (UV absorbance at ~220 nm), and available literature on ibuprofen-silica systems for comparison. Ibuprofen has been employed to act as a model drug for a whole range of applications using many different drug delivery systems, including liposomes [106-108], dendrimers [109-111], carbon nanoparticles [112], and of course silica [113-115]. There has been little published on the loading mechanics of the BIS system and it has been speculated, but not proven, that embedded amine, originally employed to facilitate silica condensation, also helps to functionalise the silica [35]. This chapter will show that the BIS system can be controlled using many factors such as the choice of amine additive, pH of synthesis, kinetics of synthesis and pH of release solution. This chapter will show that BIS has several advantages over MCM-41 (such as one step formulation, simple controllability and lack of hazardous chemicals) and it will show that BIS has similar or improved drug loading and release profiles to MCM-41. These benefits give BIS real potential as a viable DDS to be further investigated.

3.1 The effect of the amine additive on the loading and release of ibuprofen

The effect of the choice of amine additive for the synthesis of BIS upon its ability to load and release calcein (a non-pharmaceutically active but "drug-like" molecule) has previously been reported [35]. As these effects are drug specific, we investigated them for an active drug molecule (ibuprofen) in the BIS system and compared earlier results for calcein, with those for ibuprofen. As a reminder drug loading efficiency is defined as the % of available drug during synthesis which was loaded into the silica, drug content is defined by the % weight of drug in the silica-drug complex (i.e. mg of drug per mg of silica-drug complex), mass loaded is defined as the absolute mass of drug loaded into 10mg of silica. Release is expressed as the % of the total drug loaded into the silica which has been released from 10mg of silica during the experiment or by normalising the total drug release at 24 hours as "100%" (i.e. total amount of drug released over 24 hours).

In order to screen for the most suitable systems, four amine additives were investigated; three small amines and one polyamine. These were chosen based on their silica precipitation performance and previous investigations into BIS [31,35,77,87]. We measured the loading efficiency (% of drug which was loaded into the silica), drug content in the DDS (% weight of drug in the silica-drug complex) and total amount of drug released (mg drug released from 10 mg DDS). Diethylenetriamine (DETA), a small amine, was immediately excluded for use as it had a loading efficiency of only <5%, Figure 3.1. The other amines used were pentaethylenehexamine (PEHA), tetraehylenepentamine (TEPA)) and poly(allylamine hydrochloride) (PAH) and they exhibited loading efficiencies of 20-

30%, while MCM-41 showed ~40% loading efficiency (Figure 3.1). The differences in loading efficiency between BIS and MCM-41 are likely due to the different methods in which the drug was loaded. For BIS, ibuprofen was loaded *in situ* and so the drug would have been entrapped within the silica particles, followed by some surface physisorption. With MCM-41, only post-synthesis loading was possible and so drug loading was entirely reliant on physisorption (hence surface area and porosity are important in this system).

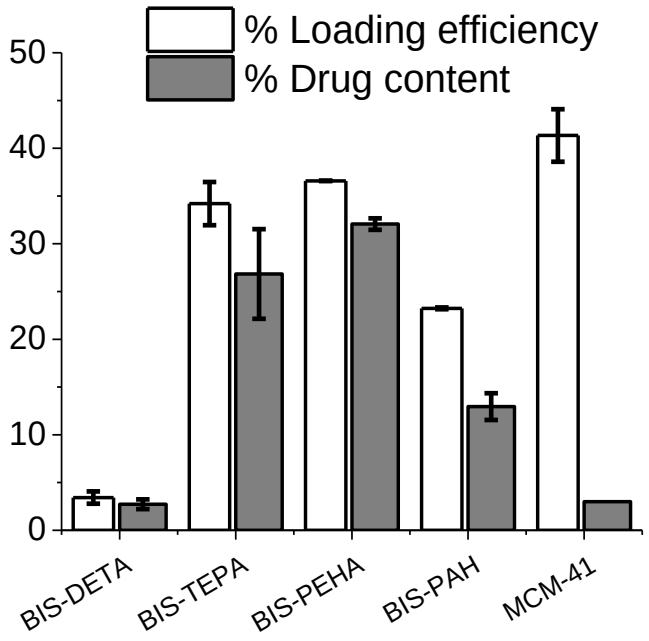

Figure 3-1 - BIS Synthesised with Different Amines, (A) % loading efficiency and % drug content (wt/wt) of ibuprofen into four different BIS and MCM-41 n=3, error bars represent one standard deviation

When the drug release was measured, despite having loading efficiencies similar to BIS-PAH, both BIS-TEPA and BIS-PEHA released <2% of loaded drug and as such these amines must also be discarded (Figure 3.2). Approximately 22% of loaded ibuprofen was released from BIS-PAH, compared to the 39% released from MCM-41 (Figure 3.2 and Table 3.1). The release data appeared to fit well using the

mathematical model shown in equation 2.1, with >0.9 R^2 values in all cases (Table 3.1). The fitting showed that BIS-DETA, BIS-TEPA and BIS-PEHA all had a very low release rate (Figure 3.2). The rates of release (Table 3.1) from MCM-41 and BIS-PAH were similar (15 and 17% per hour respectively). Figure 3.2 C shows the data presented in figure 3.2A, but normalised to 100% (i.e. 100% is calculated as the total mass of drug released from each sample after 24hours). Presenting the data like this highlights any differences in release profiles. In the data shown in figure 3.2C, the BIS profiles are all similar to MCM-41, suggesting that a similar release mechanism is taking place (i.e. only surface bound drug is being released from the different BIS systems).

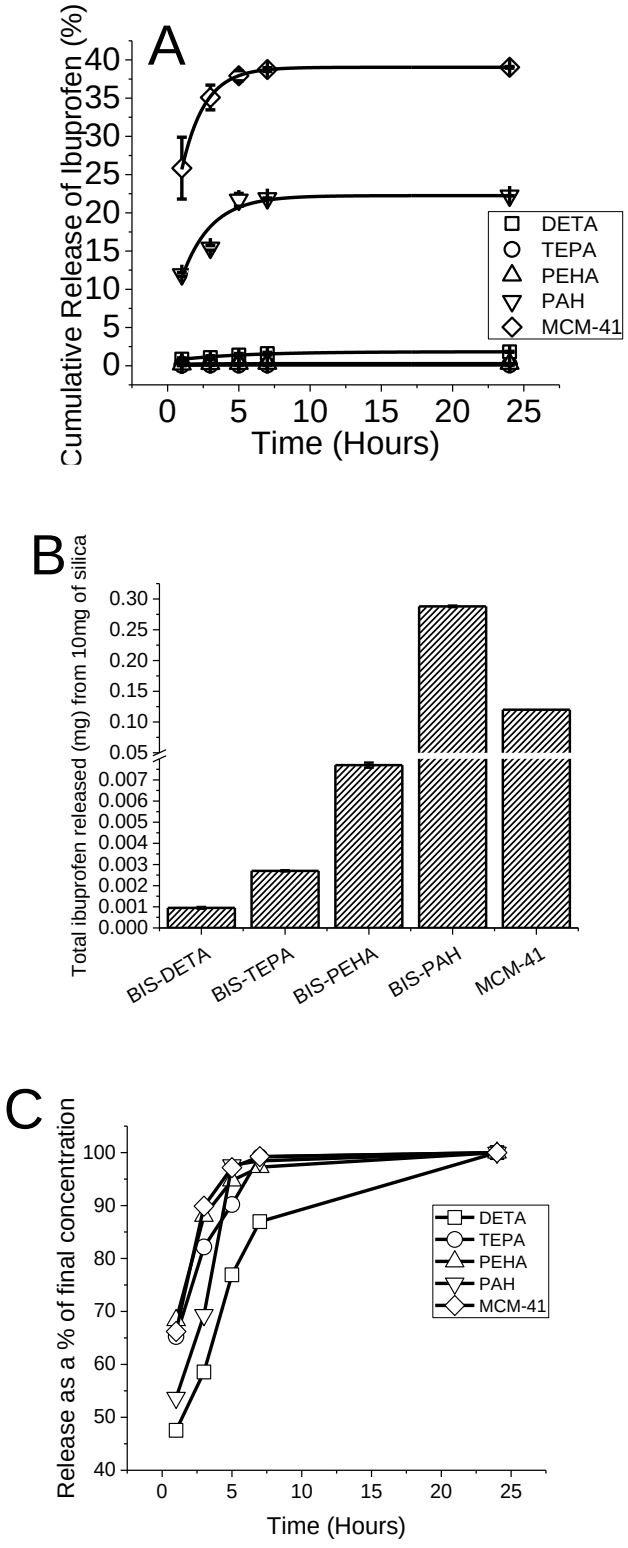

Figure 3-2 - BIS Synthesised with Different Amines (A) The % release of loaded ibuprofen from four different BIS and MCM-41 (data fitted using equation 2.1), (B) Total mass of ibuprofen (mg) released from 10mg of silica sample, (C) Release of loaded ibuprofen expressed as a % of final concentration released from BIS synthesised with different amines and MCM-41. n=3, error bars represent one standard deviation.

Table 3-1 - : Results of silica yield and of mathematical fitting (using equation 2.1) of release data presented in Figure 3-2

DDS	Silica produced (mg)	Yield (%)	Ibuprofen loaded (mg/10mg of silica)	Ibuprofen loading efficiency (%)	Max. Release (% h^{-1})	R^2	Total ibuprofen released (mg)*	Total ibuprofen released (% of loaded)
BIS-DETA	61	67	0.27	3.42	0.24	0.985	9.5×10^{-4}	1.83
DIS-TEPA	47	52	2.68	34.20	0.018	0.921	2.7×10^{-3}	0.10
BIS-PEHA	44	49	3.20	36.58	0.037	0.985	7.7×10^{-3}	0.28
BIS-PAH	79	88	1.29	23.23	17.26	0.913	0.288	22.23
MCM-41	N/A	N/A	0.33	41.34	15.46	0.998	0.12	39.03

*from 10mg of silica

The drug content on MCM-41 was found to be ~3 wt. %, while the drug content for BIS-PAH was ~13 wt. % (Figure 3.1). Despite this, MCM-41 released around half the amount of drug when compared to BIS-PAH (0.12mg compared to 0.28mg for 10 mg DDS, respectively). Doses of ibuprofen are normally administered in 400, 600 or 800mg tablets [116]. At the drug content shown in Figure 3.1 for BIS-PAH and MCM-41, a patient would have to consume 14g or 33g respectively to get a 400mg dose of ibuprofen. This is an impractical amount of silica to consume but the aim of this chapter is to first understand the mechanics of the BIS system so that it can be improved to load and release pharmaceutically relevant doses. The drug content also highlights a key benefit of using BIS over MCM-41, high doses of MCM-41 silica can result in serious toxicity issues unlike BIS [35,103]. The loading mass and % efficiency for MCM-41 (figure 3.1, 3.2 and table 3.1) may at first to be contradictory, however this is due to a difference in loading methods and the

maximum loading mass between the BIS and MCM-41. While the concentrations being loaded were the same (1mg/ml), the volumes were significantly different. BIS was synthesised in a 50ml batch, meaning that at 1mg/ml, there was 50mg of drug available to be loaded into BIS. MCM-41 on the other hand required post synthesis loading. All experiments measured the loading and release from 10mg of silica and so 10mg of MCM-41 was loaded by immersion in 1.4ml of 1.mg.ml drug, meaning that there was a maximum of 1.4mg drug available to be loaded. The loading mechanism for MCM-41 (and for BIS) is not optimal (a higher concentration of drug would increase the diffusion pressure for drug loading) and should be improved in the future.

The differences in release profiles between BIS synthesised with the different amines could potentially be attributed to a variety of factors. The lack of drug release may be because of drug crystallising upon the surface of the silica. Ibuprofen bound in MCM-41 may be amorphous and hydrogen-bonding with free silanol groups on the MCM-41 pore walls, whereas ibuprofen loaded into BIS becomes crystalline. This crystalline drug will form due to its hydrophobic nature and not be readily released form the silica surface. If the drug was amorphous rapid drug release would be observed. Further investigations would be required to verify this idea. To determine the phase of the drug and its location on or within the silica techniques such as differential scanning calorimetry (DSC) or X-ray diffraction (XRD) could be employed. DSC is able to detect phase transitions of a compound as the sample is headed up and XRD is able to identify the atomic and molecular structure of a crystal. By employing these techniques one could determine the

location and the phase of the drug molecule, thus determining if it is the hydrophobic drug crystallising on the BIS surface which is inhibiting release.

Other possible explanations for the differences in release profiles could be attributed to the porosity and morphology characteristics of the silica synthesised (Figure 3.3). In the case of MCM-41 (a mesoporous silica), it is generally accepted that porosity is a major factor in controlling the release of drugs (see chapter 1.5), and so further investigation was needed as to whether this was the case for BIS [35,117-119]. BIS and MCM-41 display a different type of adsorption isotherm which highlights the differences in porosity. Adsorption isotherms shown in appendix 2 show that all BIS display a type II adsorption isotherm which suggests a non-porous material, this is supported by the pore size distribution (figure 3.3). MCM-41 displays a type IV adsorption isotherm which suggests mesoporous, which was expected for this type of MSN. BIS-DETA, TEPA and PEHA all have a very small pore volume (~0.1 cm^3/g) and low surface areas (~20-40 m^2/g), see figure 3.3. The pore volume and surface area for BIS-PAH (0.74 cm^3/g and of 129 $m^{2/}g$ respectively) were higher than that of BIS synthesised with the other three amines. Silica particles synthesised with any of the small amines were dense when compared to BIS-PAH, which may explain the higher release from BIS-PAH within the BIS series. Interestingly, MCM-41 has a much larger surface area (989 m^2/g) than any of the BIS, but it demonstrated loading efficiency comparable with BIS-PAH.

A Common sizing technique, dynamic light scattering, was deemed inappropriate for sizing the BIS particles due to their deposition out of solution. This means that an accurate particle size could not be obtained through this technique (data not shown). SEM was chosen instead to measure the sizes of the particles. This method

may still not give a fully accurate picture of the sizes of the particles due to the aggregation of silica particles commonly occurring. Scanning electron microscopy (SEM) revealed that BIS-PAH particles were fairly uniform in shape and sizes, without and with the presence of drug (72±17 nm and 78±18 nm, Figure 3.4 and 3.5), thus suggesting that the presence of the drug did not affect the particle sizes significantly. On the other hand, MCM-41 samples used herein were not only very large in comparison (3340±1013 nm, Figure 3.4 and 3.5) but also non-uniform with large variations in sizes and shapes. The BIS particles measured are likely primary particles which will aggregate together to form larger particles. When MCM-41 was measured using the SEM image, it likely that large silica aggregates were being measured, since the primary particles could not be clearly observed (this explains the large variance in sizes). At this point in time, a direct comparison between these two DDS is not possible simply based on SEM results because of their distinctly different drug loading mechanisms and further analysis in future is necessary. Due to BIS and MSN both being precipitated silica, the particles aggregate and sediment out of solution. This has important ramifications for the loading and release profiles, the ability to size the particles and the particles level of biocompatibility. The way BIS aggregates together could also provide a reason for the differences in drug release from BIS synthesised with monoamines (DETA, TEPA and PEHA) when compared to BIS-PAH. As show in in figure 3.6, small amines may result in a more close packed aggregation of BIS. This creates a non-porous aggregate and prevents embedded and surface bound drug from being released. When BIS is synthesised with a longer amine (i.e. PAH), this may create a more open aggregate structure, linking the individual silica particles together but allowing for space between to

allow for drug release (a schematic of this is shown in figure 3.6). This idea requires further investigation to prove, however previous work has observed an "increasingly open structure" when BIS was synthesised using larger amines, which provides some evidence to support this idea [120].

Despite the variance in sizes the comparison between BIS and MCM-41 is still valid and important. In all drug release experiments the mass of silica remained constant and drug release was often comparable between MCM-41 and BIS. Previous studies have shown that particle size does not have any impact on release data but rather pore morphology is more important [121,122].

A

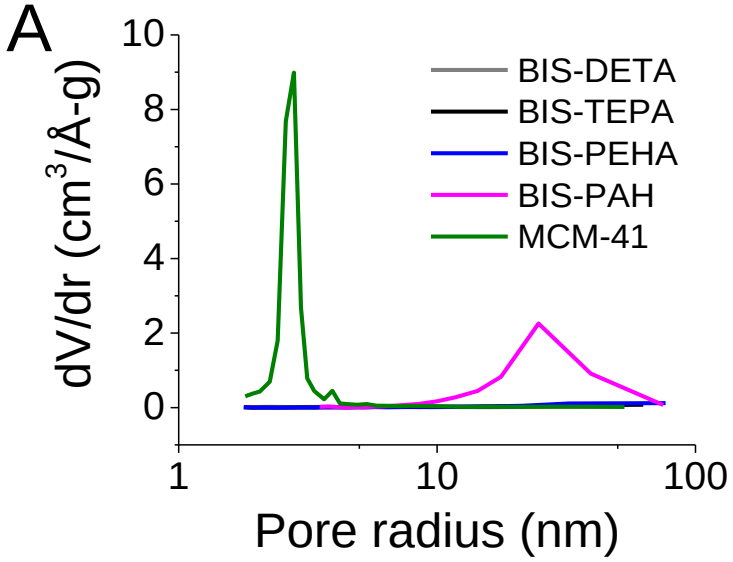

B	Surface area (m^2/g)	Pore volume (cm^3/g)	Pore size (nm)
BIS-DETA	16	0.095	*
BIS-TEPA	33	0.095	*
BIS-PEHA	36	0.131	*
BIS-PAH	129	0.91	23
MCM-41	983	0.74	2

Figure 3-3 – (A) Pore size distribution of four different BIS and MCM-41, (B) Surface area, pore volume and pore size figures for four different BIS and MCM-41 (* due to broad pore size distributions, specific pore sizes are not applicable) n=1

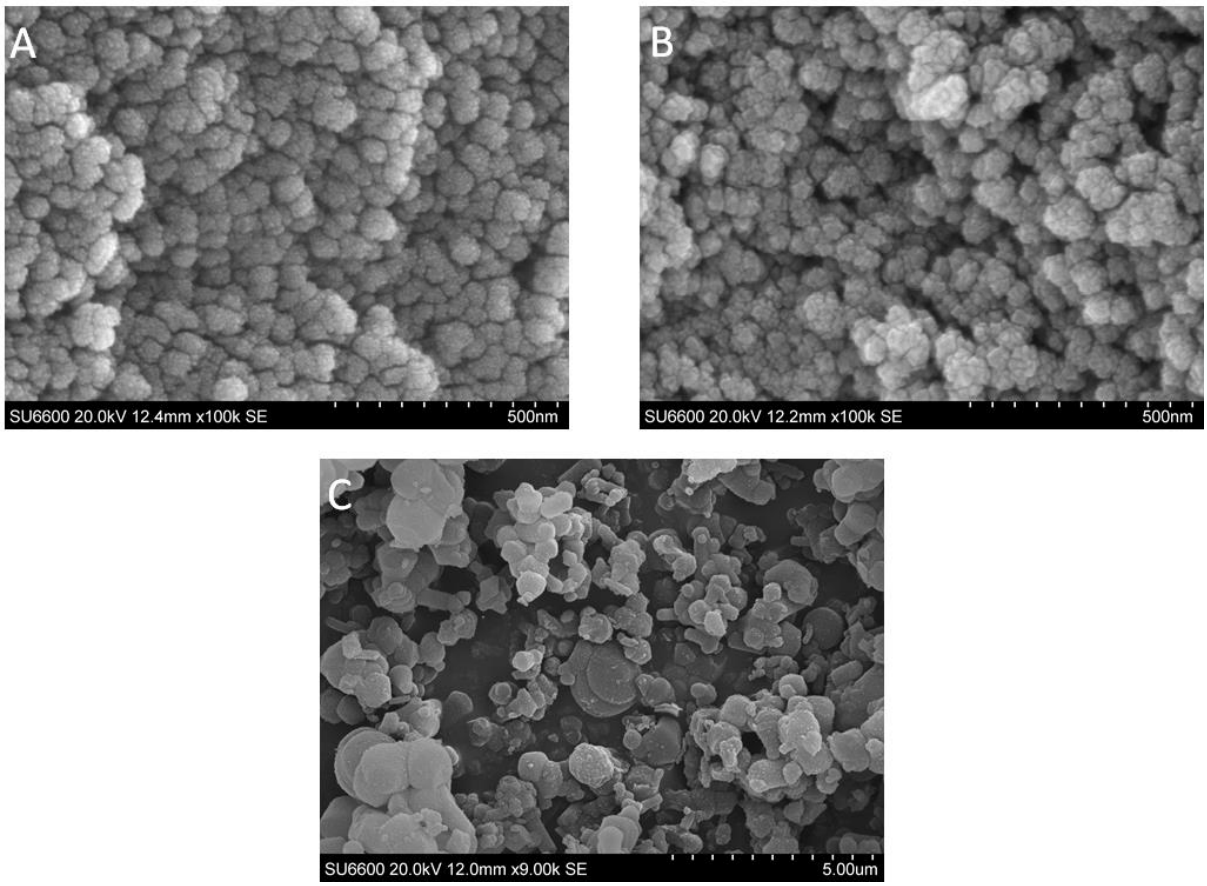

Figure 3-4 SEM images of (A) BIS-PAH, (B) Ibuprofen loaded BIS-PAH, and (C) MCM-41

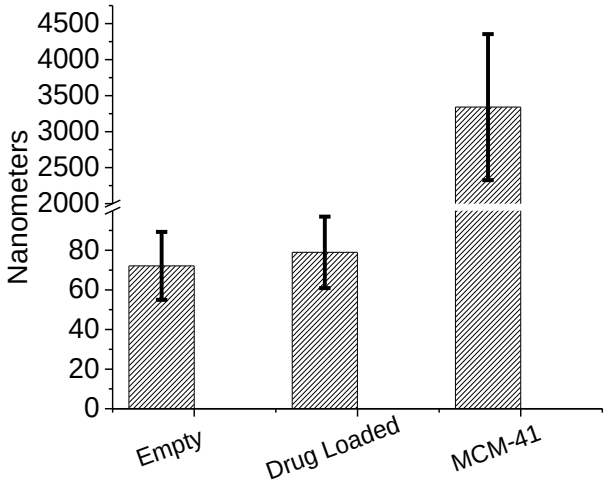

Figure 3-5 - Average size of different BIS-PAH particles (empty and ibuprofen loaded) and MCM-41 measured via SEM images. Average and standard deviation error bars were calculated from one image (Figure 3-4)

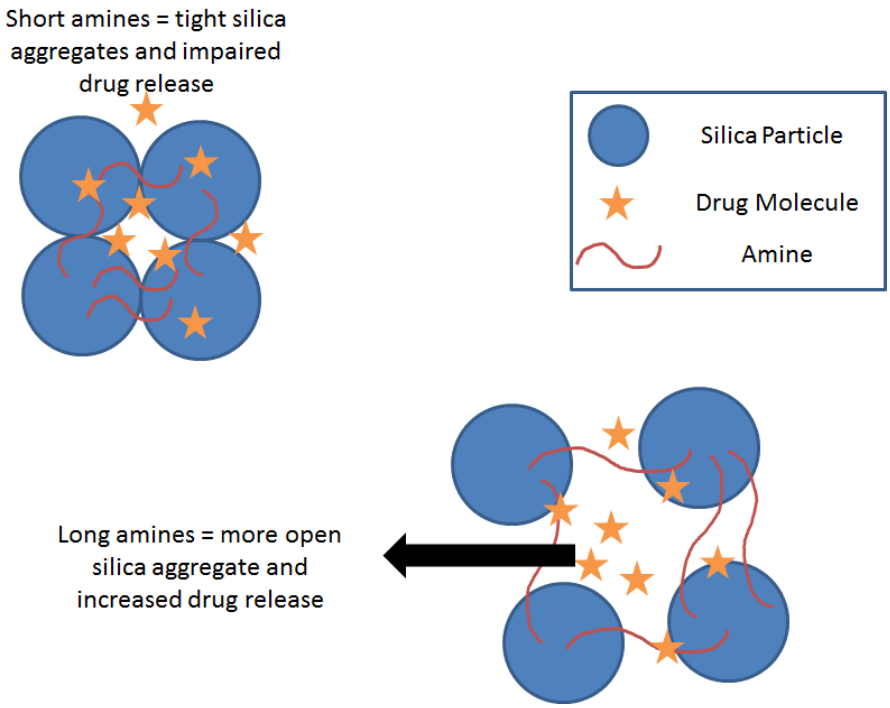

Figure 3-6 :- Schematic of the effect of amine on BIS aggregation. Where short amines result in a tight silica aggregate which traps drug molecules and longer amines result in a more open silica aggregate structure, allowing for increased drug release.

Along with porosity altering the release of ibuprofen, it has been reported that amine-ibuprofen interaction is important in loading [35,123,124]. Since BIS-TEPA and BIS-PEHA showed over 30% drug loading efficiency, it is possible that the amine additives facilitate ibuprofen loading through favourable amine-drug interactions as reported elsewhere [119,123-125], but they also form non-porous silica by fully encapsulating ibuprofen within the dense silica particles thus resulting in no release. BIS-PAH, however, allows ibuprofen loading through favourable interactions with amine groups and release occurs through the silica pores. These observations are consistent with the literature where it has been reported that these small amines lead to the formation of dense and non-porous silica, while PAH forms porous silica [77,87].

3.2. Altering reactant concentrations to understand the silica-drug system

The main aim here is to understand BIS and investigate how controllable it is with ibuprofen so that this knowledge can be implemented for other drugs. As such, our next step was to study the effects of reaction chemistry on BIS performance as a DDS. There has been evidence that altering reactant concentrations can alter the loading and release profiles of calcein from BIS synthesised with PAH [35]; however, the reasons behind this effect were not fully investigated. Therefore, a systematic approach by varying synthesis conditions and evaluating their effects on drug loading and release has been taken while keeping the starting concentration of ibuprofen in the reaction mixture constant (1 mg ml^{-1}).

Figure 3.7 and Table 3.2 show that for MCM-41 (as reported in section 3.1), the loading efficiency was ~40% and the drug content was ~3 wt%. The loading efficiency and drug content for the 1:1 BIS-PAH sample (30mM solution of sodium metasilicate and a 1mg ml^{-1} solution of PAH) were ~22% and 13 wt%. When the concentrations of silicate and PAH were doubled (2:2) there was a doubling of ibuprofen loading efficiency (Figure 3.7). This was attributed simply to more silica being formed (Table 3.2) since the drug content did not change (Figure 3.7). When only the silicate concentration was increased but the PAH concentration was kept at 1mg ml^{-1} (2:1), there was a slight increase in ibuprofen loading efficiency (Figure 3.6) but drug content remained constant and so increased loading was again attributed to an increased silica yield (Table 3.2). Producing more silica means that more ibuprofen was loaded (and so less was wasted by being left in the reaction mixture).

Interestingly, when a synthesis ratio of 1:2 (increasing PAH concentration but maintaining silicate concentration) was investigated, drug loading efficiency increased three fold to 75% from the 1:1 sample (Figure 3.8). The loading efficiency for 1:2 was significantly higher than that found for MCM-41 (~40%), despite a significantly lower silica yield (Table 3.2). The drug content also increased substantially from ~10% for 1:1 to ~70% for 1:2. This is likely due to a drug-amine interaction, suggesting that the amine can have a dual function of facilitating silica condensation as well as acting as a functionalisation agent to facilitate drug loading (see section 3.3 for further discussion). These loading studies highlight that the synthetic conditions can readily modulate the loading efficiency of BIS and even reach loadings that are significantly higher than what is achievable with MCM-1.

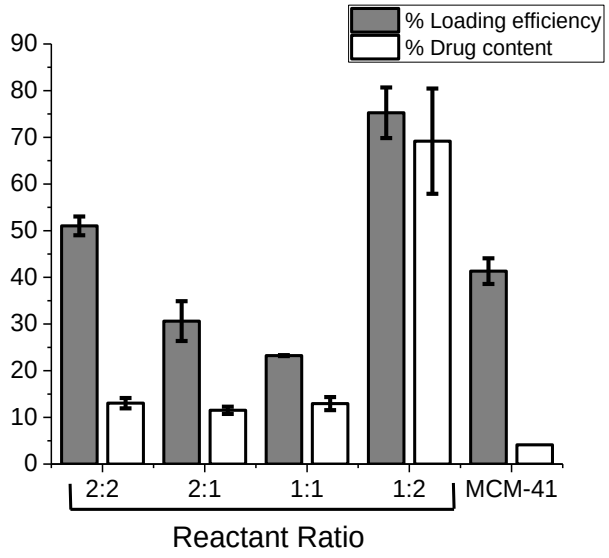

Figure 3-7- Effect of reactant concentrations on the % loading efficiency and % drug content (wt/wt) of ibuprofen into BIS synthesised with different reactant ratios and MCM-41 , n=3, error bars represent one standard deviation.

Table 3-2: - Results of silica yield and of mathematical fitting (using equation 2.1) of release data presented in Figure 3.6

DDS	**Silica produced** (mg)	**Yield** (%)	**Ibuprofen loaded** (mg/10mg of silica)	**Ibuprofen loading efficiency** (%)	**Max. Release** (% h^{-1})	**R^2**	**Total ibuprofen released** (mg)*	**Total ibuprofen released** (% of loaded)
2:2	172	95	1.30	51.02	18.65	0.996	0.62	45.40
2:1	105	58	1.15	30.63	24.01	0.99	0.63	50.27
1:1	79	88	1.29	23.23	17.26	0.913	0.288	22.23
1:2	22	25	6.91	75.26	3.38	0.996	0.41	6.06
MCM-41	N/A	N/A	0.33	41.34	15.46	0.998	0.12	39.03

* from 10mg of silica

When the release of ibuprofen from these samples was investigated and it was found that the overall release of ibuprofen varied greatly. BIS-PAH (1:1) released 22% of the loaded ibuprofen and 2:2 and 2:1 both achieved higher releases (45% and 50% respectively), which were greater than the 39% released from MCM-41 (Figure 3.8). It is possible that release was higher from 2:2 and 2:1 than 1:1 due to faster silica condensation since the silica precursor concentration used was doubled [46]. This resulted in lower pore volumes and smaller pores (Figure 3.9), leading to less drug being entrapped within the silica, leaving more drug surface bound, making release easier. In contrast, 1:2 ratio released only 6% of loaded ibuprofen (Figure 3.8), despite a very high loading efficiency and a larger pore size (Figure 3.7 & 3.9).

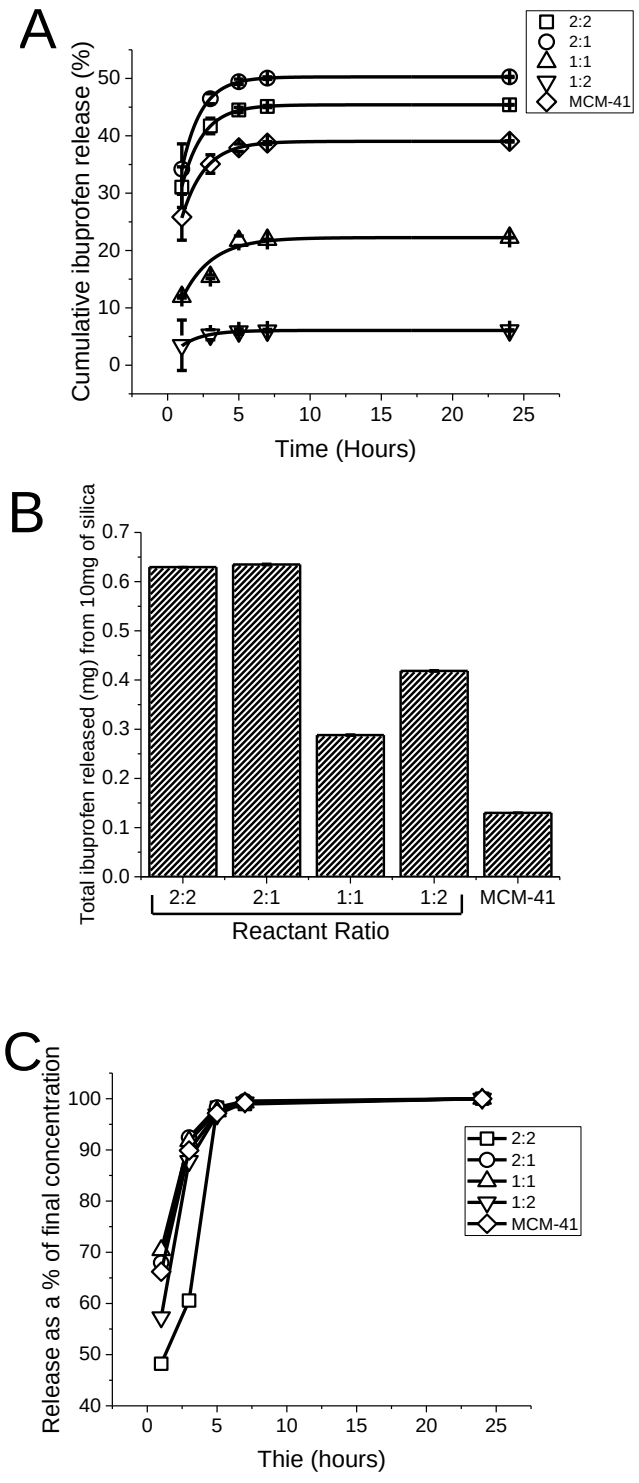

Figure 3-8 - Effect of reactant ratios on the release of ibuprofen (A) The % release of loaded ibuprofen from BIS synthesised with different reactant ratios, and MCM-1, data fitted using equation 2.1 ,(B) Total mass of ibuprofen (mg) released from 10mg of silica sample, (C) Release of loaded ibuprofen expressed as a % of final concentration released from BIS synthesised with different reactant ratios, and MCM-41. n=3, error bars represent one standard deviation.

A

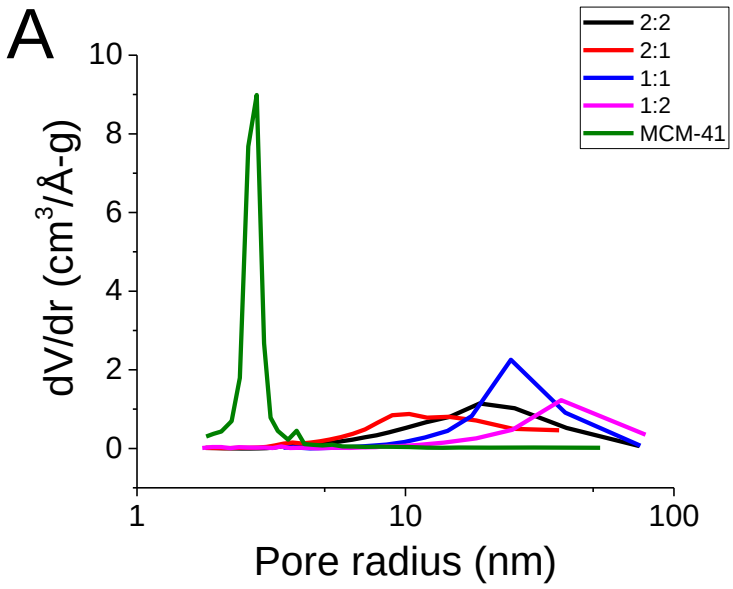

B	Surface area (m^2/g)	Pore volume (cm^3/g)	Pore size (nm)
2:2	157	0.73	15.9
2:1	180	0.531	11.3
1:1	129	0.91	23
1:2	76	0.69	28.94
MCM-41	983	0.74	2

Figure 3-9 – (A) Pore size distribution of BIS synthesised with different reactant concentrations and MCM-41, n=1 (B) Surface area, pore volume and pore size figures for BIS synthesised with different reactant concentrations, and MCM-41

Figure 3.8 C shows the data presented in figure 3.8A, but normalised to 100% (i.e. 100% is calculated as the total mass of drug released from each sample after 24hours) in order to highlight any differences in release profiles. When the release profiles were considered (Figure 3.7C), all but 1:2 samples exhibited burst release, where the majority of drug was released over the first five hours and very little release was observed after this point (Table 3.2). This suggests that the ibuprofen

that is able to escape is mainly surface bound and any ibuprofen embedded within the silica particles is trapped and unable to be released. This idea is supported by Figure 3.7C where all the BIS release profiles were similar to the release profile of MCM-41, which only had surface bound ibuprofen loaded. However, the 1:2 system had a much lower maximum release rate than the other systems (Table 3.2) as well as low total release (Figure 3.8). Table 3.2 also shows that the mass of ibuprofen released from all the BIS systems were higher than from MCM-41, some BIS samples releasing 5x more drug per weight of silica than MCM-41. This is important since if more mg of drug is released then less silica will need to be administered to a patient.

3.3. Understanding additive-drug interactions to control DDS formulation

Ibuprofen contains a carboxylic acid group, which is expected to interact with amines. Several studies have exploited these favourable amine-ibuprofen interactions by post-synthetically functionalising MSN [119,123-125]. In addition, from the results presented above, there was an indication that the PAH-ibuprofen interactions are important for the drug loading and release. Therefore, we investigated whether drug loading and release could be controlled by tuning PAH-ibuprofen interactions by varying the synthesis pH (and in turn the protonation). In this study silica was usually formed at pH 7 since silica formation is the quickest at neutral pH for this synthesis method [35,46]. BIS will not readily form outside the pH ranges shown (pH 5-9), hence we have focused on exploring drug loading under this

pH range and monitored the effect of formulation pH on the drug release (Figure 3.10).

When silica was condensed at pH ≥7, the loading efficiency was not altered (remaining at ~20%, Figure 3.10). When synthesis pH was more acidic, on the other hand, ibuprofen loading efficiency could be enhanced up to three times, to 60%, at pH 5. A similar picture was observed for the drug content (wt. %) shown in Figure 3.10.

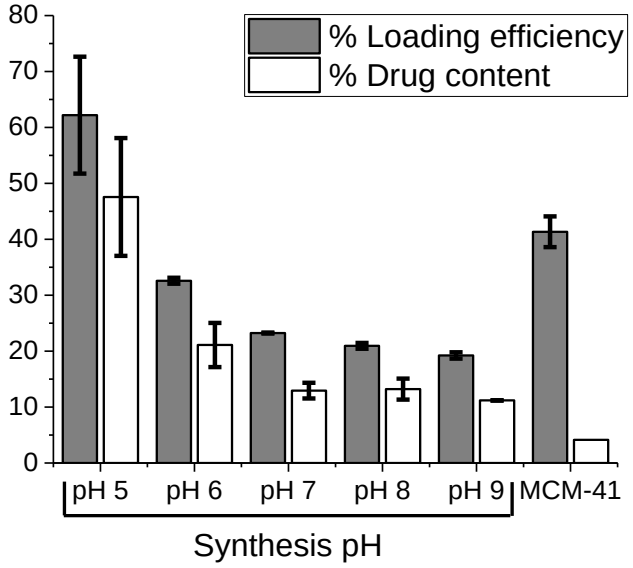

Figure 3-10 - Effect of reaction pH on the % loading efficiency and % drug content (wt/wt) of ibuprofen into BIS synthesised at different pH, and MCM-41 n=3, error bars represent one standard deviation

The % drug release for samples formulated at pH ≤7 were similar (Figure 3.11 & Table 3.3), whereas DDS formulated at pH ≥7 had greatly diminished release. It should be noted that all release experiments were carried out in PBS at pH 7.2. Interestingly, despite the higher drug loading at pH5, there was not a

correspondingly higher % release observed when compared with DDS formulated at pH7 (Figure 3.11). Despite this, the total ibuprofen (mg) released per weight of silica was 10 times higher for the pH 5 sample than MCM-41 (Figure 3.11).

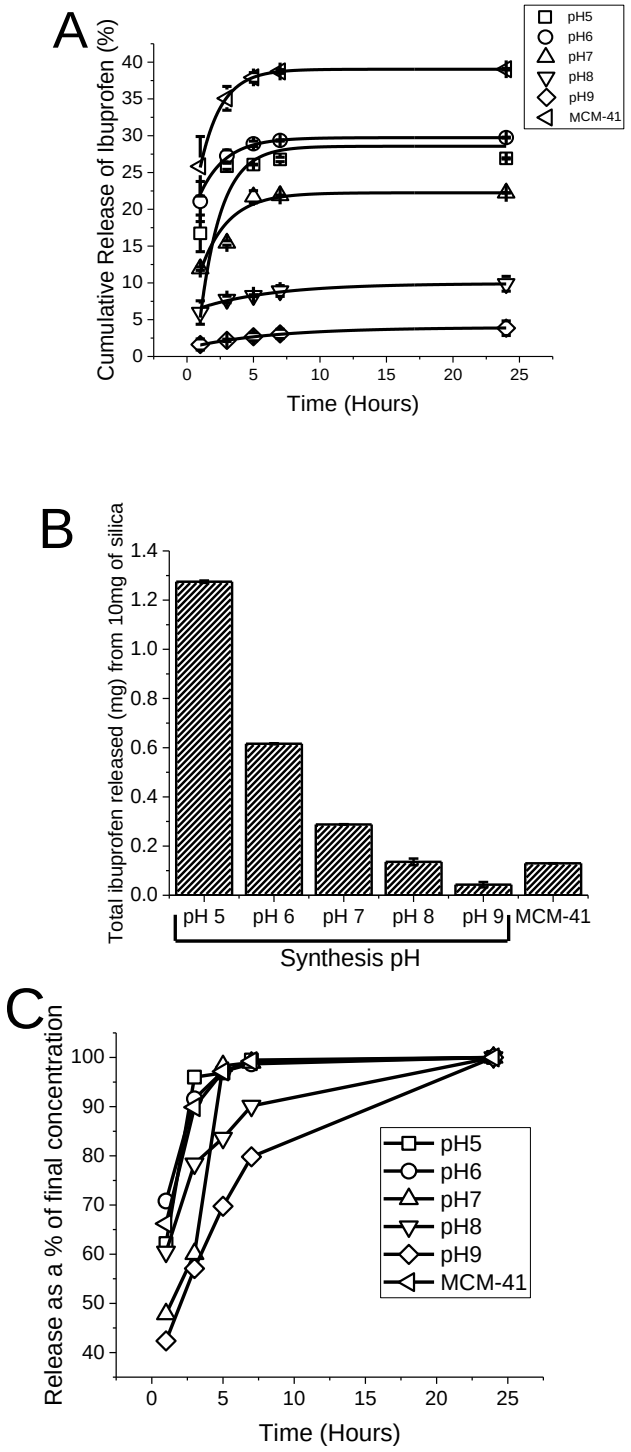

Figure 3-11 – Effect of reaction pH on the release of ibuprofen (A) The % release of loaded ibuprofen from BIS synthesised at different pH and MCM-1, data fitted using equation 2.1, (B) Total mass of ibuprofen (mg) released from 10mg of silica sample, (C) Release of loaded ibuprofen expressed as a % of final concentration released from BIS synthesised at different pH and MCM-41. n=3, error bars represent one standard deviation.

Table 3-3 - Results of silica yield and of mathematical fitting (using equation 2.1) of release data presented in Figure 3-10

Sample	**Silica produced** (mg)	**Yield** (%)	**Ibuprofen loaded** (mg/10mg of silica)	**Ibuprofen loading efficiency** (%)	**Max. Release rate** (% h^{-1})	**R^2**	**Total ibuprofen released** (mg)*	**Total ibuprofen released** (% of loaded)
pH 5	34	38	4.75	62.19	2.83	0.802	1.27	26.91
pH 6	62	69	2.11	32.59	6.53	0.971	0.61	29.73
pH 7	79	88	1.29	23.23	17.26	0.913	0.288	22.23
pH 8	69	77	1.32	20.94	0.67	0.900	0.13	9.91
pH 9	72	80	1.11	19.22	0.417	0.993	0.04	3.93
MCM-41	N/A	N/A	0.33	41.34	15.46	0.998	0.12	39.03

* from 10mg of silica

Figure 3.11 C shows the data presented in figure 3.10A, but normalised to 100% (i.e. 100% is calculated as the total mass of drug released from each sample after 24hours) in order to highlight any differences in release profiles. When release was plotted as a fraction of total release over time, two different release profiles became apparent (Figure 3.11). BIS-PAH synthesised at pH ≤7 exhibited similar burst release profile observed for BIS samples reported above (also evident from high release rates, Table 3.3), where the majority of ibuprofen was released from the silica in the first 5 hours and very little was released after this. This burst release profile was similar to that seen for MCM-41, suggesting that the main mechanism for release in these systems was release from the surface. However, silica synthesised at pH >7 appeared to have a slow and sustained release profile, which also reflected in slow release rates (Table 3.3). Release did not plateau for 24 hours and ibuprofen maintained a slow release over the course of the experiment. This slow release suggested that the loaded ibuprofen was embedded within the silica rather than bound to the surface, making release more prolonged. While the total amount of

ibuprofen released from these samples under the 24 hour observation window was low, this system does show some promise as a prolonged release system.

It is clear from the results presented about the DDS formulation that pH was able to control the loading and release of ibuprofen. The reason for these differences could be attributed to differences in porosity, morphology and/or additive-drug interaction. We explored these possibilities as discussed next. SEM results suggested that pH did not have a significant effect on the morphology or the particle sizes of DDS (Figure 3.12). When surface area and pore volume were measured for BIS-PAH DDS formulated at different pH conditions, there were no significant differences observed (Figure 3.13).

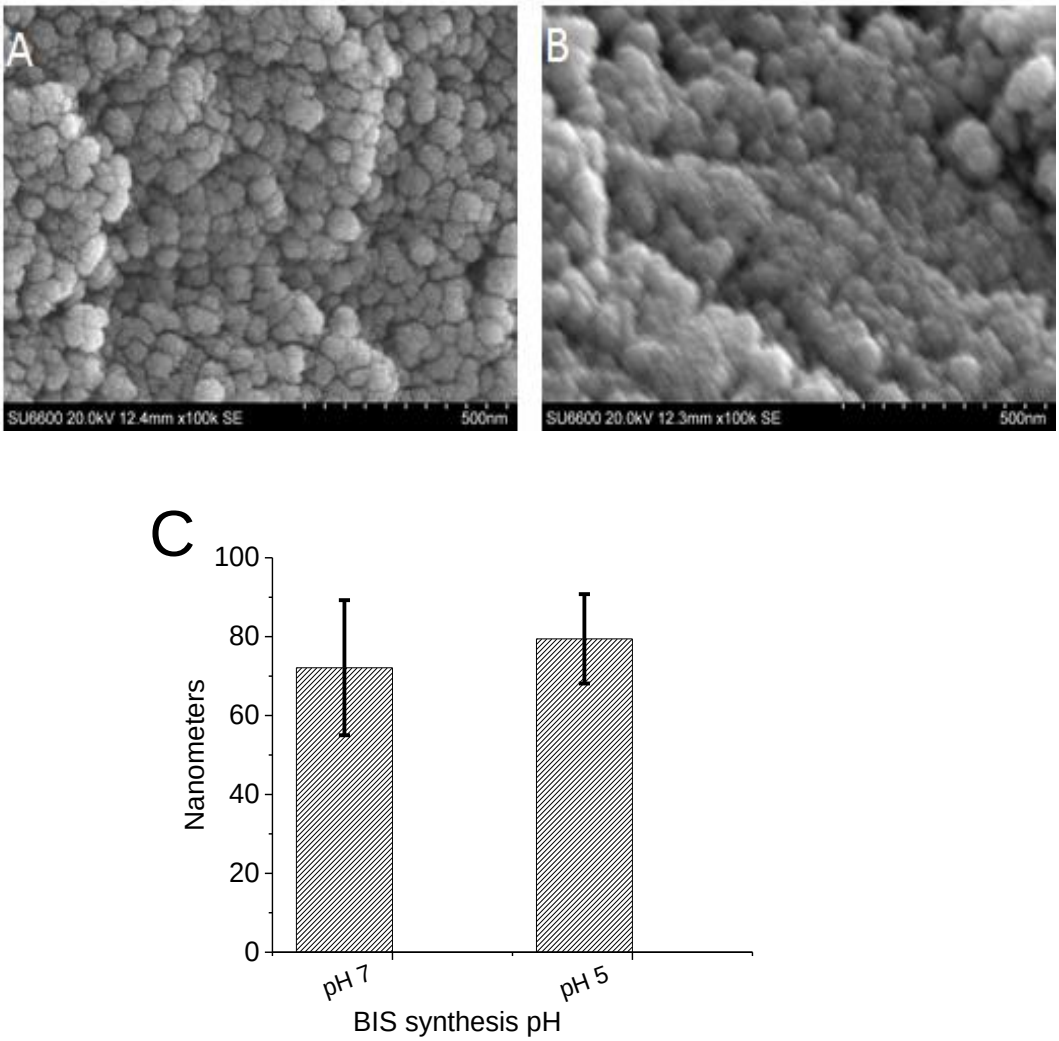

Figure 3-12 - (A) SEM image of BIS-PAH synthesised at pH 7 (B) SEM images of BIS-PAH synthesised at pH 5 (C) Average size of different BIS-PAH particles (synthesised at pH 7 or pH 5) measured via SEM images. Average and standard deviation error bars were calculated from one image (Figure 3-4)

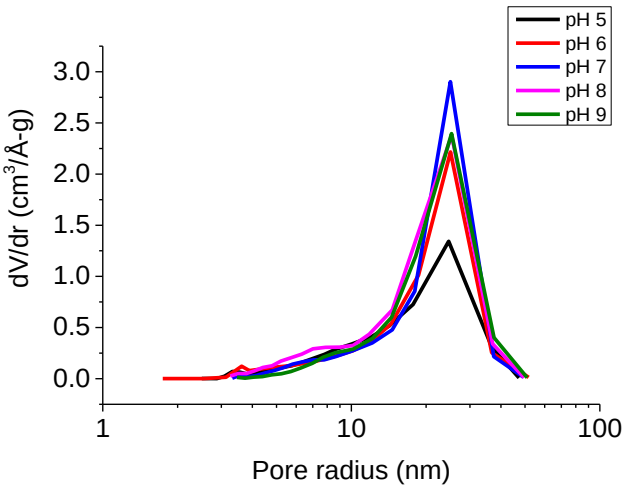

B	**Surface area** (m^2/g)	**Pore volume** (cm^3/g)	**Pore size** (nm)
5	142	0.60	21
6	149	0.67	21
7	129	0.91	23
8	161	0.84	25
9	140	0.68	25

Figure 3-13 - (A) Pore size distribution of BIS synthesised at different pH and MCM-41, n=1 (B) Surface area, pore volume and pore size figures for BIS synthesised at different pH and MCM-41

The differences in ibuprofen loading in these systems could be attributed to the ionisation of the three components present (silica, amine additive and drug) in the reaction mixture, as well as the silica formation pathways. A scheme showing how the proportions of ionised reactants vary as the reactant pH is altered can be seen in Figure 3.14 and Table 3.4. The results here suggest that the negative charge on silica can have an inhibitory effect on loading efficiency. Both the silica surface and ibuprofen are negatively charged at pH ≥7 (table 3.14) and so silica and drug will repel one another, thus explaining low loading efficiencies at pH ≥7 (only ~20% of

ibuprofen was loaded under these conditions, Figure 3.10 and Table 3.3). For DDS formulations occurring under acidic conditions, and particularly at pH5, the silica and ibuprofen are both significantly less charged, thus allowing for ibuprofen to be more efficiently loaded (30-60% of ibuprofen was loaded under acidic conditions, Figure 3.10 and Table 3.3).

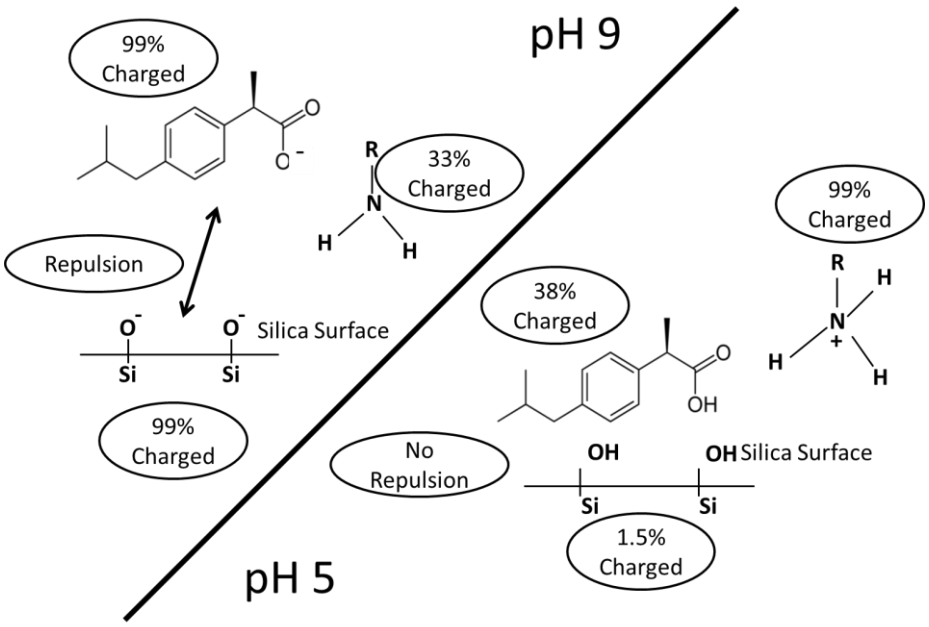

Figure 3-14 - Scheme to illustrate the differences in charge of silica, amine and ibuprofen during synthesis at pH ranging from 9 to 5.

Table 3-4 - Percentage ionisation of the three relevant species involved during the synthesis of BIS at various pH

pH	% Ibuprofen negatively ionised (pKa 5.2)	% PAH positively ionised (pKa 8.7)	% Silica negatively ionised (pKa 6.8)
5	38	99.9	1.5
6	86	99.9	13
7	98	98	61
8	99	83	94
9	99	33	99

It is clear that pH has a drastic effect on the loading efficiency of ibuprofen into BIS, with more acidic conditions resulting in increased loading. There is also strong evidence of an amine-drug interaction playing a major role in the ability of BIS to load drug. This interaction, when too strong, can also inhibit drug release.

3.4. Investigating the release of ibuprofen from BIS under different pH

Finally, a brief experiment was carried out which investigated release pH. BIS-PAH 2:2 (chapter 3.2) was used and the release of ibuprofen measured under different pH conditions. PBS was used for pH 7 (as described in chapter 3.2), for pH 1, 1M HCl was used and pH 2 and 5 were obtained by diluting HCl with dH_2O. These pH values were chosen to mimic the pH a DDS would be exposed to during its journey through the digestive system, from pH 1 in the stomach, to the increasingly neutral pH in the intestines.

As stated before for the BIS-PAH 2:2 sample the loading efficiency was 51% and the drug content was 13% (Figure 3.7). Interestingly at pH 1 and 3 there was a release of 15-20% over a 24 hour period with similar amounts of drug being released (0.31 mg and 0.32 mg respectively) (Figure 3.15 and Table 3.5). When pH rose to pH 5 there was a significant decrease in release (reaching only 4.5% and 0.06 mg released). When pH was increased to pH 7, the release rose to 45% and 0.43 mg

While there is a significant amount of drug released at pH 1 and 3, the rate is lower than at pH 7 (Figure 3.15 and Table 3.5). This would decrease the amount of drug being released in the stomach (food is only in the stomach for 2-5 hours [126]), before reaching the more neutral parts of the intestine, where most absorption occurs (food can be in the intestine for up to 40 hours [126]).

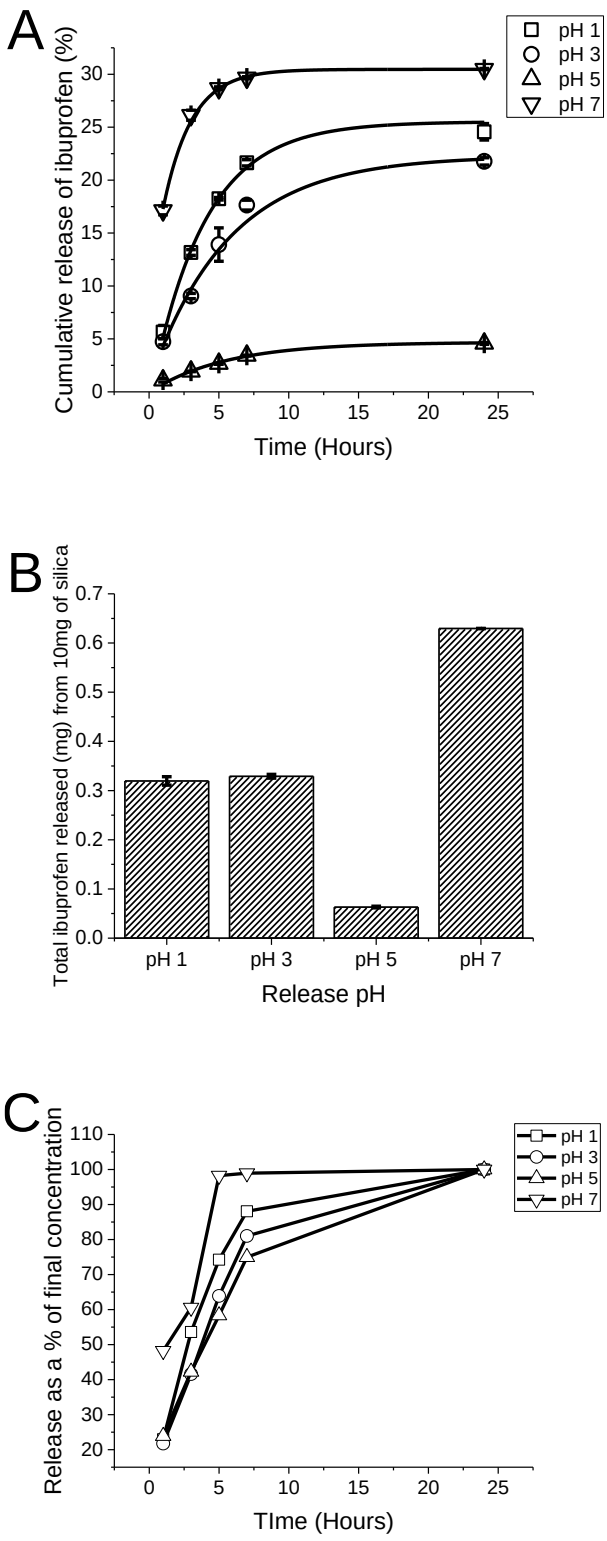

Figure 3-15 – Effect (A) The % release of loaded ibuprofen at different pH values from BIS-PAH 2:2, data fitted using equation 2.1 ,(B) Total mass of ibuprofen (mg) released at different pH values from 10mg of silica sample, (C) Release of loaded ibuprofen expressed as a % of final concentration released at different pH from BIS-PAH 2:2. n=3, error bars represent one standard deviation.

Table 3-5 - Results of silica yield and of mathematical fitting (using equation 2.1) of release data presented in Figure 3-14

DDS	Silica produced (mg)	Yield (%)	Ibuprofen loaded (mg/10mg of silica)	Ibuprofen loading efficiency (%)	Release pH	Max. Release (% h^{-1})	R^2	Total ibuprofen released (mg)*	Total ibuprofen released (% of loaded)
2:2	172	95	1.30	51.02					
	-	-	-	-	1	6.83	0.98	0.31	24
	-	-	-	-	3	4.34	0.97	0.32	21
	-	-	-	-	5	0.86	0.98	0.06	4.5
	-	-	-	-	7	18.65	0.99	0.43	45

Table 3-6 - Percentage ionisation of the three relevant species during drug release at various pH

pH	% Ibuprofen negatively ionised (pKa 5.2)	% PAH positively ionised (pKa 8.7)	% Silica negatively ionised (pKa 6.8)
1	6.3 X10 -3	100	1.5 X10-4
3	0.62	99.9	1.5 X10 -2
5	38	99.8	1.5
7	98	98	61

The reason behind the results presented here are likely due to the changing charges of the three main components (drug, amine and silica) as the pH changes. These varying charges ultimately control the release of drug, by either promoting or hindering it. Release at pH 1 and 3 are similar because the % of charged molecules are similar (table 3.6), where there was no significant attraction or repelling forces.

At pH 5, ibuprofen becomes much more negatively charged and so became attracted to the positively charged amine, impeding release. As the pH rises to pH 7, the silica also becomes more negatively charged. Despite there still being an attraction between the negatively charged ibuprofen and positively charged amine, the abundance of negatively charged silica repels the ibuprofen and results in an increased release of the drug from the system.

This experiment is simple and does not fully reflect the passage of BIS through the digestive system. For example, pH remained constant throughout the experiment for each sample rather than changing and the system was static which does not simulate what occurs *in vivo*. However, it is an important and often forgotten part of developing orally delivered DDS, since if drug is being released too early in the digestive system it could be broken down by the stomach acid or not be absorbed into the blood stream effectively.

3.5. Conclusions

The primary aim of this chapter was to develop an *in situ* drug loading and release system using bio-inspired silica (BIS). The BIS system can be controlled using many factors such as the choice of amine additive, pH of synthesis, kinetics of synthesis and pH of release solution. The results presented here suggest that the ideal formulation would be BIS-PAH synthesised with a reactant concentration of 2:2 because of its favourable performance in loading and releasing drug. Formulation under acidic pH was found to be suitable for designing DDS for fast targeted release, while basic pH was preferred for sustained release. Ultimately, BIS appears to have several advantages over MCM-41 (such as one step formulation,

simple controllability and lack of hazardous chemicals) and we found that BIS has similar or improved drug loading and release profiles to MCM-41. These benefits give BIS real potential as a viable DDS to be further investigated and this is the subject of the next chapter.

Chapter 4: Investigating the use of bio-inspired silica to improve adrenocorticoid insufficiency treatment with hydrocortisone

This chapter aims to determine whether BIS is a suitable DDS for hydrocortisone. While BIS proved to have some potential for delivering ibuprofen, hydrocortisone faced a major issue. Hydrocortisone was unstable when exposed to the alkaline conditions found at the beginning of the BIS synthesis process and so could not be loaded using the *in situ* method employed for ibuprofen. To avoid the degradation of hydrocortisone, it must only be loaded post-synthesis. This has the consequence of very low loading efficiencies onto BIS due to the relatively low porosity and surface area of BIS. This low loading also appears to be unaffected by increasing the length of time BIS and hydrocortisone has to interact. Therefore, unfortunately, BIS must be deemed an inappropriate system for loading hydrocortisone and cannot be used for improving adrenocorticoid insufficiency treatments.

4.1. An introduction to hydrocortisone

Corticosteroids influence the majority of the body's functions, including those of the heart, muscles, endocrine and nervous systems, as well as influencing virtually every stage of inflammatory and immune responses (either through induction or suppression). Corticosteroids are also involved in regulating the metabolism and can accelerate glucose or glycogen synthesis, especially in the liver [127,128]. This chapter will focus on one corticosteroid, specifically a glucocorticoid; Cortisol.

Cortisol is an adrenal steroid hormone and has a role in response to stress as well as dramatic effects on the immune system, specifically acting as an anti-inflammatory agent [128]**.** It slows the migration of phagocytic cells into an injury site

and also dampens the activity of any phagocytic cells already in this area. Thus, inflammation, swelling and further irritation is greatly reduced [129].

Cortisol is produced (as seen in Figure 4.1) when the pituitary gland in the brain releases adrenocorticotropic hormone (ACTH), which is the carried through the blood to the kidneys where it induces the adrenal glands to produce and release the glucocorticoid. This secretion is ultimately regulated by a negative feedback loop, where high levels of glucocorticoid in the blood, inhibit the production of corticotrophin-releasing hormone (CRH) (in the hypothalamus) and of ACTH in the pituitary gland [129].

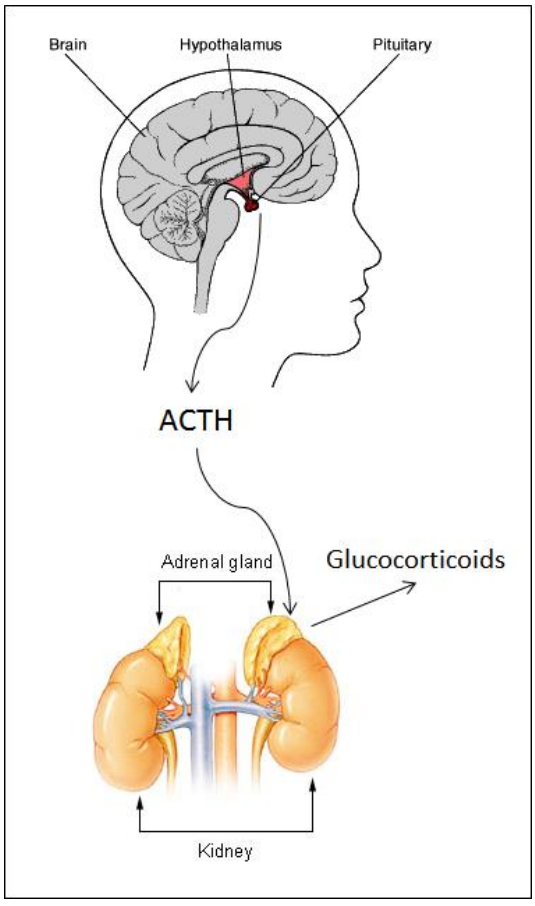

Figure 4-1 - The hormonal responses which induce the production and release of glucocorticoids (i.e. cortisol) (figure created using images from [130,131])

Another characteristic of cortisol is its distinct circadian rhythm in terms of release. Figure 4.2 shows work done by Debono *et al.*, who measured the cortisol levels in 33 normal individuals' blood over the course of a day. Cortisol is at its lowest blood concentration at midnight and then levels begin to rise around 2-3am, reaching a peak around 8.30am before steadily decreasing over the rest of the day.

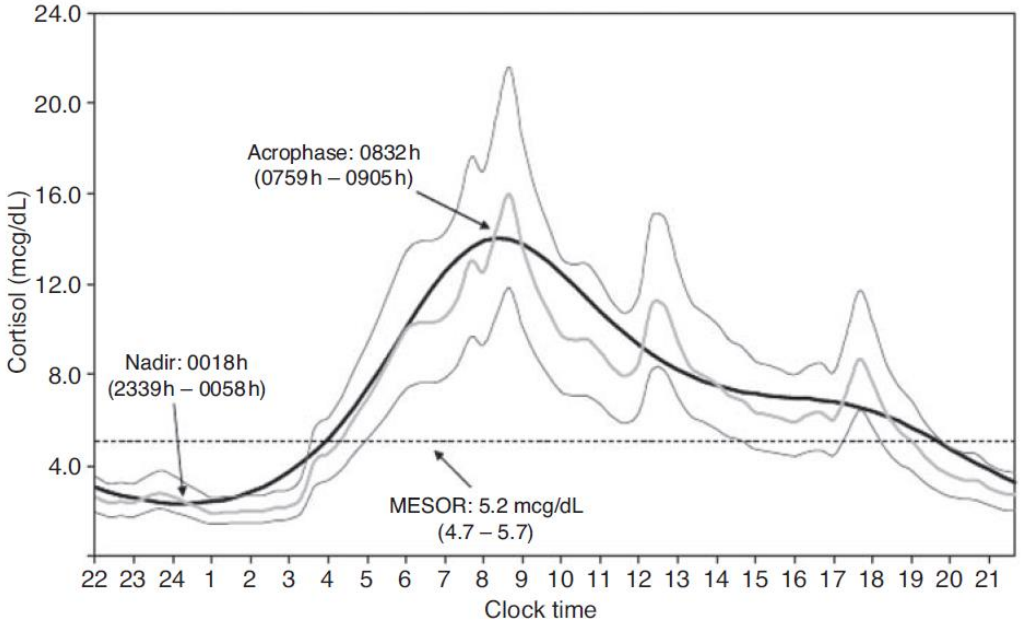

Figure 4-2- The measurement of blood cortisol levels in normal individuals over the course of a day. Figure reproduced from reference [132]

4.1.1. Adrenocortical insufficiency

The importance of glucocorticoids in the body becomes very clear when they are not present. There are several disorders which can result in the lack of circulating corticoids (known as adrenocorticoid insufficiency). This can arise from disorders such as Addison's disease (a lack of corticoids due to the destruction of the adrenal cortex) and congenital adrenal hyperplasia (a genetic mutation which inhibits the biosynthesis of cortisol) [133]. However, there are a whole host of other causes of

adrenal insufficiency including, AIDS, bacterial and fungal infections, mitochondrial DNA deletions, tumours, receptor mutations, adrenal haemorrhage and head traumas [134,135].

Addison's disease is a rare disorder of the adrenal glands which affects the production of glucocorticoids. Addison's disease affects around 8,400 people in the UK and is most commonly diagnosed in women between the ages of 30-50 [136]. In the UK 70-90% of Addison's disease cases are due to an autoimmune attack on the adrenal cortex [136]. This immune attack then impairs the normal production of cortisol in the adrenal gland. However, worldwide, the leading cause of Addison's disease is Tuberculosis infections. Here, the bacteria (normally found infecting the lungs) can migrate to and damage the adrenal glands (on the kidneys). Other, less common, causes of Addison's disease are haemorrhages into the adrenal glands (often due to meningitis), cancer of the adrenal glands or surgical removal of the adrenal glands (often due to tumour growth) [137,138]. Addison's disease can be difficult to diagnose as early symptoms (including lethargy, muscle weakness, low mood and appetite loss) are similar to many other health conditions. Prolonged suffering from Addison's disease can lead to lowered blood pressure, lowered blood sugar and hyperpigmentation (a darkening of the skin, lips and gums, particularly seen in the creases of the palms). The treatment for Addison's disease has remained largely unchanged since the 1950's [139]. It is treated via glucocorticoid replacement therapy where a patient takes hydrocortisone (the synthetic pharmaceutical replacement for cortisol) [140]. Hydrocortisone is normally administered in doses of 10-20 mg/m^2 when required throughout the day [141,142].

Congenital adrenal hyperplasia (CAH) occurs at a range of frequencies (from 1 in 5000 to 1 in 15000 people) depending on ethnicity and race [143]. Adrenocortical insufficiency, in this case, is caused by a genetic mutation in the CYP21A2 gene which results in a deficiency in 21-hydroxylase activity which is essential in the biosynthesis of cortisol [143]. The clinical features of CAH vary across a large spectrum (depending on the specific mutation) and patients can also have varying symptoms throughout their lives. In infant and young females CAH causes ambiguous genitalia and premature pubarche (growth of pubic hair before the age of 8 for girls and 9 for boys) and premature growth. In infant and young boys, genital development is normal but CAH results in poor weight gain, vomiting, hyperkalemia (elevated levels of blood potassium) and hyponatremia (low levels of blood sodium). In adults, CAH causes acne, alopecia, hirsutism (excessive growth of coarse hairs) and can result in problems achieving pregnancy [143,144]. Due to the wide range of symptoms associated with CAH, there is considerable focus on treatment. To treat the adrenocortical insufficiency associated with CAH, hydrocortisone is again employed. Children are given 6-15 mg/m^2 per day of hydrocortisone in three doses throughout the day and can also have increased doses (45mg/m^2 per day) for times of high stress. Adults are often given dexamethasone (0.25-0.4 mg at bedtime or in 2 doses during the day) or prednisone (5-7.5 mg in 2 doses a day) [143,145,146].

4.1.2. Issues with the treatment of adrenocortical insufficiency

The issue of treating corticoid insufficiency with several doses of hydrocortisone tablets is because hydrocortisone has a short plasma half-life and this treatment does not emulate the natural circadian rhythm of cortisol production in the body [140].

Figure 4.3 shows a simulation of a patient's blood cortisol level over the course of a day. The solid line shows a healthy patient and the dotted line represents an Addison's patient taking three doses of hydrocortisone throughout the day. It is obvious how ineffective this type of treatment is in replicating the normal circadian rhythm of cortisol [87,147]. Normally cortisol production begins during random eye movement (REM) sleep, in the early hours of the morning and results in a spike in blood cortisol upon awakening. For Addison's disease and other corticoid insufficiency patients, who must take a dose of hydrocortisone in the morning, this spike in blood hydrocortisone occurs a few hours later than in normal individuals. This can result in fatigue, mild nausea or headaches, which are only relieved 30-60 minutes after taking the morning dose of hydrocortisone [148].

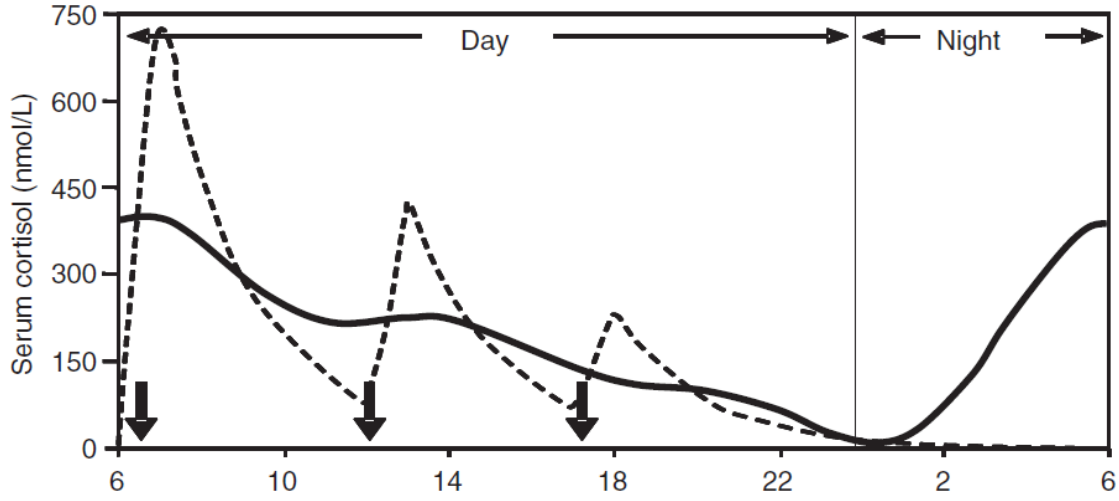

Figure 4-3 - A simulated profile of patient's blood cortisol levels. Solid line represents a healthy patient. Dotted line represents an Addison's disease patient taking three doses of hydrocortisone [140,147].

Another issue with this type of cortisol replacement is the number of tablets a patient must take; this is especially problematic for children. Some liquid suspensions have been investigated which would make administering medicine to children easier, but inadequate suspension of hydrocortisone was achieved [145].

Therefore, a drug delivery system which would both reduce the number of tablets a patient has to take, and is also able to release hydrocortisone in a manner which more closely reproduces natural cortisol levels, would clearly be favourable.

4.2. Potential hydrocortisone delivery systems

There are some drug delivery systems, aimed at mimicking hydrocortisones normal circadian rhythm of release, currently in clinical trials or on the market. But none of them are perfect. A company called Diurnal has produced a delivery system called Chronocort® which is currently in phase 3 of clinical trials and aims to be on the market as soon as 2018. However, there is potential for this system to fail or have better competition, and so there is still a need to investigate a novel drug delivery system which can mimic the circadian rhythm of cortisol release [149].

There is also an approved system on the market called Plenadren®, which has a slow release core surrounded by an outer shell which quickly releases hydrocortisone [150,151]. Plenadren® was recently approved by the Committee for Medicinal Products for Human Use (CHMP) in Europe and was made available first in Denmark in 2012 [152]. This system (either in 5 or 20mg doses) releases a physiological concentration of hydrocortisone within 20 minutes followed by an extended release over the next 24 hours [153]. The main issue with this system is the cost. To administer Plenadren® 20mg daily, it costs the NHS £224. Immediate release systems of hydrocortisone only cost £81 for 20mg daily [23]. The cost of production of any new drug or DDS is important, since there will always be a cost: benefit analysis.

As yet only two papers have been published using silica for the delivery of hydrocortisone. Lopez, *et al*. 2009, synthesised four MSNs using different templates so as to produce particles with different pore properties [154]. The MSNs were loaded via immersion in a solution of hydrocortisone for 2 hours and then dried at room temperature for three days, compressed into a tablet and the release of hydrocortisone was measured. They showed that the release of hydrocortisone from MSNs occurs in two stages; the first burst release followed by a slower release (resulting from the diffusion of the drug molecules through the nanopore structure). One of their MSN released hydrocortisone at a much slower rate than the others and so it was proposed as a candidate for long term release of drug (such as those required for Addison's disease treatment, described above) [154]. In reality, however, this delivery system is far from perfect. Firstly the synthesis of MSN takes several hours and also uses some harmful chemicals (such as TEOS). The length of time it takes to load the MSNs with drug (3 days) is also a detriment to this type of drug delivery system. Secondly the burst release of hydrocortisone over the first 26 hours does not mimic cortisol's natural circadian rhythm and the system also has the potential for drug release during storage, making dosages unreliable.

Andrade, *et al*., 2009 describes the much quicker loading of hydrocortisone onto silica bio-glass [155]. This method took several hours to synthesise and drug load the bioglass. The authors observed ~65% of loaded hydrocortisone being released in the first 24 hours. The mass of hydrocortisone released after 24 hours was seen to not be statistically different [155]. While this method of synthesis and loading of hydrocortisone is substantially quicker than that of MSNs described above, it still requires the use of harmful chemicals (mainly TEOS) to synthesise; additionally this

release also does not emulate the natural release of cortisol. Therefore a synthesis process which does not require TEOS and can have hydrocortisone loaded relatively quickly would be more favourable.

It is clear then that there is room for a more effective DDS for hydrocortisone to be developed and BIS has the potential to address issues faced by other silicas. This chapter aims to use the knowledge of the BIS system to investigate the loading and release profiles of hydrocortisone in order to develop a controlled release of hydrocortisone to improve upon current technologies.

4.3. Stability of Hydrocortisone during *in situ* loading into BIS

The method of loading that is unique for BIS among silica based DDS is the *in situ* loading method. This method allows for the synthesis of ones' DDS and drug loading all in one step, compared to the multi-step process required for MSN, for example. Briefly, BIS is synthesised by neutralising a solution of sodium metasilicate, amine additive and drug molecule. Hydrocortisone was chosen as a drug in real need for an effective DDS (as described in section 4.1), however, it became apparent through the use of HPLC that the hydrocortisone molecule was not stable under the conditions it was being exposed to during BIS synthesis.

It is obvious in the HPLC traces that hydrocortisone was being degraded during BIS synthesis. Figure 4.4A shows the HPLC trace of hydrocortisone on its own and clearly shows one peak at 7.1 minutes representing hydrocortisone being detected. Figure 4.4B shows the HPLC trace of the supernatant of the synthesis reaction (which is taken to determine the loading efficiency of drug into BIS) and multiple peaks were observed, one at 7.1 minutes representing hydrocortisone and another

peak at 2.2 minutes which is likely to be a hydrocortisone degradation product (since no other chemical used in the process gave a peak during HPLC shown in appendix 3).

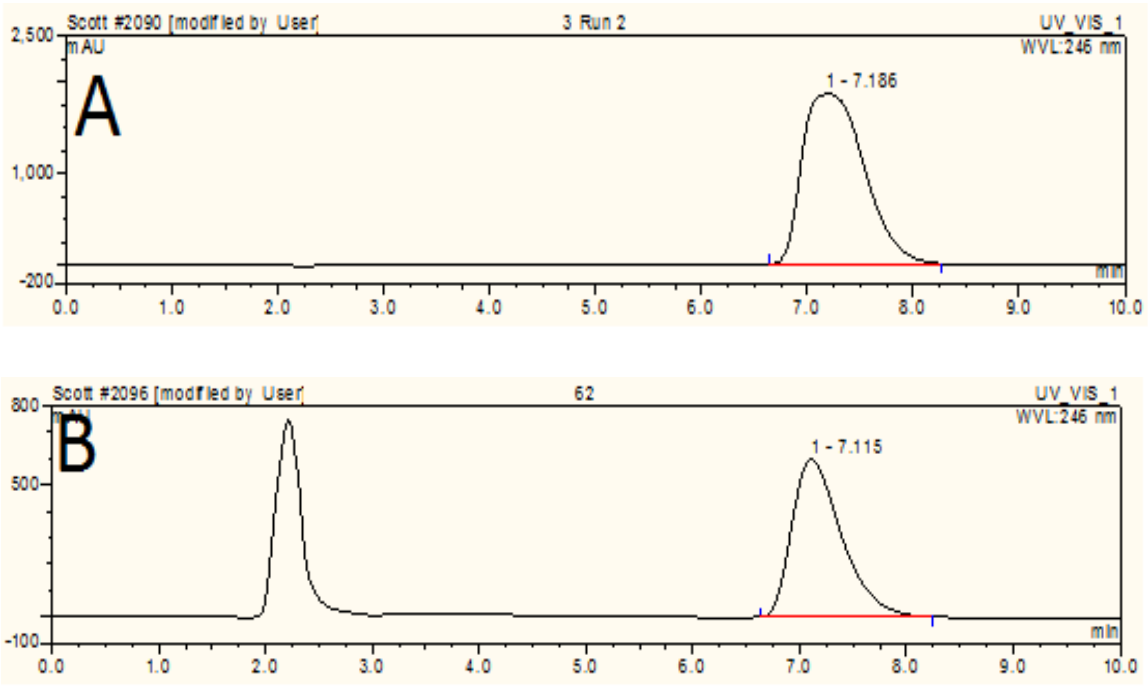

Figure 4-4– Hydrocortisone detected using an isocratic reverse phase HPLC method, with 40 µl injection volume and a mobile phase of acetonitrile: water (7:3) at a flow rate of 1ml min^{-1} through a ACE 5 C-18 column (150X4.6 nm with 5 µm particle size). , Hydrocortisone retention time is approximately 7.1 minutes and was detected using UV absorbance at the wavelength 246 nm. (A) HPLC trace of hydrocortisone in 70% ethanol, where the drug is not degrading and peak at ~7.1 minutes is visible (B) HPLC trace of hydrocortisone exposed to BIS synthesis conditions, , where the normal hydrocortisone peak can be seen at 7.1 minutes along with an additional peak at 2.2 minutes, associated with a degradation product

Next, to fully deduce what was causing the degradation of hydrocortisone, the drug was systematically exposed to each reactant and a range of pH occurring in BIS synthesis. Figure 4.5 shows the % degradation of hydrocortisone (i.e. the % of undetectable drug). There is minimal loss of hydrocortisone under acidic conditions (HCl and PAH) and neutral conditions (70:30 ethanol: water/PBS and neutralised sodium metasilicate). There is also no drug degradation when the solution was heated to 85 ^{o}C. The small apparent loss of hydrocortisone under these conditions

may also be due to incomplete dissolution of hydrocortisone in these solutions since no degradation products are observed in the HPLC traces (appendix 3).

Significant hydrocortisone loss and degradation products were observed is when hydrocortisone is exposed to basic conditions. >40% of hydrocortisone was lost when it was exposed to pH 12 30 mM sodium metasilicate (Figure 4.5). This degradation was pH dependent rather than via chemical reaction with the metasilicate solution since minimal degradation was observed when hydrocortisone was exposed to neutralised metasilicate (pH 7). Further to this ~65% of hydrocortisone was lost when exposed to another basic solution (NaOH) (Figure 4.5).

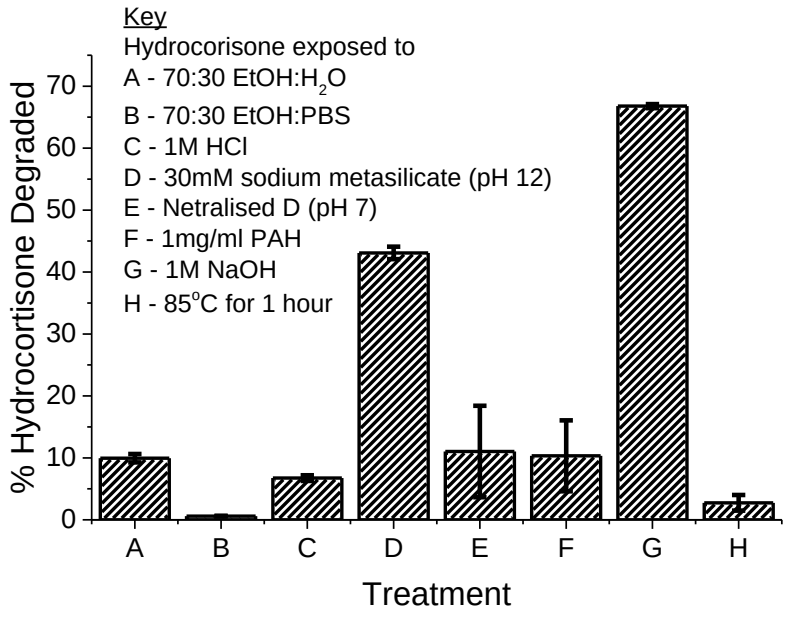

Figure 4-5 - The % degradation of hydrocortisone when exposed to various conditions (A) 70:30 - EtOH:H2O (pH 7.4), (B) 70:30 - EtOH:PBS (pH 7.2), (C) 1M HCl (pH 1), (D) 30mM Sodium metasilicate (pH 12), (E) 30mM Sodium metasilicate (pH 7), (F) 1mg/ml PAH (pH5), (G) 1M NaOH (pH 14), (H) Heated at 85ºC for 1 hour

The stability of hydrocortisone (HC) and its degradation has been well studied in the literature. Degradation most often occurs as a result of reactions on the C_{17}-dihydroxyacetone side chain (Figure 4.6) with several oxidative and non-oxidative reactions being able to take place [156]. Less commonly, degradation can also occur as a result of chemical reactions in ring A of the HC molecule (Figure 4.6) [157]. The degradation of HC is dependent on three main conditions; pH, temperature and the solvent used. Under basic conditions, HC degrades into several different products through both oxidative and non-oxidative reactions. Figure 4.7 shows these degradation products [156].

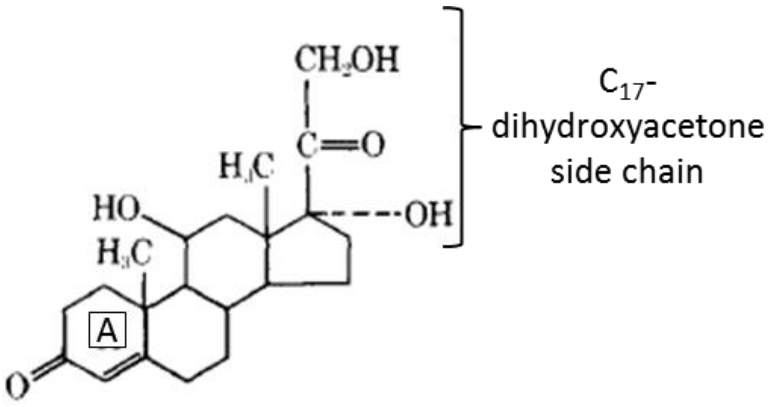

Figure 4-6 - The structure of hydrocortisone with the two main sites of degradation (C17 side chain and ring A) labelled [157].

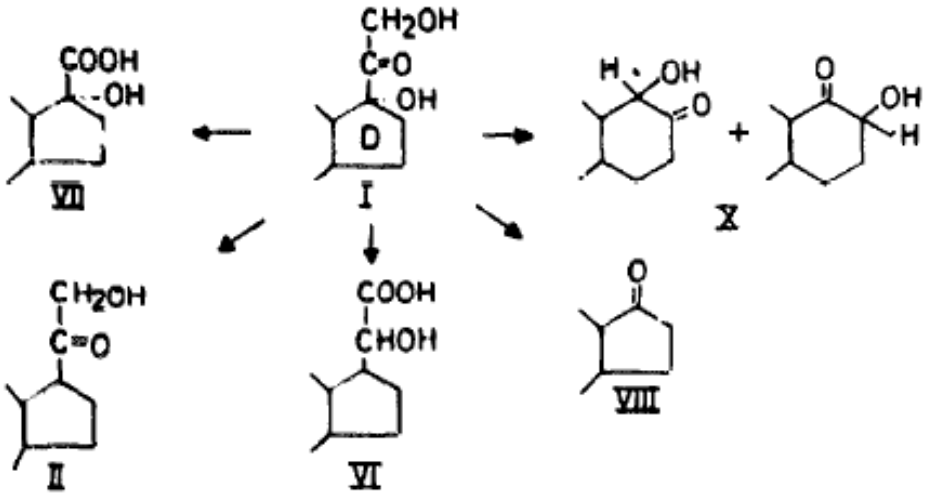

Figure 4-7 - Degradation products of HC under basic conditions. The following is a list of the names of molecules shown in this Figure, it should be noted that since the paper this Figure was taken from is from 1980, some of the nomenclature may be out of date. I (hydrocortisone), II (corticosterone), , VI (11β,20-dihydroxy-3-oxo-4-pregene-21-oic acid), VII (11β,17α-dihydroxy-3-oxo-4-androsten-17β-carboxylic acid) ,VIII (11β-hydroxy-4-androsteb-3,17-dione and X are D-homosteroids [156]

A more recent paper used HPLC and mass spectrometry to look into the auto-oxidation of betamethasone and its analogues (including hydrocortisone) under alkaline conditions [158]. Figure 4.8 shows the structure of betamethasone 17-acid, a breakdown product which also occurs in the hydrocortisone side-chain and was not suggested by Hansen *et al.* The degradation of betamethasone to betamethasone 17-acid through an auto-oxidation reaction was observed to occur after 30-50 in 1M NaOH. Increasing the strength of the base or increasing the base:drug ratio also increased degradation. Due to all the possible by-products of exposing hydrocortisone to basic conditions, these pH levels must be avoided during drug loading and release.

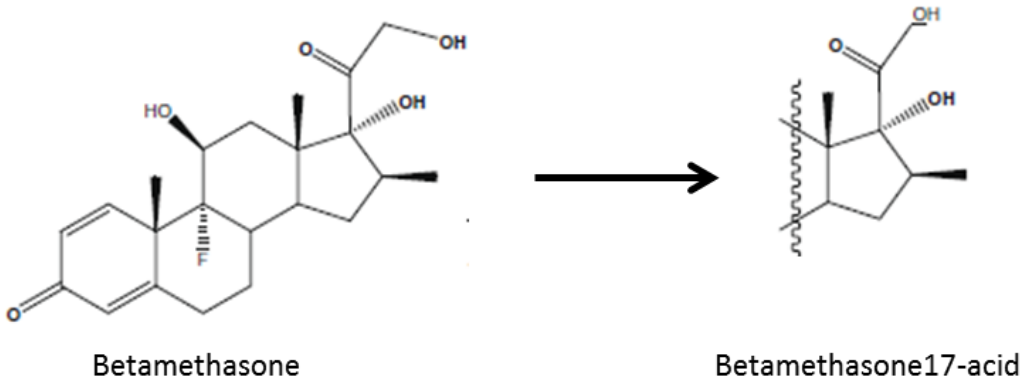

Figure 4-8 - Degradation of betamethasone to betamethasone 17-acid under basic conditions. A reaction which also occurs in HC [158].

While less important than pH, temperature can also have an effect on the degradation of hydrocortisone. Allen and Gupta (1974) calculated the rate equation for the temperature dependent HC degradation and by using these equations, Figure 4.9 could be plotted. Figure 4.9 shows the % degradation of HC at various temperatures over a range of times and it can be seen that HC can be exposed to up to 90 ^{o}C for up to 8 hours with very little degradation. When exposed to higher temperatures for longer periods of time, the degradation increases. However, even under the harshest conditions presented (90 ^{o}C for 7 days) only 8 % of HC is degraded [159]. We also observed minimal hydrocortisone degradation when exposed to 85^{o}C for an hour (Figure 4.5). However, to remove the potential for hydrocortisone degradation under high temperatures, drug loaded BIS should be dried at a lower temperature after synthesis.

While pH degradation mainly occurs on the C-17 side chain, heat generally impacts upon the A ring in the molecule, with greater A ring degradation with increasing temperature. Figure 4.10 shows some products from A ring degradation.

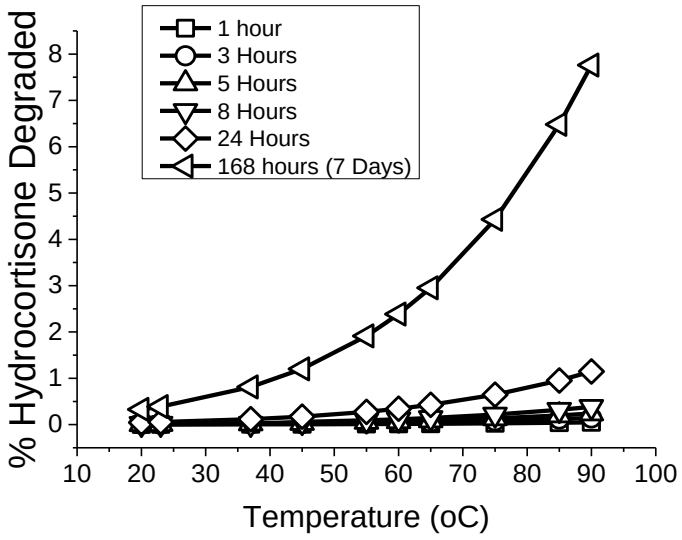

Figure 4-9 – The degradation of HC at various temperatures over time as calculated using the published HC degradation rate equation ci/ct = $10^{t\,(K/2.303)}$, where ci is the initial concentration, ct is the concentration at time t, t is the time and K is the rate constant [159].

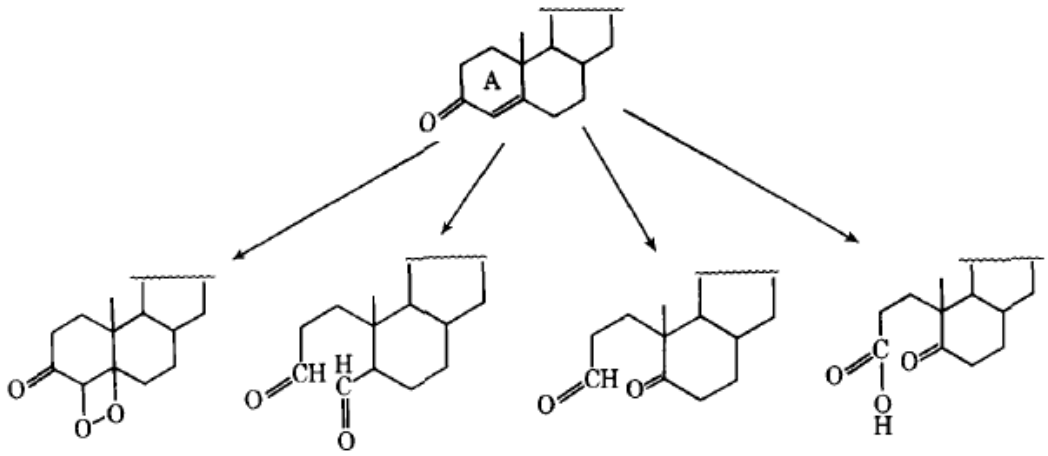

Figure 4-10 - Products from the degradation of ring A in the hydrocortisone molecules. Figure reproduced with permission from reference [159].

Due to the sensitivity of hydrocortisone to both basic pH and prolonged exposure to heat, the method of BIS synthesis must be modified for loading this drug. Before the BIS synthesis solution is neutralised (for silica condensation) the solution is very basic (pH 12). So hydrocortisone must only be added to the solution once it is neutral (and BIS has already begun forming) in order to reduce the risk of

drug degradation. To avoid any temperature related degradation, drug loaded BIS was dried at 40^{o}C.

4.4. Effect of different amines in the loading and release of hydrocortisone into BIS

It has previously been shown in chapter 3 with ibuprofen work and in the work carried out by Stevens *et al.,* that the choice of amine used in BIS synthesis can greatly impact the loading and release of drug [35]. Due to the instability of hydrocortisone under basic conditions, it could not be loaded fully "*in situ"* as with ibuprofen. Instead, a solution of hydrocortisone had to be added once the silica reaction mixture had been neutralised and the silica had started forming. This had a great impact on the loading efficiency of hydrocortisone into this system as well as drug location on the DDS. As a reminder drug loading efficiency is defined as the % of available drug during synthesis which was loaded into the silica, drug content is defined by the % weight of drug in the silica-drug complex (i.e. mg of drug per mg of silica-drug complex), mass loaded is defined as the absolute mass of drug loaded into 10mg of silica. Release is expressed as the % of the total drug loaded into the silica which has been released from 10mg of silica during the experiment or by normalising the total drug release at 24 hours as "100%" (i.e. total amount of drug released over 24 hours).

The choice of amine additive had very little effect on the loading efficiency of hydrocortisone to BIS (Figure 4.11). For BIS synthesised with DETA, TEPA or PEHA the loading efficiency was between 6-8%. For BIS-PAH the loading is slightly enhanced to 13%, which was still low when compared to the 48% loading

efficiency of MCM-41. The wt % for all the types of silica was low with the BIS systems having a wt% of between 0.03 and 0.6 % (Figure 4.11). With similar loading efficiencies for all BIS systems, the differences in wt% are likely to be due to the differences in yield with the larger amines resulting in higher yields (e.g. 31% for DETA and 96% for PAH) (Table 4.1). MCM-41 also had an obvious advantage over all the BIS systems in that it has a much higher surface area (Figure 4.12 shows 983 m^2/g compared to 16-129 m^2/g of BIS). Surface area and porosity become more important for loading hydrocortisone than it was for loading ibuprofen due to the altered method of drug loading and so *in situ* entrapment may be limited. The loading of hydrocortisone onto BIS could be improved either by increasing the surface are of BIS or by creating a supersaturated solution of drug. This increases the diffusion pressure and allows for drug to precipitate onto the silica nucleation sites, resulting in increased drug loading.

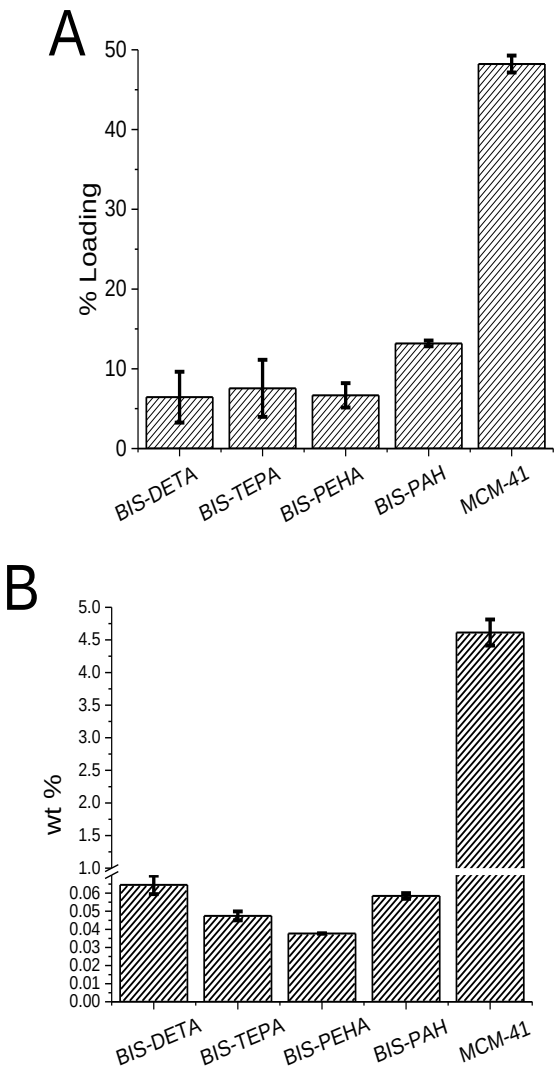

Figure 4-11 - Effect of amine additive on (A) % loading efficiency of hydrocortisone into BIS synthesised with different amine additives and MCM-41, (B) hydrocortisone content per mg of silica into four different BIS and MCM-41. n=3, error bars represent one standard deviations

Table 4-1 - Results of mathematical fitting (using equation 2.1) of release data presented in Figure 4.13

Sample	Mass of silica produced (mg)	% yield	Release % per hour	R^2	Mass (mg) of HC loaded in 10mg of silica	% of HC loaded	Total mass (mg) of HC released from 10mg of silica	Total % of loaded HC Released
BIS-DETA	53.8	31.96	0.755	0.99	0.006	6.4	$2.5 X10^{-4}$	3.64
DIS-TEPA	76.01	56.09	0.185	0.99	0.004	7.5	$5.6X10^{-5}$	1.20
BIS-PEHA	88.56	69.83	0.108	0.99	0.004	6.6	$6.5X10^{-5}$	1.68
BIS-PAH	97.5	80.08	9.7	0.99	0.009	17.6	0.0026	29.1
MCM-41	N/A	N/A	2.29	0.99	0.47	48.2	0.05	10.8

A

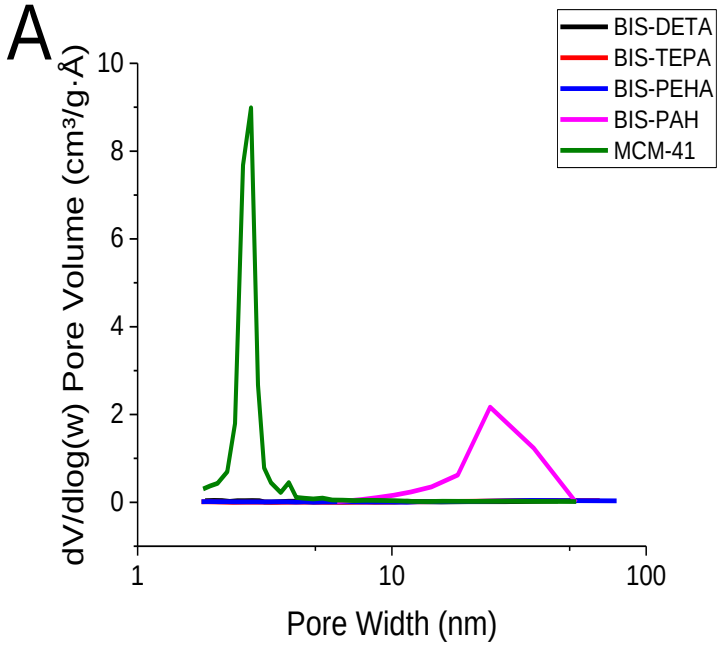

B	BET Surface area (m^2/g)	Pore volume (cm^3/g)	Pore size (nm)
BIS-DETA	11	0.04	*
BIS-TEPA	11	0.04	*
BIS-PEHA	15	0.04	*
BIS-PAH	93	0.52	22.4
MCM-41	983	0.74	2

Figure 4-12 - (A) Pore size distribution of BIS synthesised with amines and MCM-41, (B) Surface area, pore volume and pore size figures for BIS synthesised with amines and MCM-41 (* due to broad pore size distributions, specific pore sizes are not applicable), n =1

Interestingly when release profiles were fitted (all with $R^2 > 0.9$); there was a wide difference between the different types of silica (Figure 4.13). BIS-DETA, TEPA and PEHA had very low release % (<4 %). These three BIS systems (as with ibuprofen) were then deemed inappropriate for drug delivery application as they showed poor loading and release profiles. MCM-41 fares better with 10% of loaded hydrocortisone being released. Finally, while BIS-PAH performed poorly on its

loading efficiency, it was able to release 29% of loaded hydrocortisone. Based on % released, BIS-PAH was the most favourable system; however, it is also important to note the actual mg of hydrocortisone being released. 10 mg of BIS-PAH released $2.6x10^{-3}$ mg of hydrocortisone but, due to its higher loading, MCM-41 releases the highest mg of hydrocortisone (0.05mg per 10 mg). This is important to note because, for a DDS system to be viable, there needs to be a feasible dosages of drug loaded silica that a patient has to consume.

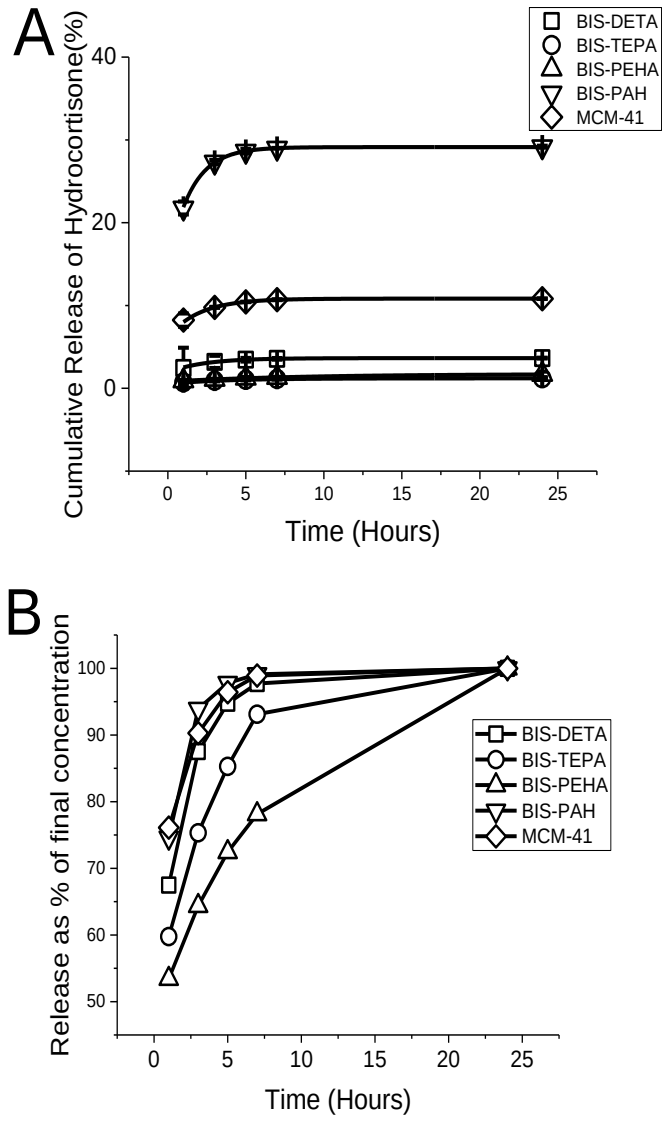

Figure 4-13 - (A) The % release of loaded hydrocortisone from four different BIS and MCM-41, data fitted using equation 2.1, (B) Release of loaded hydrocortisone expressed as a % of final concentration released from four different BIS and MCM-41. F n=3, error bars represent one standard deviations

A normal dose of hydrocortisone is 10-20 mg [141,142]. Based on the release efficiencies of these silica systems one would be required to consume 31 g of BIS-PAH to achieve a 10 mg dose (an obviously impractical and potentially dangerous dosage of silica). A lower dosage of MCM-41 would be required (2 g); however this is still a large amount for a patient to take in an oral dose. The release for all systems (apart from BIS-PEHA) is a burst release (Figure 4.13) where the majority of drug is

released in the first 5 hours. BIS-PEHA provides a more prolonged release which could be useful for the desired delivery profile for hydrocortisone (if one was able to load and release a significant amount of drug).

The reason for the difference in release profile in the BIS systems using small amines (DETA, TEPA and PEHA) and polymeric amines (PAH) is likely to involve porosity. Small amines produce micoporous silica (<2nm), while PAH generates mesoporous silica (2-50nm). MCM-41 may have poorer than expected release profile due to its small pores (2 nm) and lack of functionalisation which may impede hydrocortisone release since they are more easily blocked than the much larger pores of BIS (~22 nm). Another reason for poor release is the release media being used (PBS). Hydrocortisone was loaded in a solution of 70% ethanol since it has a soluility of 15mg/ml in ethanol at 25ºC [160]. When the release experiment is set up, the media is not ideal since it is largely aqueous and hydrocortisones solubility is only 0.32 mg/ml is water at 25ºC [160,161]. While release could potentially be improved by changing the release media to (for example) 70% ethanol, this does not replicate a biologically relevant environment for clinical use. To resolve these issues, a hydrocortisone salt (which is much more water soluble) could be employed.

4.5. The effect of maturation time on the *In situ* loading onto and release of hydrocortisone from BIS-PAH

It was hypothesised that since hydrocortisone solution would be added to the silica reaction mix after the solution had been neutralised (and thus the silica had begun condensing) there would be impeded loading. As such, an experiment was set up to investigate the effect of adding hydrocortisone after the BIS synthesis solution

had been neutralised and leaving the reaction mixture for various lengths of time (i.e. maturation time) before the reaction is stopped (via centrifugation).

Contrary to what was hypothesised, increased loading time (up to 120 minutes) did not increase the loading efficiency but rather it decreased it slightly (from 17.6% at 0 minutes to 10.9% at 120 minutes) (Figure 4.14). This is reflected in the wt % (Figure 4.8B) which also reduces (~0.09-~0.045%) when the loading time is increased. This is a real reduction in the loading efficiencies as (shown in Table 4.2). The yield of silica remains similar for all BIS samples (yields over 100% are attributed to the incomplete removal of water during drying since a lower temperature, 45^{o}C, was used in order to protect the structure of hydrocortisone). As before the loading efficiency of hydrocortisone into MCM-41 was 48% and the wt % was 4.6; much higher than the BIS systems.

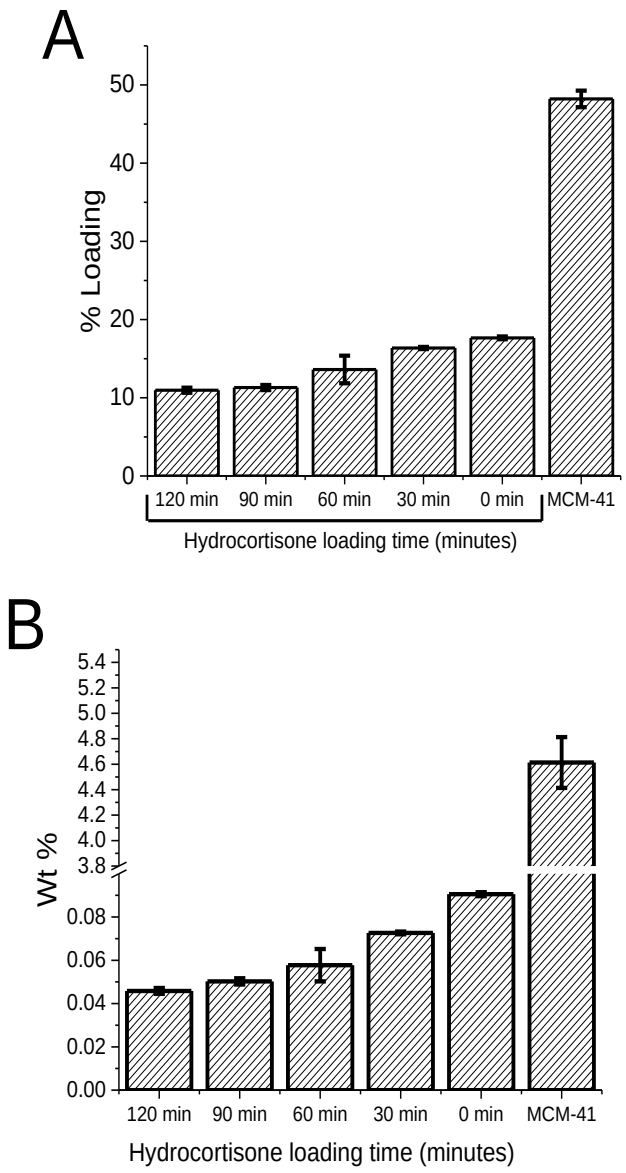

Figure 4-14 - Effect of drug loading time (A) % loading efficiency of hydrocortisone into BIS with various drug loading times and MCM-41, (B) Average hydrocortisone content per mg of silica into BIS with various drug loading times and MCM-41, n=3, error bars represent one standard deviations

Table 4-2 - Results of mathematical fitting (using equation 2.1) of release data presented in Figure 4.16

Sample	Mass of silica produced (mg)	% yield	Release % per hour	R^2	Mass (mg) of HC loaded in 10mg of silica	% of HC loaded	Total mass (mg) of HC released from 10mg of silica	Total % of loaded HC Released
120	119.58	104.1	16.49	0.99	0.004	10.9	0.0030	66.3
90	112.5	96.45	16.89	0.99	0.005	11.3	0.0024	48.2
60	117.92	102.73	7.99	0.99	0.005	13.6	0.0020	35.1
30	112.62	96.65	9.14	0.98	0.007	16.3	0.0023	32.7
0	97.5	80.08	9.7	0.99	0.009	17.6	0.0026	29.1
MCM-41	N/A	N/A	2.29	0.99	0.47	48.2	0.05	10.8

The slight differences in loading efficiencies for the BIS systems cannot be attributed to their physical properties. Figure 4.15 clearly show that the pore sizes, volumes and surface areas do not change significantly when the maturation time is changed. It appears then that hydrocortisone loading will occur quickly but some loaded drug will release back into solution over 120 minutes, thus lowering the loading efficiency slightly.

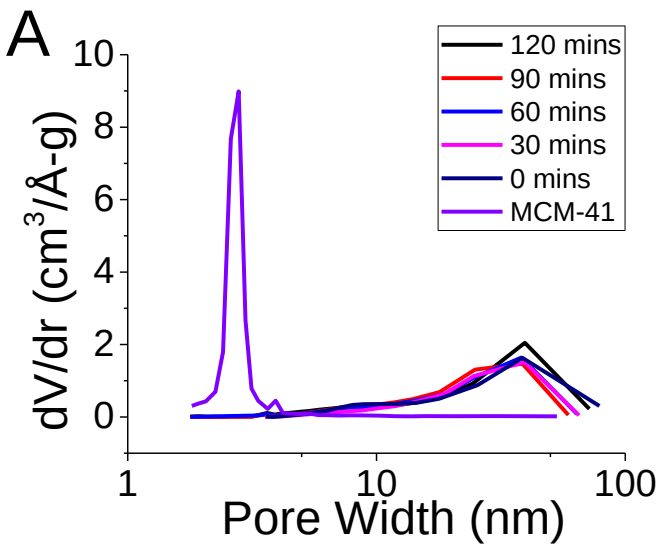

B Maturation Time (mins)	BET Surface area (m^2/g)	Pore volume (cm^3/g)	Pore size (nm)
120	179	1.05	22
90	177	0.91	20
60	173	0.97	22
30	132	0.87	24
0	155	0.98	24
MCM-41	983	0.745	2

Figure 4-15 - (A) Surface area, pore volume and pore size figures for BIS with various drug loading times and MCM-41, (B) The % release of loaded hydrocortisone from BIS with various drug loading times and MCM-41, n=1

While loading efficiencies were similar regardless of maturation time, when drug released was measured there were great differences (Figure 4.16). With longer maturation times a higher % of loaded drug was released, from 29% with 0 minutes maturation time to 66 % with 120 minutes maturation time. All BIS systems performed better than MCM-41 (for % release), however, due to low loading efficiencies, the mg of drug was lower (0.003 mg in BIS-120, compared to 0.05mg for MCM-41. All release profiles exhibit burst release with the majority of drug

release occurring within the first 5-7 hours. Since such a small mass of hydrocortisone was released from these samples, the differences in release were not deemed to be important.

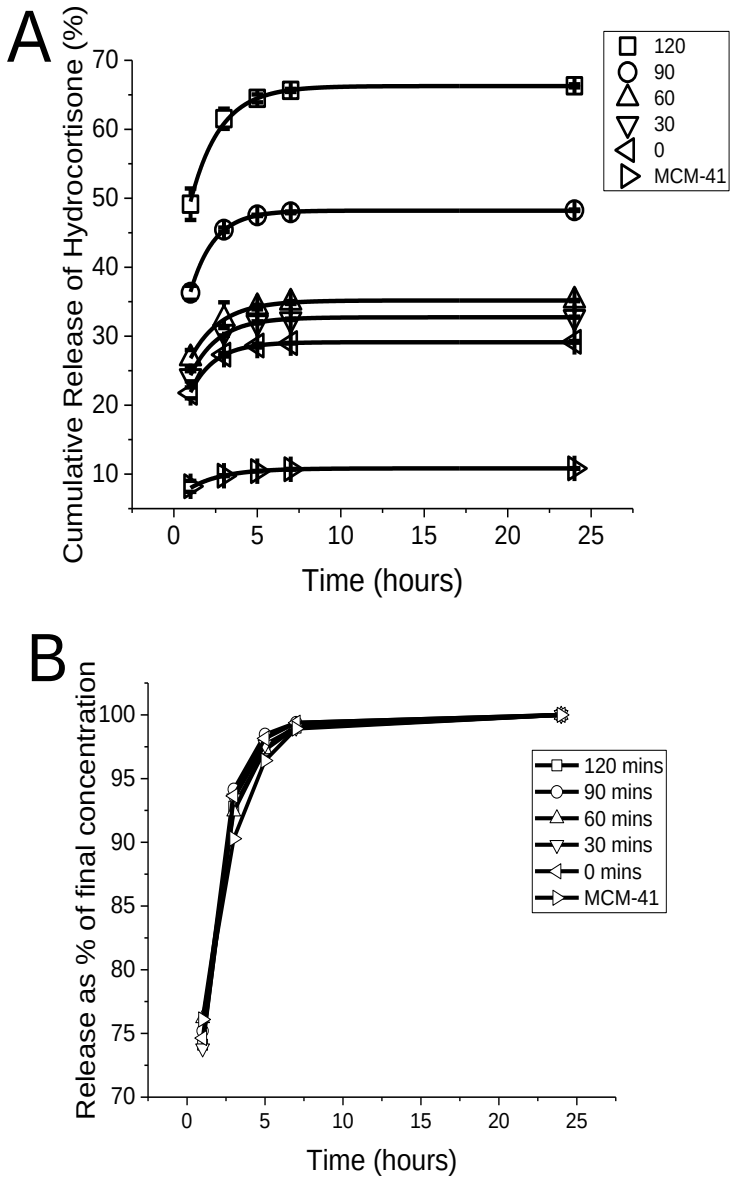

Figure 4-16 - (A) The % release of loaded hydrocortisone from BIS with various drug loading times and MCM-41, data fitted using equation 2.1,(B) Release of loaded hydrocortisone expressed as a % of final concentration released from BIS with various drug loading times and MCM-41. n=3, error bars represent one standard deviation.

4.6. Conclusions

While BIS does have several advantages over other types of DDS (e.g. short synthesis time, *in situ* drug loading and robustness), due to the instability of hydrocortisone under BIS synthesis conditions, all these advantages were not able to be utilised. To avoid the degradation of hydrocortisone, it must only be loaded post-synthesis. This has the consequence of very low loading efficiencies onto BIS due to the relatively low porosity and surface area of BIS. This low loading also appears to be unaffected by increasing the length of time BIS and hydrocortisone has to interact. Therefore, unfortunately, BIS must be deemed an inappropriate system for loading hydrocortisone and cannot be used for improving adrenocorticoid insufficiency treatments.

Chapter 5: Determining the biocompatibility of bio-inspired silica

This final results chapter investigates briefly the biocompatibility, bio-translocation and bioaccumulation of BIS. Previous studies have shown that higher dosages of MCM-41 can lead to cytotoxic effects in epithelial cells and so there is potential for gut wall damage, whereas BIS-PAH was found to be less cytotoxic. The results presented in this chapter show that BIS-PAH is able to pass through the gut wall (which is useful for targeted treatments, e.g. anti-cancer) into the blood stream and haemolytic activity was found to be minimal (significantly less than MCM-41). Once in the blood silica will not dissolve (which may be useful for prolonged release systems) and has been shown in the literature to be effectively cleared from rats with no adverse effects (as long as the dosage is low enough).

5.1. An introduction to biocompatibility

Biocompatibility "refers to the ability of a biomaterial to perform its desired function with respect to a medical therapy, without eliciting any undesirable local or systemic effects in the recipient or beneficiary of that therapy, but generating the most appropriate beneficial cellular or tissue response in that specific situation, and optimising the clinically relevant performance of that therapy" [162]. Put simply, to be biocompatible a material must have no adverse effects on the patient (or the benefits should outweigh the risks). Biocompatibility studies are often left out of drug delivery publications; however, a DDS could have the most desirable loading and release profiles but without biocompatibility it can never be approved for clinical use.

To fully determine a materials biocompatibility several adverse factors of a DDS must be tested; including cytotoxicity (i.e. toxic effects against mammalian cells usually *in vitro*) and non-fatal effects (e.g. morphological changes, growth rate changes and immunological response). Also important is the bio-translocation of the DDS (how the material is going to be taken up into cells), bio-distribution of the DDS (how the material moves around the body) and finally how and if the material is metabolised/degraded and excreted. Determining biocompatibility and receiving FDA approval is one of the biggest hurdles facing developing DDS and is the main reason why so few DDS are currently on the market. Most FDA approved DDS are either lipid-based systems or PEGylated systems designed for the delivery of anti-cancer agents or for treating dangerous chronic infections [12,15].

Silica, and specifically MSN (which has received most focus for drug delivery applications) has many desirable properties for drug delivery such as high surface area and tailorable pore size and structure [33,34]. Silica has also been accepted as "generally recognised as safe" by the FDA due to its natural abundance [36,163]. Despite this, MSN and BIS can have very different properties from "natural" silica (e.g. sand) and so their biocompatibility must be researched. The majority of studies on silica toxicity are carried out *in vitro*, which, while a useful first step, will never fully reflect what happens *in vivo*. There is also an issue in the literature impeding the effective evaluation of MSN biocompatibility, and that is consistency. Different studies will use different types of silica, of different sizes and concentrations and test them on different cell lines.

A review of the literature suggests that size, porosity and surface charge all have an impact upon the cytotoxicity of silica particles, but the literature does not always

agree. A study by He, *et al*., (2009) observed that mesoporous silica particles which are not in the nanoscale (1220 nm in diameter**)** resulted in very little cytotoxicity, regardless of concentrations; 10-480 µg/ml. When nanoscale mesoporous silica (190nm in diameter) was exposed to the same cell types, there was a significant cytotoxic effect (above a concentration of 25 µg/ml). For both sizes of mesoporous silica, cytotoxicity increased as the concentration increased, however, the results are not as simple as this. Two different cell types, MDA-MB-468 cells (a human breast cancer cell line) and COS-7 fibroblast cells showed very different responses to the MSNs. The cancer cells were much more robust and remained at 80% viability even when exposed to the highest concentrations of MSNs, whereas the COS-7 cells viability decreased to 40% when exposed to the same concentrations (between 200-500 µg/ml) [164].

Conversely, a different study by Hudson, *et al*. (2008) found that differences in particle size (from 150-4000 nm) had no impact on the level of *in vitro* cytotoxicity. This study also observed greater cytotoxic effects occurring as the concentration of MCM-41 and SBA-15 increased, and also that the levels of cytotoxicity differed depending on cell type. This paper reported that macrophages were the most robust cell type, with their survival rates only reducing to 70-80% (and only after exposure to the highest concentration, 0.5µg/ml, for 4 days). Mesothelial and muscle cells, on the other hand, were much more sensitive to increasing concentrations of MCM-41 and SBA-15. Both these cells types' survival rates reduced to 40-50% at the higher concentrations after 4 days exposure [70].

Porosity has also been observed to have an impact on the cytotoxicity of silica. Nanoparticles with large surface areas have an increased risk of the

generation of reactive oxygen species, which results in toxicity [165]. In theory, MSN should be more cytotoxic than Stöber nanoparticles (which are non-porous); however, from experiments reported from several papers, the opposite appears to be true. When macrophages were exposed to silica with different levels of porosity it was found that that non-porous colloidal silica NPs were much more cytotoxic than MSNs [166]. At 100 µg/ml colloidal silica nanoparticles reduced cell viability to approximately 20%, whereas macrophages exposed to the same concentration of MSNs remained largely unaffected.

The surface charge of silica is also an important factor in biocompatibility, with positively charged particles being internalised into cells at a greater rate than negatively charged particles [167]. The cytotoxicity of certain charges appears to be controversial with one paper reporting with an increased negative charge the particle makes it more cytotoxic [164] and another stating that amine modified (and therefore cationic) MSNs were less cytotoxic that their bare counterparts (with anionic charges) [168]. This apparent contradiction may be due to the fact that the type of cell used can result in great differences in the measured levels of cytotoxicity.

It is clear that despite large volumes of literature on the biocompatibility of silica and it being "generally recognised as safe" by the FDA, that the biocompatibility of silica is not yet fully understood and there is still a great need to investigate the safety of using silica as a drug delivery system in humans. The following sections will investigate the biocompatibility of BIS as it passes through the digestive tract, into the blood system and becomes systemic since the aim is to develop BIS for oral drug delivery applications. The biocompatibility of BIS over

MCM-41 could provide a major advantage for the use of BIS for drug delivery applications over other types of silica particles.

5.2. Effects of silica in the GI tract

Due to ease and non-invasive nature of administration, oral delivery of drugs is the most preferred route for patients [169]. Silica is an ideal material for oral drug delivery due to its stability under the conditions found in the GI tract, especially the low pH found in the stomach (pH1-3) and so it is able to protect loaded drug molecules from the changes in pH as well as degradative enzymes and bile salts [170,171].

Since we wished to develop BIS as an orally administered DDS, it is important to uncover the fate of orally administered silica and determine its impact on the efficacy of the DDS and the biocompatibility of the silica. Depending on the drug being delivered, one may wish the silica to pass through the gut wall so it can be targeted to a specific area (e.g. for anti-cancer drugs) or one may wish for the drug to be released in the GI tract and have the silica pass through without being absorbed systemically. We explored both possibilities by performing silica dissolution experiments and also gut transport followed by haemolysis studies.

The cytotoxicity of silica has been shown to be dose dependent. A study in 2011 investigated the cytotoxicity of Stöber silica on human oesophageal epithelial cells (NE083) [172]. They found that at concentrations <2.5μg/ml there was no decrease in cell viability over 48 hours. Higher concentrations may result in increased toxicity (as reported by Yuan, *et al*., although this was carried out on a different cell type [173]).

Previous work in our group used fibroblasts (3T3) and found that MCM-41 has high toxicity to this cell type, with an IC_{50} of 20µg/ml. BIS-PEHA was found to have very low toxicity (IC_{50} of >500µg/ml) and BIS-PAH (the BIS focused mostly in this paper) had an IC_{50} of 100µg/ml [35]. Due to the evidence for dose dependent cytotoxicity, bioaccumulation resulting in cytotoxicity could be a major problem.

Our limited study focuses on the fate of BIS-PAH once it had been administered orally. If BIS-PAH is able to pass through the gut wall then there is potential for bioaccumulation and cytotoxic effects. A simple, yet highly valuable, experiment was set up using sections of rat gut to measure the movement of fluorescently tagged BIS-PAH (FITC-BIS-PAH) across the gut wall over an hour. Initially, gut health was tested by measuring the passage of glucose through the gut wall and its inhibition by DNP. DNP inhibits all energy requiring cellular processes (including the active transport of glucose) by preventing the uptake of phosphates into the mitochondria which inhibits the production of adenosine triphosphate (ATP) during the oxidative phosphorylation process [100-102]. Figure 5.1 clearly shows that ~140mM of glucose is able to pass through the gut wall over an hour. This transport is completely stopped by exposing the gut sections to 1mM of DNP for 15 minutes before glucose solution was added. This shows that the sections of rat gut were alive during the experiment and the experiments measuring silica transport (shown next) are valid.

Figure 5-1 - mM of Glucose transported across the inverted gut wall of a rat over an hour in the absence or presence of DNP. Details on method can be found in chapter 2.7, n=3 and error bars are one standard deviation.

Next, FITC-BIS-PAH was synthesised using FITC-tagged PAH, so that its movement through the gut wall could be measured. From Figure 5.2 It is clear that ~22% of silica moved across the gut wall during the hour long incubation. This movement is through passive diffusion since it is not inhibited significantly by the addition of DNP. Longer time points were not carried out since gut tissue only remains viable *in vitro* in balanced salt solution for 1-2 hours.

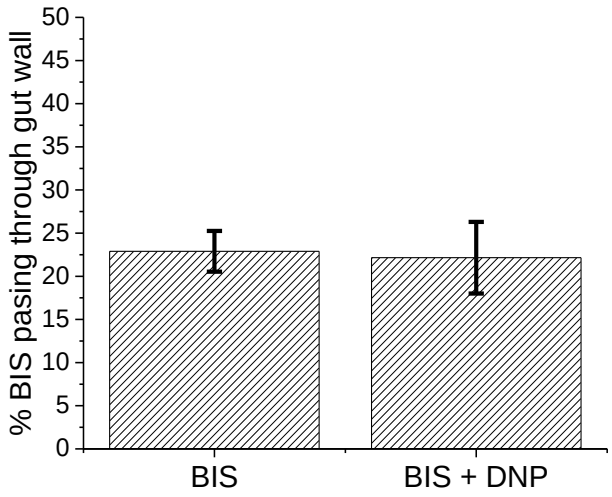

Figure 5-2 - Average percentage of FITC-BIS-PAH passing through a section of rat gut over an hour at 37ºC, with and without the presence of DNP (an active transport inhibitor), n=3 and error bars represent one standard deviation.

To further observe the movement of silica particles through the gut wall, fluorescence microscopy images of the inner and outer surfaces of the rat gut were taken (Figure 5.3). When no silica was present (control) there were no defined points of fluorescence but when the sections of rat gut were exposed to fluorescent silica and silica with DNP, defined points of silica associated fluorescence were observed. Silica was found to be clearly localised on both sides of the gut wall, confirming its movement. Due to the ability of BIS-PAH to pass through the gut wall, it is now important to investigate its biocompatibility with other cell types and tissues (e.g. blood) as well as its bioaccumulation in tissue.

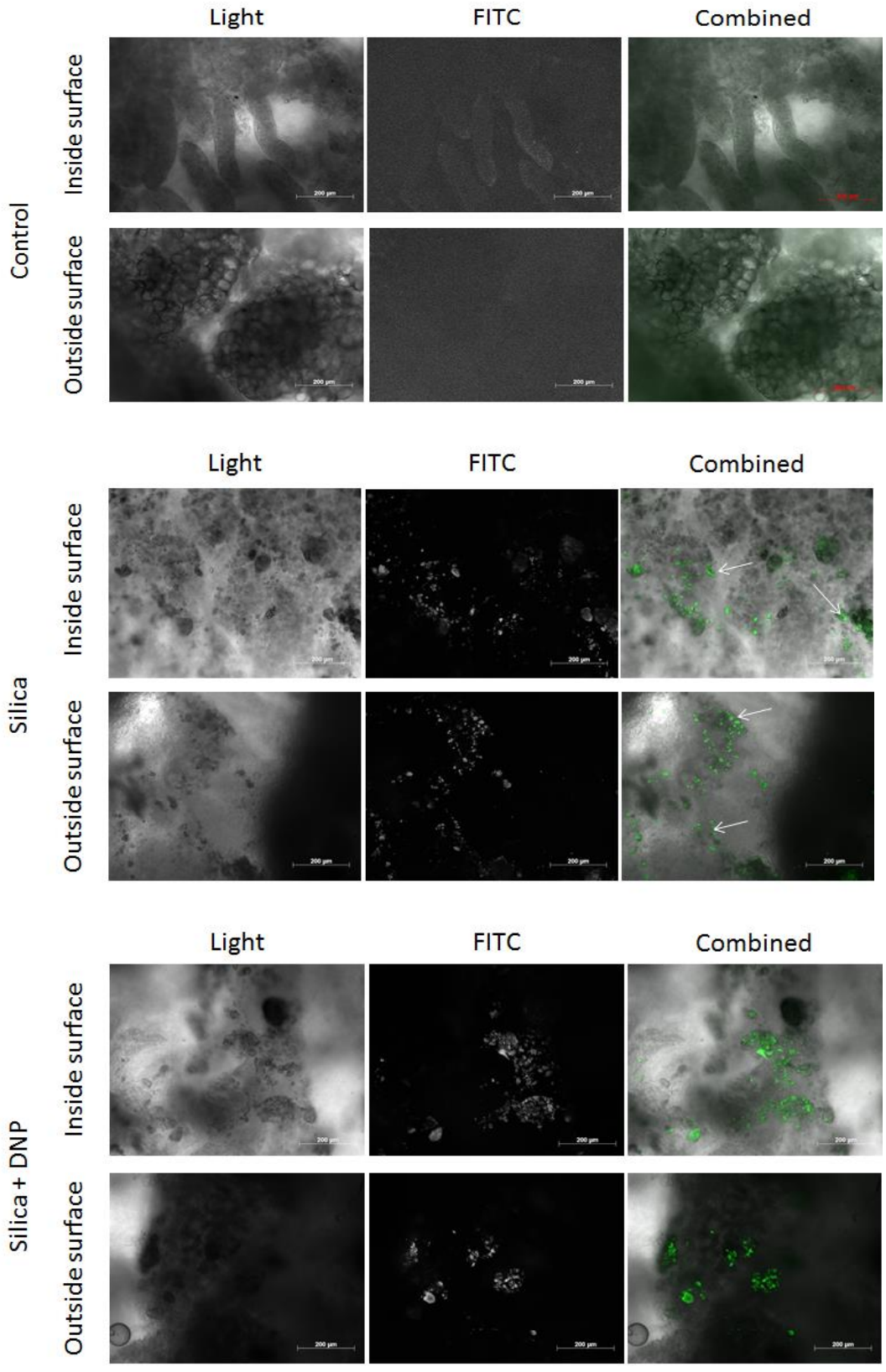

Figure 5-3 - Light and FITC microscopy images of the inside and outside surfaces of rat gut with the addition of no silica (Control), fluorescent silica or fluorescent silica and DNP

5.3. Haemolytic activity of silica

A clear understanding of the haemolytic activity (i.e. lysis of red blood cells) of silica is difficult to determine from the literature due to the many variables involved [171]. However, haemolysis appears to be dependent on the size of MSN that the red blood cells (RBC) are exposed to. It has been shown that as the size of MSN increased from 42nm to 225nm, there was an increase in the TC_{50} (the concentration of MSN where 50% of RBC are lysed) and therefore a decrease in toxicity [174,175].

As a comparison the size of BIS-PAH and MCM-41 used in our study were measured using SEM (images in Figure 3.4 and sizes in Figure 3.5). The SEM images show that all BIS particles were spherical and the particles were 78±18 nm in diameter. The MCM-41 particles were much larger, 3340±1013 nm in diameter. As discussed in section 3.1 this sizing may not be entirely accurate, however

To determine the potential haemolytic activity of BIS, we exposed BIS-PAH and MCM-41 to red blood cells (RBC). Figure 5.4 shows that BIS-PAH had very low haemolytic activity, only lysising 2% of RBS at the highest concentration used (500 µg/ml) and only 0.6% at the concentration which passed through the gut wall (~250 µg/ml). MCM-41 exhibited a higher haemolytic activity, rising to 10% at 500 µg/ml. The data were extrapolated by fitting a line through the straight part of the graph (Figure 5.4). This was between 100-500 µg/ml for MCM-41 and between 250-500 µg/ml for BIS-PAH. The equations of the lines were Y=0.0228X-0.359 and Y= 0.0063X-0.9319 respectively (where Y represent % of RBC lysed and X represents silica concentration). Using these equations allowed for the calculation of a TC_{50} value (assuming toxicity is linear) of 2.2 mg/ml for MCM-41. If this was

scaled for humans (who have an average of 5 litres of blood) the TC_{50} would be a 0.1g dose). The TC50 for BIS-PAH was calculated to be 8.08 mg/ml (0.4g dose for a human). The differences in toxicity between BIS and MCM-41 may be related to the size of the particles. A study in 2010 found that as the size of MSN increased from 42nm to 225nm there was an increase in the TC_{50} (the concentration of MSN where 50% of RBC are lysed) [174]. BIS-PAH particles are 78±18 nm in diameter (S2 A & B) whereas the MCM-41 used were found to be 3340±1013 nm in diameter. Interestingly the non-porous BIS-PAH is less toxic than other non-porous silica measured in the literature. Lin, *et al*, investigated haemo-biocompatibility of non-porous Stöber silica and found it to be much more haemolytic than BIS-PAH, with a TC_{50} of only 20µg/ml (0.1g per 5 litres of blood) [176].

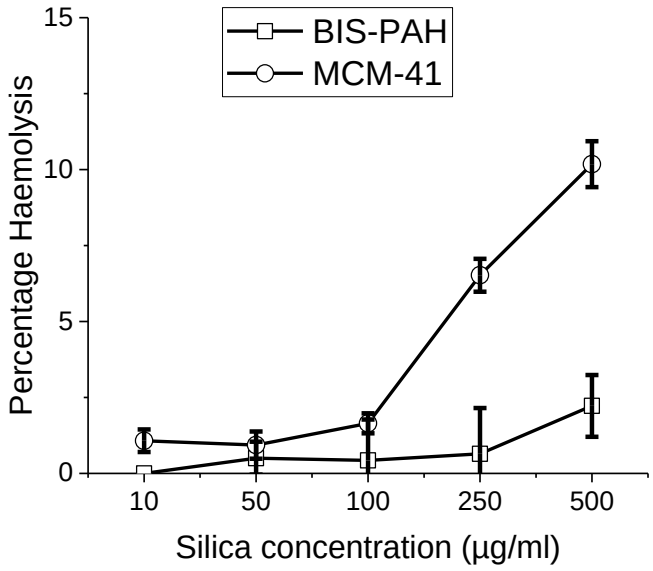

Figure 5-4 - Percentage haemolysis induced by varying concentrations of BIS-PAH and MCM-41. n=3, error bars represent one standard deviation.

5.4. Potential bioaccumulation of silica

Once silica is in the blood system the next stage of investigating bio-compatibility is to look at bio-distribution, bio-accumulation and clearance of the silica. The possible dissolution of BIS-PAH and MCM-41 in an aqueous environment at 37°C over the course of a month was investigated. Here 10mg of either BIS-PAH or MCM-41 were immersed in 1.5ml of dH_2O and incubated at 37°C for 30 days. Molybdic acid colorimetric assay was employed to determine the concentration of silicic acid and therefore the amount of silica which had dissolved over the course of the experiment.

From this experiment, the dissolution of BIS-PAH and MCM-41 were found to be very similar (Figure 5.5). After 30 days the supernatant contained ~2.7 mM of silicic acid for both types of silica, with the majority of the silica samples remaining settled and not dissolving, this corresponds to ~6-10% silica dissolution over the course of 30 days. The solubility of amorphous silica ranges from 70-150 ppm (1.1-2.5mM) at 25°C [39]. This experiment was carried out at 37°C (core body temperature) and so there is a slight increase in the dissolution limit of the silica.

Another study investigated the dissolution of MSN in simulated body fluid (to emulate the *in vivo* environment more accurately) and found very similar results to those presented in Figure 5.5 (where water was used) [177]. MSN dissolution in SBF occurred in the first 2 hours and did not significantly increase over the course of the next 8 hours. The maximum dissolution was 2.2mM (~4% of the weight of the initial silica) and this level of dissolution did not change when MSN was immersed in 10 ml or 210 ml [177]. This suggests that silica would not fully dissolve within the

blood *in vivo* and while these static dissolution experiments do not fully reflect the situation found *in vivo*, it does show that silica cannot simply dissolve in the body and be easily excreted.

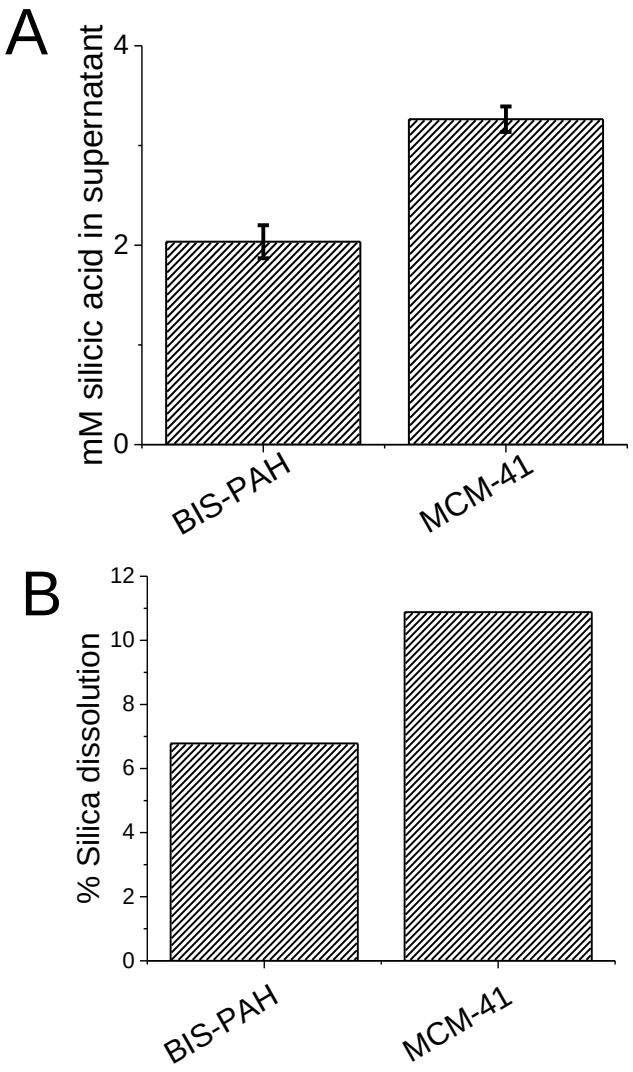

Figure 5-5 – Dissolution of silica (A) mM of silicic acid released from 10mg of BIS or MCM-41 when incubated for 30 days at 37ºC in 1.5ml of dH_2O, (B) % of silica dissolved under these conditions n=3, error bars represent one standard deviation.

Due to the low levels of silica dissolution, bioaccumulation may be an issue. To investigate the potential for silica bioaccumulation, Huang, *et al*. injected mice intravenously with 20mg/kg of 70 nm MSN [178]. They tracked the location of silica

over the course of 7 days and found that it mainly accumulated in the liver, lungs and spleen. After a week, they reported that all the silica had been effectively excreted in the faeces and urine and no blood or tissue toxicity was found. There may have been some effect on the glomerular filtration in the kidneys but the MSN were deemed to have very good biocompatibility. Another study injected 10mg/kg of two sizes of silica (20 nm and 80 nm) into mice and found accumulation in similar places (i.e. liver, lungs and spleen) [179]. The larger particles were less likely to accumulate and over the course of the 30 day experiment the amount of accumulated silica reduced; however a significant amount remained (especially the 20nm silica in the liver). This study reported that they did not observe any significant changes in the morphology of any of the organs but did see some inflammation in the liver. It is thought that the persistence of smaller silica nanoparticles in the liver is due to macrophages, which effectively take up the silica particles which are then difficult to degrade due to the inherent stability of silica. Along with the size of the particles, dosage can have a great effect on biocompatibility. Hudson, *et al*. injected rats with 30mg of MSN and found no major signs of toxicity; however, when this same dose was administered to mice, they all died. This is due to the large difference in dose/weight between rats (0.17g/kg) and mice (1.2g/kg) [70]. It is thought that the mice died due to a pulmonary embolism and/or thrombosis.

5.5. Conclusions

Silica has the potential to be an orally administered DDS due to its robust nature and also because it is "generally recognised as safe" by the FDA. However, dosage is important to remember. Higher dosages of MCM-41 can lead to cytotoxic effects in epithelial cells and so there is potential for gut wall damage. BIS-PAH was found

to be less cytotoxic. BIS-PAH is also able to pass through the gut wall (which is useful for targeted treatments, e.g. anti-cancer) and haemolytic activity was found to be minimal (significantly less than MCM-41). Once in the blood silica will not dissolve (which may be useful for prolonged release systems) and has been shown in the literature to be effectively cleared from rats with no adverse effects (as long as the dosage is low enough).

From these preliminary studies we have shown that the biocompatibility of BIS is greater than for MCM-41, giving BIS a key advantage for drug delivery applications. However, more studies are required, especially *in vivo* studies to fully elucidate the biocompatibility of BIS.

Chapter 6: Conclusions and Future Work

The development of drug delivery systems is essential to solve the many limitations of free drug molecules, including poor solubility, high toxicity and non-specificity [11]. Many materials have been investigated for use for drug delivery applications (Liposomal and PEGylated systems are most commonly on the market [12,15)], although none are perfect. Silica has received ever increasing attention in the drug delivery field due to its chemical and thermal stability, along with its versatility. This research aimed to investigate BIS which has several advantages of other types of silica including a one-step synthesis and drug loading method which occurs under benign conditions [75].

Firstly this project aimed to develop an *in situ* drug loading and release system using bio-inspired silica (BIS). Ibuprofen was first used as a model drug to aid in the understanding of the BIS system and how it can be controlled in order to develop favourable loading and release profiles for drug molecules. It was found that the choice of amine additive, pH of synthesis, kinetics of synthesis and pH of the release solution, all had dramatic impacts upon the loading and release of ibuprofen. From the results gathered using ibuprofen, it can be suggested that the ideal formulation for drug delivery applications would be BIS-PAH synthesised with reactant concentration of 2:2 (where the concentrations of sodium metasilicate and PAH are doubled but the concentration of drug remains at 1 mg ml^{-1}). Release could be controlled through synthesis pH where acidic conditions were found to be suitable for designing DDS for fast targeted release, while basic conditions were preferred for sustained release. The pH of the release solutions also impacted upon release, where high release was observed under highly acidic and neutral conditions but at low

acidity (pH 5) release was greatly impaired. This release profile could enhance the efficacy of loaded drug if administered orally.

While predictive rules based on synthesis chemistry to influence drug loading and release were found for ibuprofen, they could not be applied for use with hydrocortisone. Hydrocortisone is a drug in real need of an effective drug delivery system but its instability during BIS synthesis meant that doses could not be accurately measured and the released drug may have been non-functional. Due to this hydrocortisone had to be added once the BIS synthesis solution of neutral and silica particles had already formed. BIS-PAH was the only BIS tested that allowed for drug release (likely due to the larger pores when compared to BIS synthesised using other amines). Maturation time of the BIS-PAH did not greatly impact upon the loading efficiency of hydrocortisone but future work could increase the times tested and increase the concentration of hydrocortisone within the system to increase the diffusion pressure. Ultimately hydrocortisone loading onto BIS was greatly limited due to the inability to *in situ* load drug.

An essential criterion for any DSS is biocompatibility. Silica has the potential to be an orally administered DDS due to its robust nature and also because it is regarded as "generally recognised as safe" by the FDA. However, there is still a lot of contradictory literature on the biocompatibility of silica, which means that more biocompatibility studies of BIS are essential. MCM-41 was found to be toxic to epithelial cells in higher dosages which is concerning since this could cause serious damage to the gut wall [35]. BIS-PAH was found to be less toxic to this cell type which enhances the argument for the use of bio-inspired silica over MSN. BIS-PAH was observed to be able to pass through the gut wall which means it has the potential

to be useful as a more targeted drug delivery system (e.g. anti-cancer), where the aim is to get the drug delivery system to the exact site of action, thus avoiding systemic flow of the drug (i.e. avoid giving the drug free range throughout the entire body) and reducing side-effects. Once through the gut wall into the blood stream BIS-PAH has very little haemolytic activity, whereas MCM-41 induced a significant amount of haemolysis. Haemolytic activity is extremely undesirable in a drug delivery system, for obvious reasons. Finally, due to silica's chemical stability, minimal silica dissolution was observed over the course of a month. This may be useful for prolonged release systems; however there are also concerns over bioaccumulation of silica resulting in unknown negative effects. Although some studies have observed the effective clearance of silica from rats, a full *in vivo* study using BIS is essential for it to be developed for drug delivery applications.

The main limitation of the study using ibuprofen is the unrealistic release conditions.All release was carried out in a low volume (1.4ml of PBS) in a static environment, which does not emulate the passage through the digestive tract. This low volume will also impede the release of hydrophobic drugs since there is not a large enough diffusion pressure for the hydrophobic drug to be released into a hydrophilic environment. Future investigations could look into the effect of sink volume (i.e. the volume of liquid that a drug is able to diffuse into from the DDS), which may result in increased drug release because of the higher diffusion pressures in the system and will stop the sink volume becoming saturated with drug. The loading mechanism for BIS or MCM-41 is not optimal and should be improved in the future. Throughout this investigation the loading concentration was relatively low (1mg/ml), which resulted in a low loading efficiency. If a higher concentration

of drug or a super-saturated solution was used, then hydrophobic drugs would be more likely to bond with the silica surface. An increased concentration of drug may also increase the drug loading into BIS. Creating a more saturated solution of drug could be done simply by increasing the concentration of drug being dissolved and heating the solution to allow for more drug molecules to dissolve. However, the *in situ* drug loading method for BIS presented here may also result in a more saturated solution of drug. A study in 2005 used a similar "*in situ"* loading method for loading ibuprofen into their DDS (dextran). Here they used a solution of dextran and ibuprofen (to a final concentration of 1 mg/ml) in NaOH and slowly reduced the pH. As the pH is reduced the solubility of ibuprofen reduces (at pH12 solubility is 31.53 mg/ml, pH 7 solubility is 1.46 mg/ml and at pH 1 solubility is 0.02 mg/ml). This decrease in solubility creates a more saturated solution and inducing ibuprofen precipitation with dextran, resulting in increased loading [180]. The creation of a more saturated drug solution could result in the potential issue of drug crystallisation. This phase change could inhibit release of loaded drug [181]. Future work will require a more detailed investigation into this for the BIS system to discover is supersaturated solutions of drug increase loading and its effect on the drug release. In doing so, drug dosages being released from BIS could be increased more therapeutically relevant concentrations.

Other improvements on the release experiment could include increasing the time of the release experiment (to observe any prolonged drug release), observing the effect movement has upon release (shaking may increase drug release which could result in a decrease in drug efficacy since it is being released higher up the digestive tract), the effect of pH changes (this was briefly investigated but requires a more focused

study and with changes in the pH of the release solution over time, similar to how it would change within the human body), and the effect of the release solution itself (PBS does not fully replicate the environment within the digestive tract). Finally to improve drug loading and release, synthesis conditions in tandem should be investigated, for example, reactant concentration ratio of 2:2 and BIS-PAH synthesised at pH 5 both showed favourable loading and release conditions, would this improve further if both synthesis conditions were together? Other additives could also be studied in order to improve the physical characteristics of BIS. Larger surface areas and controllable pore sizes are important factors in the drug loading and release efficiencies of a DDS and changing the additive could vastly improve these characteristics of BIS, resulting in more pharmaceutically relevant amounts of drug being loaded and released. The BIS with the highest surface area in the present research was BIS-PAH, with a surface area of 129 $m^2 g^{-1}$. The use of alternative additives has been shown to produce silicas with surface areas of >500 $m^2 g^{-1}$ (with the use of amino acid derived surfactants to condense silica)[182] and even up to 1030 $m^2 g^{-1}$(with the use of polyethylene glycol) [183]. This high surface area rivals MCM-41 (983 $m^2 g^{-1}$) and could allow for much improved drug loading efficiencies.

The HPLC system and calibration curve for ibuprofen will also require improvement in future studies. The HPLC calibration curve for ibuprofen has an R^2 of 0.95, which ideally should have a better fit and have an R^2 of 0.99. The lowered R^2 value was deemed appropriate during this investigation but is not perfect. The R^2 could be improved by adding more data points to the graph (figure 2.1), especially between 0.2mg/ml and 1 mg/ml. The experiment could also benefit from the use of two calibration curves, one for the higher concentrations (mg/ml) (usually detected

when measuring drug loading) and one for the low concentrations (µg/ml) (usually when drug release is being detected). This would help resolve subtle differences in drug loading and release.

The sizing of particles was a major issue. As previously discussed dynamic light scattering, was deemed inappropriate for sizing the BIS particles due to their deposition out of solution. SEM was employed instead; however this may not have given an accurate representation of the silica particle sizes. When measuring the sizes of BIS particles, the primary particles were measured; however these particle aggregate into larger particles in solution and so this measurement may not be a true representation. When measuring MCM-41, the primary particles were not resolved and so large particles of varying sizes were measured. Future work should include a more accurate sizing experiment for these particles. TEM (transmission electron microscopy) was not employed to investigate the BIS and MCM-41 pore structure simply due to the lack of access to this equipment. TEM images of BIS have been previously observed and found that a similar aggregation of primary particles occurred and a slight increase in particle size was measured when using TEM rather than SEM [120].

The porosity of BIS was too small to compete with MSN using post-synthesis hydrocortisone loading and so future work should entail developing BIS with a larger pore size and volume, without the use of surfactants, which will facilitate increased post-synthesis loading (as discussed above). The synthesis protocol for BIS has the benefit of allowing *in situ* drug loading. However, because of the chemical instability of hydrocortisone during *in situ* loading, BIS was deemed inappropriate for use as a DDS for hydrocortisone. Future work would have to

involve a comprehensive screening of drug stability under the basic pH conditions encountered during BIS synthesis. This may significantly limit the number of drug molecules that a BIS DDS could be used for. Investigating potential degradation products is greatly important because, not only could the drug become non-functional, but it may degrade into a toxic product (for example, pralidoxin degrades to cyanide under basic conditions [184]). It is the C_{17}-dihydroxyacetone side chain of hydrocortisone which is susceptible to degradation under basic conditions [156], meaning that drugs with this side chain would also be inappropriate candidates for the BIS system. Degradation often occurs as a result of hydrolysis and so pH-rate profiles of drugs are important to investigate in order to determine the stability of a drug molecule under the conditions found during BIS synthesis [185]. Some drug molecules which are also unstable under basic pH include cefazolin and flomexef [186]. Even though BIS is an inappropriate drug delivery system for hydrocortisone there are other systems being developed such as Chronocort® (which is currently in phase 3 of clinical trials and aims to be on the market as soon as 2018) and Plenadren®, which has a slow release core surrounded by an outer shell which quickly releases hydrocortisone [150,151].

While there is evidence for good biocompatibility for BIS (especially when compared with MSN), this has all been investigated with *in vitro* work. This is the major limitation of the biocompatibility study in the present study. It has focused only on small parts of the journey of BIS through the digestive tract and into the blood stream, but studies looking at the system as a whole are required. To fully uncover the safety of BIS, *in vivo* biocompatibility studies are essential and would involve the use of a model animal (usually a rat) and administering a dose of BIS.

This is most commonly done via intravenous injection, but to fully investigate BIS for oral delivery, the model animals would have to eat the silica. The model animals would then be sacrificed and an autopsy would reveal bio-distribution, bio-degradation and bio-accumulation of the silica within a body, as well as the potential deleterious effects BIS could have upon vital organs. An example of this type of study was carried out by He, *et al*., who administered different sized MSN to rats [187].

Another issue to regarding the biocompatibility of BIS is the use of amine additives. It has been previously shown that free amines (specifically PEHA) were toxic to human monocytes, however when this amine was used to synthesise BIS (and so is likely to be entrapped in the silica particles, this toxicity was removed [35].

Due to the importance of amines in synthesising and functionalising the BIS system and the amines potential toxicity if released from BIS, it is important to measure the mass of amines in BIS and the location of these amines. The ability to do this is quite difficult. IR spectroscopy is not useful for detecting surface amines because the amine peaks will be too small to detect next to the very large silica peaks and are also obscured by peaks representing water, meaning that the use of IR is inappropriate for this issue. NMR is a possible solution, however ^{14}N goes not provide a signal and so amine additives would have to be synthesised with ^{15}N to be detected using this technique. This is expensive and labour intensive but some work had been carried out previously [77].

What is also currently unknown is whether amine molecules are released from the silica, which could have great implications upon cytotoxicity. Future work

should be carried out exposing BIS to various conditions found within the body and measuring whether amine is released (likely through use of HPLC).

Also impacting on biocompatibility is surface charge. The zeta potential (i.e. the surface charge) was not measured during this investigation, due to issues with the silica particles remaining in suspension (see sizing issues above). However the surface charge of a particle can have drastic impacts upon its biocompatibility and should be measured in future work. The surface charge of the nanoparticle is greatly important with positively charged particles being internalised into cells at a greater rate than negatively charged particles [167]. The cytotoxicity of charged silica does not appear to be concise in the literature, with one paper reporting with an increased negative charge being more cytotoxic [164] and another stating that amine modified (and therefore cationic) MSNs were less cytotoxic that their bare counterparts (with anionic charges) [168]. This is another reason that measuring biocompatibility of all new DDS is essential.

If BIS was found to be safe, clinical trials on humans would be approved, which occur in four phases, with increasing numbers of test subjects [188]. If BIS passes these four phases a licence will be granted by the Medicines and Healthcare Regulatory Agency (MHRA); the government body in charge of regulating medicines and medical devices in the UK. Once a licence is granted, BIS would finally be allowed to be sold and used for treating humans [189]. All drugs or medical devices will have some side-effects and so can never be regarded as 100% safe, but if the advantages outweigh the disadvantages, then a new drug delivery system, like BIS, could have a huge potential.

This thesis has shown promising results for BIS as a drug delivery system and has argued its benefits over other DDS and other types of silica, and so there is potentially a great future ahead for this technology. Developing drug delivery systems is also financially logical since the development of new DDS cost approximately $20-50 million and take around 3-4 years to develop, whereas developing new drug molecules can cost around $500 million and take 10-12 years [13]. The drug delivery technology market is predicted to be worth 1.5 trillion US by 2020 [14], meaning that development of BIS for drug delivery applications has the potential for huge financial returns.

Along with the controllability provided through synthesis conditions, the additions of "smart"/"stimuli-responsive materials to BIS could bring more control over drug release (either at specific times or locations). For example coating the surface of drug loaded BIS with poly(acrylic acid) (PAA), allows for pH dependent drug release [73]. PAA remains attached to the BIS under acidic conditions (thus holding in the drug), but under neutral conditions, it will detach from the silica and allow for drug release. This will protect drug molecules from the low pH found in the stomach and release it in the small intestine where highest absorption occurs.

This would avoid the problem of burst release profiles and allow for the use of BIS for prolonged release treatments. Prolonged and sustained released systems are very useful for treating a while range of conditions, since they reduce the amount of doses a patient is taking. Some examples of these include anti-cancer treatments, anti-depressants, Hormone replacement therapy, Ritalin for treatment of attention deficit disorder, or any other treatment that requires the patient to take a drug for prolonged periods of their lives). Due to the ease of control of BIS properties and

the ease of synthesis, there is a real potential in the future for BIS to be used in personalised medicines. This could greatly improve the efficacy of drugs (since doses are specific to each patient), as well as improve the lives of patients with long-term conditions, since they could take fewer doses of medicine and potentially synthesise their treatments at home. This idea is still many years of research and development away, but the advantages of BIS (such as one-step formulation, simple controllability, lack of hazardous chemicals and superior biocompatibility) and the fact that BIS has similar or improved drug loading and release profiles to MCM-41 when using ibuprofen, means that, with further drug and biocompatibility research, BIS as real potential as a viable DDS.

References

1 Davidson, S., Lamprou, D. A., Urquhart, A. J., Grant, M. H. & Patwardhan, S. V. Bioinspired Silica Offers a Novel, Green, and Biocompatible Alternative to Traditional Drug Delivery Systems. *ACS Biomaterials Science & Engineering* **2**, 1493-1503 (2016).

2 Chan, C. P., HL ; Liu, G ; McIlwrath, K ; Zhang, XF ; Huggins, RA ; Cui, Y. High-performance lithium battery anodes using silicon nanowires. *Nat. Nanotechnol* **3**, 31-35 (2008).

3 Horie, M., Kato, H., Fujita, K., Endoh, S. & Iwahashi, H. In vitro evaluation of cellular response induced by manufactured nanoparticles. *Chemical research in toxicology* **25**, 605-619 (2012).

4 Birrenbach, G. S., P P. Polymerized Micelles and Their Use as Adjuvants in Immunology. *J. Pharm. Sci.* **65**, 1763-1766 (1976).

5 Etheridge, M. C., SA ; Erdman, AG ; Haynes, CL ; Wolf, SM ; McCullough, J. The big picture on nanomedicine: the state of investigational and approved nanomedicine products. *Nanomed. Nanotech. Biol. Med.* **9**, 1-14 (2013).

6 Ventola, C. L. The nanomedicine revolution: Part 2: Current and future clinical applications. *P and T* **37**, 582-591 (2012).

7 Chou, L. Y. T. M., Kevin ; Chan, Warren C W. Strategies for the intracellular delivery of nanoparticles. *Chem. Soc. Rev* **40**, 233-245 (2011).

8 Clift, M. J. D. R.-R., B. ; Brown, D.M. ; Duffin, R. ; Donaldson, K. ; Proudfoot, L. ; Guy, K. ; Stone, V. The impact of different nanoparticle surface chemistry and size on uptake and toxicity in a murine macrophage cell line. *Toxicol. Appl. Pharmacol.* **232**, 418-427 (2008).

9 Litzinger, D. C. B., A M ; Van Rooijen, N ; Huang, L. Effect of liposome size on the circulation time and intraorgan distribution of amphipathic poly(ethylene glycol)-containing liposomes. *Biochimica et biophysica acta* **1190**, 99-107 (1994).

10 O'Neal, D. P. H., L.R. ; Halas, N.J. ; Payne, J.D. ; West, J.L. Photo-thermal tumor ablation in mice using near infrared-absorbing nanoparticles. *Cancer Lett.* **209**, 171-176 (2004).

11 Parveen, S. M., R. ; Sahoo, S.K. Nanoparticles: A boon to drug delivery, therapeutics, diagnostics and imaging. *Nanomed. Nanotech. Biol. Med.* **8**, 147-166 (2012).

12 Zhang, Y. C., H. F. ; Leong, K. W. Advanced materials and processing for drug delivery: the past and the future. *Adv. Drug Deliv. Rev.* **65**, 104-120 (2013).

13 Verma, R. K. a. G., S. Current Status of Drug Delivery Technologies and Future Directions. *Pharm. Technol* **25**, 1-14 (2001).

14 marketsandmarkets.com. *Drug Delivery Technology Market worth 1,504.7 Billion USD by 2020*, <http://www.marketsandmarkets.com/PressReleases/drug-delivery-technologies.asp> (2015).

15 Allen, T. M. & Cullis, P. R. Drug delivery systems: entering the mainstream. *Science* **303**, 1818-1822 (2004).

16 Northfelt, D. W. *et al.* Doxorubicin encapsulated in liposomes containing surface-bound polyethylene glycol: pharmacokinetics, tumor localization, and safety in patients with AIDS-related Kaposi's sarcoma *J. Clin. Pharmacol.* **36**, 55-63 (1996).

17 Glue, P. *et al.* A dose-ranging study of pegylated interferon alfa-2b and ribavirin in chronic hepatitis C. *Hepatology* **32**, 647-653 (2000).

18 Kwon, S. *et al.* Silica-based mesoporous nanoparticles for controlled drug delivery. *J. Tissue Eng* **4** (2013).

19 Chonn, A. & Cullis, P. R. Recent advances in liposomal drug-delivery systems. *Curr. Opin. Biotech* **6**, 698-708 (1995).

20 Goyal, P. G., K; Kumar, S. G. V.; Sing, A.; Katare, O. P.; Mishra, D. N. Liposomal drug delivery systems - Clinical applications. *Acta pharmaceutica* **55** (2005).
21 Gabizon A., P. D. Liposome formulations with prolonged circulation time in blood and enhanced uptake by tumors. *Proceedings of the National Academy of Sciences of the United States of America* **85** (1988).
22 Tiwari, G. *et al.* Drug delivery systems: An updated review. *International journal of pharmaceutical investigation* **2**, 2 (2012).
23 Matthews, O. A., Shipway, A. N. & Stoddart, J. F. Dendrimers—Branching out from curiosities into new technologies. *Prog. Polym. Sci* **23**, 1-56 (1998).
24 McNerny, D. Q., Leroueil, P. R. & Baker, J. R. Understanding specific and nonspecific toxicities: a requirement for the development of dendrimer-based pharmaceuticals. *WIREs Nanomed. Nanobiotechno.* **2**, 249-259 (2010).
25 Soliman, G. M., Sharma, A., Maysinger, D. & Kakkar, A. Dendrimers and miktoarm polymers based multivalent nanocarriers for efficient and targeted drug delivery. *J. Chem. Soc., Chem. Commun.* **47**, 9572-9587 (2011).
26 Bianco, A., Kostarelos, K. & Prato, M. Applications of carbon nanotubes in drug delivery. *Curr. Opin. Chem. Biol.* **9**, 674-679 (2005).
27 Yamashita, T. *et al.* Carbon Nanomaterials: Efficacy and Safety for Nanomedicine. *Materials* **5**, 350 (2012).
28 Chen, Y.-C. *et al.* Non-metallic nanomaterials in cancer theranostics: a review of silica-and carbon-based drug delivery systems. *Science and Technology of Advanced Materials* (2016).
29 Xavier Le, G., Nicole, D. & Marc, S. Synthesis and characterization of human transferrin-stabilized gold nanoclusters. *Nanotech.* **22**, 275103 (2011).
30 Liu, Y., Zhang, B. & Yan, B. Enabling Anticancer Therapeutics by Nanoparticle Carriers: The Delivery of Paclitaxel. *Int. J. Mol. Sci.* **12**, 4395 (2011).
31 Forsyth, C. & Patwardhan, S. V. Controlling performance of lipase immobilised on bioinspired silica. *J. Mater. Chem. Chemistry* **1**, 1164-1174 (2013).
32 Idris, S., Robertson, C., Morris, M. & Gibson, L. A comparative study of selected sorbents for sampling of aromatic VOCs from indoor air. *Analytical Methods* **2**, 1803-1809 (2010).
33 Hoffmann, F., Cornelius, M., Morell, J. & Fröba, M. Silica-based mesoporous organic–inorganic hybrid materials. *Angew. Chem. Int.* **45**, 3216-3251 (2006).
34 Huang, Y., Trewyn, B. G., Chen, H.-T. & Lin, V. S. Y. One-pot reaction cascades catalyzed by base- and acid-functionalized mesoporous silica nanoparticles. *New J. Chem* **32**, 1311 (2008).
35 Steven, C. R. B., G. A. ; Mather, C. ; Tariq, B. ; Briuglia, M. L. ; Lamprou, D. A. ; Urquhart, A. J. ; Grant, M. H. ; Patwardhan, S. V. Bioinspired silica as drug delivery systems and their biocompatibility. *J. Mater. Chem. B* **2**, 5028-5042 (2014).
36 Tang, F., Li, L. & Chen, D. Mesoporous silica nanoparticles: synthesis, biocompatibility and drug delivery. *Adv. Mater.* **24**, 1504-1534 (2012).
37 Tan, W. *et al.* Bionanotechnology based on silica nanoparticles. *Med. Res. Rev.* **24**, 621-638 (2004).
38 Duncan, R. & Gaspar, R. nanomedicine(s) under the microscope. *Mol. Pharm.* **8**, 2101-2141 (2011).
39 Iler, R. K. *The chemistry of silica. Solubility, polymerisation, colloid and surface properties, and biochemistry*. 3, 15-22 (John Wiley & Sons, 1979).
40 Iler, R. K. *The chemistry of silica.*, 462-463 (John Wiley & Sons, 1979).

41 Plumeré, N., Ruff, A., Speiser, B., Feldmann, V. & Mayer, H. A. Stöber silica particles as basis for redox modifications: Particle shape, size, polydispersity, and porosity. *J. Colloid Interface Sci.* **368**, 208-219 (2012).
42 Green, D., Jayasundara, S., Lam, Y.-F. & Harris, M. Chemical reaction kinetics leading to the first Stober silica nanoparticles–NMR and SAXS investigation. *J. Non-Cryst. Solids* **315**, 166-179 (2003).
43 Stöber, W., Fink, A. & Bohn, E. Controlled growth of monodisperse silica spheres in the micron size range. *J. Colloid Interface Sci.* **26**, 62-69 (1968).
44 Ahola, M. S. *et al.* In vitro release of heparin from silica xerogels. *Biomat.* **22**, 2163-2170 (2001).
45 Albarran, L., López, T., Quintana, P. & Chagoya, V. Controlled release of IFC-305 encapsulated in silica nanoparticles for liver cancer synthesized by sol–gel. *Colloids Surf., A* **384**, 131-136 (2011).
46 Iler, R. K. *The Chemistry of silica*. 94-99 (John Wiley & sons, 1979).
47 Coradin, T. & Lopez, P. J. Biogenic Silica Patterning: Simple Chemistry or Subtle Biology? *Chembiochem : a European journal of chemical biology* **4**, 251-259 (2003).
48 Beck, J. S. *et al.* A new family of mesoporous molecular sieves prepared with liquid crystal templates. *J. Am. Chem. Soc.* **114**, 10834-10843 (1992).
49 Kim, T.-W., Chung, P.-W. & Lin, V. S. Y. Facile Synthesis of Monodisperse Spherical MCM-48 Mesoporous Silica Nanoparticles with Controlled Particle Size. *Chem. Mat.* **22**, 5093-5104 (2010).
50 Hiyoshi, N., Yogo, K. & Yashima, T. Adsorption characteristics of carbon dioxide on organically functionalized SBA-15. *Micropor. Mesopor. Mat.* **84**, 357-365 (2005).
51 Selvam, P., Bhatia, S. K. & Sonwane, C. G. Recent advances in processing and characterization of periodic mesoporous MCM-41 silicate molecular sieves. *Ind. Eng. Chem. Res.* **40**, 3237-3261 (2001).
52 Wang, S. Ordered mesoporous materials for drug delivery. *Micropor. Mesopor. Mat.* **117**, 1-9 (2009).
53 Schumacher, K., Grün, M. & Unger, K. Novel synthesis of spherical MCM-48. *Micropor. Mesopor. Mat.* **27**, 201-206 (1999).
54 Zhao, D. *et al.* Triblock copolymer syntheses of mesoporous silica with periodic 50 to 300 angstrom pores. *Science* **279**, 548-552 (1998).
55 Beck, J. S. *et al.* A New Family of Mesoporous Molecular-Sieves Prepared with Liquid-Crystal Templates. *J Am Chem Soc* **114**, 10834-10843, doi:Doi 10.1021/Ja00053a020 (1992).
56 Kresge, C. T., Leonowicz, M. E., Roth, W. J., Vartuli, J. C. & Beck, J. S. Ordered Mesoporous Molecular-Sieves Synthesized by a Liquid-Crystal Template Mechanism. *Nature* **359**, 710-712, doi:Doi 10.1038/359710a0 (1992).
57 Idris, S. A., Robertson, C., Morris, M. A. & Gibson, L. T. A comparative study of selected sorbents for sampling of aromatic VOCs from indoor air. *Anal. Methods* **2**, 1803 (2010).
58 Moller, K., Kobler, J. & Bein, T. Colloidal suspensions of nanometer-sized mesoporous silica. *Advanced Functional Materials* **17**, 605-612, doi:10.1002/adfm.200600578 (2007).
59 Couvreur, P. Nanoparticles in drug delivery: past, present and future. *Advanced drug delivery reviews* **65**, 21-23 (2013).
60 Vallet-Regi, M., Rámila, A., del Real, R. P. & Pérez-Pariente, J. A New Property of MCM-41: Drug Delivery System. *Chem. Mat.* **13**, 308-311 (2001).
61 Giraldo, L. *et al.* in *Macromol. Symp.* 129-141 (Wiley Online Library).

62 Uhrich, K. E., Cannizzaro, S. M., Langer, R. S. & Shakesheff, K. M. Polymeric systems for controlled drug release. *Chem. Rev.* **99**, 3181-3198 (1999).
63 Horcajada, P., Rámila, A., Pérez-Pariente, J. & Vallet-Regí, M. Influence of pore size of MCM-41 matrices on drug delivery rate. *Micropor. Mesopor. Mat.* **68**, 105-109 (2004).
64 Izquierdo-Barba, I., Martinez, A., Doadrio, A. L., Perez-Pariente, J. & Vallet-Regi, M. Release evaluation of drugs from ordered three-dimensional silica structures. *Eur. J. Pharm. Sci.* **26**, 365-373 (2005).
65 Qu, F. *et al.* A controlled release of ibuprofen by systematically tailoring the morphology of mesoporous silica materials. *J. Solid State Chem.* **179**, 2027-2035 (2006).
66 Wang, S. Ordered mesoporous materials for drug delivery. *Micropor. Mesopor. Mat.* **117**, 1-9 (2009).
67 Muñoz, B., Rámila, A., Pérez-Pariente, J., Díaz, I. & Vallet-Regí, M. MCM-41 Organic Modification as Drug Delivery Rate Regulator. *Chem. Mat.* **15**, 500-503 (2003).
68 Balas, F., Manzano, M., Colilla, M. & Vallet-Regi, M. L-Trp adsorption into silica mesoporous materials to promote bone formation. *Acta. Biomater.* **4**, 514-522 (2008).
69 Vallet-Regí, M. Ordered mesoporous materials in the context of drug delivery systems and bone tissue engineering. *Chemistry–A European Journal* **12**, 5934-5943 (2006).
70 Hudson, S. P., Padera, R. F., Langer, R. & Kohane, D. S. The Biocompatibility of Mesoporous Silicates. *Biomat.* **29**, 4045-4055 (2008).
71 Zhou, Z., Zhu, S. & Zhang, D. Grafting of thermo-responsive polymer inside mesoporous silica with large pore size using ATRP and investigation of its use in drug release. *J. Mater. Chem.* **17**, 2428-2433 (2007).
72 Wang, Y. *et al.* Mesoporous silica nanoparticles in drug delivery and biomedical applications. *Nanomed. Nanotech. Biol. Med.* **11**, 313-327 (2015).
73 Song, S. W., Hidajat, K. & Kawi, S. pH-Controllable drug release using hydrogel encapsulated mesoporous silica. *Chem. Commun.*, 4396-4398 (2007).
74 Yang, Q. *et al.* pH-responsive carrier system based on carboxylic acid modified mesoporous silica and polyelectrolyte for drug delivery. *Chem. Mater.* **17**, 5999-6003 (2005).
75 Sano, K., Minamisawa, T. & Shiba, K. Autonomous silica encapsulation and sustained release of anticancer protein. *Langmuir* **26**, 2231-2234 (2010).
76 Wan, M. M. *et al.* In Situ Loading of Drugs into Mesoporous Silica SBA-15. *Chem. Eur. J.* **22**, 6294-6301 (2016).
77 Belton, D. J. P., S. V. ; Perry, C. C. Spermine, spermidine and their analogues generate tailored silicas. *J. Mater. Chem.* **15**, 4629-4638 (2005).
78 Nelson, D. M., Tréguer, P., Brzezinski, M. A., Leynaert, A. & Quéguiner, B. Production and dissolution of biogenic silica in the ocean: revised global estimates, comparison with regional data and relationship to biogenic sedimentation. *Global Biogeochem. Cycles* **9**, 359-372 (1995).
79 Sumper, M. & Brunner, E. Silica biomineralisation in diatoms: the model organism Thalassiosira pseudonana. *ChemBioChem* **9**, 1187-1194 (2008).
80 Hildebrand, M. Diatoms, Biomineralization processes and Genomics. *Chem. Rev.* **108**, 4855–4874 (2008).
81 Sumper, M. & Kroger, N. Silica formation in diatoms: the function of long-chain polyamines and silaffins. *J. Mater. Chem* **14**, 2059-2065 (2004).

82 Kroger, N., Deutzmann, R., Bergsdorf, C. & Sumper, M. Species-specific polyamines from diatoms control silica morphology. *Proceedings of the National Academy of Sciences of the United States of America* **97**, 14133-14138 (2000).
83 Shimizu, K., Cha, J., Stucky, G. & Morse, D. Silicatein alpha: Cathepsin L-like protein in sponge biosilica. *Proceedings of the National Academy of Sciences of the United States of America* **95**, 6234-6238 (1998).
84 Kröger, N., Deutzmann, R. & Sumper, M. Polycationic peptides from diatom biosilica that direct silica nanosphere formation. *Science* **286**, 1129-1132 (1999).
85 Patwardhan, S. V. Biomimetic and bioinspired silica: recent developments and applications. *Chem. Commun. (Camb)* **47**, 7567-7582 (2011).
86 Fowler, C. E., Khushalani, D. & Mann, S. Facile synthesis of hollow silica microspheres. *J. Mater. Chem.* **11**, 1968-1971 (2001).
87 Belton, D. J., Patwardhan, S. V., Annenkov, V. V., Danilovtseva, E. N. & Perry, C. C. From biosilicification to tailored materials: optimizing hydrophobic domains and resistance to protonation of polyamines. *Proceedings of the National Academy of Sciences of the United States of America* **105** (2008).
88 Forsyth, C. & Patwardhan, S. V. Controlling performance of lipase immobilised on bioinspired silica. *J. Mater. Chem. B* **1**, 1164-1174 (2013).
89 Forsyth, C., Yip, T. W. & Patwardhan, S. V. CO 2 sequestration by enzyme immobilized onto bioinspired silica. *Chem. Commun.* **49**, 3191-3193 (2013).
90 Drummond, C., McCann, R. & Patwardhan, S. V. A feasibility study of the biologically inspired green manufacturing of precipitated silica. *Chem. Eng. J.* **244**, 483-492 (2014).
91 Begum, G., Laxmi, M. & Rana, R. Entrapped polyamines in biomimetically synthesized nanostructured silica spheres as pH-responsive gates for controlled drug release. *J. Mater. Chem.* **22**, 22174-22180 (2012).
92 Vallet-regí, M., F., B. & Arcos, D. Mesoporous materials for drug delivery. *Angewandte Chemie (International ed. in English)* **46**, 7548-7558 (2007).
93 Lechner, C. C. & Becker, C. F. Modified silaffin R5 peptides enable encapsulation and release of cargo molecules from biomimetic silica particles. *Bioorganic & medicinal chemistry* **21**, 3533-3541 (2013).
94 Huang, Y., Trewyn, B. G., Chen, H.-T. & Lin, V. S.-Y. One-pot reaction cascades catalyzed by base-and acid-functionalized mesoporous silica nanoparticles. *New J. Chem* **32**, 1311-1313 (2008).
95 Agilent Technologies, I. *HPLC basics - Findamentals of Liquid Chromatography (HPLC)*, <http://polymer.ustc.edu.cn/xwxx_20/xw/201109/P020110906263097048536.pdf > (unknown).
96 El-Kattan, A. F. A., Charles S ; Michniak, Bozena B. The effect of terpene enhancer lipophilicity on the percutaneous permeation of hydrocortisone formulated in HPMC gel systems. *Int. J. Pharm* **198**, 179-189 (2000).
97 Sing, K. S. Reporting physisorption data for gas/solid systems with special reference to the determination of surface area and porosity (Recommendations 1984). *Pure Appl. Chem* **57**, 603-619 (1985).
98 Brunauer, S., Emmett, P. H. & Teller, E. Adsorption of Gases in Multimolecular Layers. *J. Am. Chem. Soc* **60**, 309-319 (1938).
99 Barrett, E. P., Joyner, L. G. & Halenda, P. P. The Determination of Pore Volume and Area Distributions in Porous Substances. I. Computations from Nitrogen Isotherms. *J. Am. Chem. Soc* **73**, 373-380, doi:10.1021/ja01145a126 (1951).
100 Simon, E. Mechanisms of dinitrophenol toxicity. *Biol. Rev.* **28**, 453-478 (1953).

101 Rognstad, R. & Katz, J. The effect of 2, 4-dinitrophenol on adipose-tissue metabolism. *Biochem. J.* **111**, 431-444 (1969).
102 Issekutz Jr, B. Effect of propranolol in dinitrophenol poisoning. *Arch. Int. Pharmacodyn. Ther.* **272**, 310-319 (1984).
103 Yu, T., Malugin, A. & Ghandehari, H. Impact of silica nanoparticle design on cellular toxicity and hemolytic activity. *ACS nano* **5**, 5717-5728 (2011).
104 Dunlap, M. A., J. E. *Introduction to the Scanning Electron Microscope*, <https://imf.ucmerced.edu/downloads/semmanual.pdf> (1997).
105 Lang, Y., Finn, D. P., Pandit, A. & Walsh, P. J. Pharmacological activity of ibuprofen released from mesoporous silica. *J. Mater. Sci. Mater. Med.* **23**, 73-80 (2012).
106 Dong, Y. *et al.* Fabrication and characterization of silk fibroin-coated liposomes for ocular drug delivery. *Eur. J. Pharm. Biopharm.* **91**, 82-90 (2015).
107 Mohammed, A., Weston, N., Coombes, A., Fitzgerald, M. & Perrie, Y. Liposome formulation of poorly water soluble drugs: optimisation of drug loading and ESEM analysis of stability. *Int. J. Pharm.* **285**, 23-34 (2004).
108 Okamoto, Y., Kishi, Y., Ishigami, T., Suga, K. & Umakoshi, H. Chiral Selective Adsorption of Ibuprofen on a Liposome Membrane. *J. Phys. Chem. B* **120**, 2790-2795 (2016).
109 Milhem, O., Myles, C., McKeown, N., Attwood, D. & D'Emanuele, A. Polyamidoamine Starburst® dendrimers as solubility enhancers. *Int. J. Pharm.* **197**, 239-241 (2000).
110 Kolhe, P., Misra, E., Kannan, R. M., Kannan, S. & Lieh-Lai, M. Drug complexation, in vitro release and cellular entry of dendrimers and hyperbranched polymers. *Int. J. Pharm.* **259**, 143-160 (2003).
111 Khaliliazar, S., Akbari, S. & Kish, M. Modification of poly (l-lactic acid) electrospun fibers and films with poly (propylene imine) dendrimer. *Appl. Surf. Sci.* **363**, 593-603 (2016).
112 Oh, W.-K., Yoon, H. & Jang, J. Size control of magnetic carbon nanoparticles for drug delivery. *Biomat.* **31**, 1342-1348 (2010).
113 Rehman, F., Rahim, A., Airoldi, C. & Volpe, P. L. Preparation and characterization of glycidyl methacrylate organo bridges grafted mesoporous silica SBA-15 as ibuprofen and mesalamine carrier for controlled release. *Mter. Sci. Eng. C* **59**, 970-979 (2016).
114 Mortazavi, Y. & Ghoreishi, S. Synthesis of Mesoporous Silica and Modified as a Drug Delivery System of Ibuprofen. *J. Nanostruct.* **6**, 83-86 (2016).
115 Charnay, C. *et al.* Inclusion of ibuprofen in mesoporous templated silica: drug loading and release property. *Eur. J. Pharm. Biopharm.* **57**, 533-540 (2004).
116 PerrigoPharmaceuticalsCompany. *Ibuprofen 800mg*, <http://www.drugs.com/pro/ibuprofen-800mg.html> (2005).
117 Lee, J. H. & Yeo, Y. Controlled drug release from pharmaceutical nanocarriers. *Chem. Eng. Sci.* **125**, 75-84 (2015).
118 Li, Z.-Z., Wen, L.-X., Shao, L. & Chen, J.-F. Fabrication of porous hollow silica nanoparticles and their applications in drug release control. *J. Controlled Release* **98**, 245-254 (2004).
119 Kamarudin, N. H. N. *et al.* Role of 3-aminopropyltriethoxysilane in the preparation of mesoporous silica nanoparticles for ibuprofen delivery: Effect on physicochemical properties. *Micropor. Mesopor. Mat.* **180**, 235-241 (2013).
120 Belton, D., Patwardhan, S. V. & Perry, C. C. Putrescine homologues control silica morphogenesis by electrostatic interactions and the hydrophobic effect. *Chemical communications*, 3475-3477 (2005).

121 Manzano, M. *et al.* Studies on MCM-41 mesoporous silica for drug delivery: effect of particle morphology and amine functionalization. *Chemical Engineering Journal* **137**, 30-37 (2008).
122 Slowing, I. I., Trewyn, B. G., Giri, S. & Lin, V. Y. Mesoporous silica nanoparticles for drug delivery and biosensing applications. *Advanced Functional Materials* **17**, 1225-1236 (2007).
123 Hwang, D. *et al.* Surface functionalization of SBA-15 particles for ibuprofen delivery. *Korean J. Chem. Eng* **27**, 1087-1092 (2010).
124 Lee, K. *et al.* Comparison of amine-functionalized mesoporous silica particles for ibuprofen delivery. *Korean J. Chem. Eng.* **27**, 1333-1337 (2010).
125 Munoz, B., Ramila, A., Perez-Pariente, J., Diaz, I. & Vallet-Regi, M. MCM-41 organic modification as drug delivery rate regulator. *Chem. Mater.* **15**, 500-503 (2003).
126 Bowen, R. *Gastrointestinal Transit: How Long Does It Take?*

, <http://arbl.cvmbs.colostate.edu/hbooks/pathphys/digestion/basics/transit.html> (2006).
127 TheScottHamiltonCaresInitiative. *Hydrocortisone*, < http://chemocare.com/chemotherapy/drug-info/hydrocortisone.aspx#.UjrOGj-JrTq> (2015).
128 Goodwin, J. S. A., D. ; Sierakowski, S. ; Lianos, E. A. Mechanism of action of glucocorticosteroids. Inhibition of T cell proliferation and interleukin 2 production by hydrocortisone is reversed by leukotriene B4. *J. Clin. Invest.* **77**, 1244-1250 (1986).
129 Martini, F., Nath, J. . *Fundamentals of anatomy and physiology*. 8th edn, 619, 629 (San Francisco: Pearsons Education, Inc., (2009)).
130 Surgeons, A. A. o. N. *The Pituitary Gland and Pituitary Tumors*, <http://www.aans.org/Patient%20Information/Conditions%20and%20Treatments/The%20Pituitary%20Gland%20and%20Pituitary%20Tumors.aspx> (
131 *Adrenal gland*, <https://en.wikipedia.org/wiki/Adrenal_gland> (
132 Debono, M. *et al.* Modified-release hydrocortisone to provide circadian cortisol profiles. *J. Clin. Endocrinol. Metab.* **94**, 1548-1554 (2009).
133 Chung, S., Son, G. H. & Kim, K. Circadian rhythm of adrenal glucocorticoid: its regulation and clinical implications. *Biochim. Biophys. ACTA - Mol. Basis Dis.* **1812**, 581-591 (2011).
134 Arlt, W. & Allolio, B. Adrenal insufficiency. *The Lancet* **361**, 1881-1893 (2003).
135 Bornstein, S. R. Predisposing factors for adrenal insufficiency. *N. Engl. J. Med.* **360**, 2328-2339 (2009).
136 NHS.uk. *Addison's disease*, <http://www.nhs.uk/conditions/addisons-disease/Pages/Introduction.aspx> (2015).
137 GOSH, N.-. *Cortisol deficiency information*, <http://www.gosh.nhs.uk/medical-information-0/search-medical-conditions/cortisol-deficiency> (2009).
138 Anglin, R. E., Rosebush, P. I. & Mazurek, M. F. The neuropsychiatric profile of Addison's disease: revisiting a forgotten phenomenon. *J. Neuropsychiatry Clin. Neurosci.* (2006).
139 Løvås, K. & Husebye, E. S. Replacement therapy for Addison's disease: recent developments. *Expert Opin. Investig. Drugs* **17**, 497-509 (2008).
140 Chan, S. & Debono, M. Review: Replication of cortisol circadian rhythm: new advances in hydrocortisone replacement therapy. *Ther. Adv. Endocrinol. Metab.* **1**, 129-138 (2010).
141 Ten, S. M. N., M.; Maclaren, N. Addison's Disease 2001. *J. Clin. Endocrinol. Metab.* **86**, 2909-2922 (2001).

142 Quinkler, M. & Hahner, S. What is the best long-term management strategy for patients with primary adrenal insufficiency? *Clin. Endocrinol.* **76**, 21-25 (2012).
143 Witchel, S. F. & Azziz, R. Congenital adrenal hyperplasia. *J. Pediatr. Adolesc. Gynecol.* **24**, 116-126 (2011).
144 Merke, D. P. & Bornstein, S. R. Congenital adrenal hyperplasia. *The Lancet* **365**, 2125-2136 (2005).
145 Merke, D. & Kabbani, M. Congenital adrenal hyperplasia. *Paediatric drugs* **3**, 599-611 (2001).
146 Speiser, P. W. & White, P. C. Congenital adrenal hyperplasia. *N. Engl. J. Med.* **349**, 776-788 (2003).
147 Mah, P. M. *et al.* Weight-related dosing, timing and monitoring hydrocortisone replacement therapy in patients with adrenal insufficiency. *Clin. Endocrinol.* **61**, 367-375 (2004).
148 Tache, Y. Cyclic vomiting syndrome: the corticotropin-releasing-factor hypothesis. *Digest. Dis. Sci.* **44**, 79S-86S (1999).
149 Diurnal, L. Treatment of Adrenal Insifficiency. (2010).
150 Information), U. U. M. *Hydrocortisone modified-release*, <http://www.medicinesresources.nhs.uk/upload/documents/Evidence/Drug%20Specific%20Reviews/NMP%20Hydrocortisone%20MR.1.pdf> (2012).
151 Agency, E. M. *Plenadren*, <http://www.ema.europa.eu/ema/index.jsp?curl=pages/medicines/human/medicines/002185/human_med_001495.jsp&mid=WC0b01ac058001d124> (
152 Unipharma. *Plenadren approved for treatment of Adrenal Insufficiency (AI)*, <http://www.unipharma.ch/134/plenadren-approved-treatment-adrenal-insufficiency-ai> (2012).
153 PituitaryFoundation. <http://www.pituitary.org.uk/information/treating-a-pituitary-condition/hydrocortisone/> (
154 Lopez, T. O., E ; Alexander-Katz, R ; Basaldella, E ; Bokhimi, X . . Cortisol controlled release by mesoporous silica. *Nanomed. Nanotech. Biol. Med.* **5**, 170-177 (2009).
155 Andrade, A. L. S., D. M. ; Vasconcellos, W. A. ; Ferreira, R. V. ; Domingues, R. Z. Tetracycline and/or hydrocortisone incorporation and release by bioactive glasses compounds. *J. Non-Cryst. Solids* **355**, 811-816 (2009).
156 Hansen, J. B., H. Studies on the stability of corticosteroids V. The degradation pattern of hydrocortisone in aqueous solution. *Int. J. Pharm.* **6**, 307-319 (1980).
157 Gupta, V. D. Effect of vehicles and other active ingredients on stability of hydrocortisone. *J. Pharm. Sci.* **67**, 299-302 (1978).
158 Li, M., Chen, B., Monteiro, S. & Rustum, A. M. Mechanism of base-catalyzed autooxidation of corticosteroids containing 20-keto-21-hydroxyl side chain. *Tetrahedron Letters* **50**, 4575-4581 (2009).
159 Allen, A. E. D. G., V. Stability of hydrocortisone in polyethylene glycol ointment base. *J. Pharm. Sci.* **63**, 107-109 (1974).
160 PubChem. *Compound Summary for CID 5754*, <https://pubchem.ncbi.nlm.nih.gov/compound/hydrocortisone#section=Solubility> (2016).
161 DrugBank. *Hydrocortisone*, <http://www.drugbank.ca/drugs/DB00741> (2016).
162 Williams, D. F. On the mechanisms of biocompatibility. *Biomaterials* **29**, 2941-2953 (2008).
163 Lewis & Harrison, L. *Silicon Dioxide GRAS Notification*, <http://www.fda.gov/ucm/groups/fdagov-public/@fdagov-foods-gen/documents/document/ucm269494.pdf> (2010).

164 He, Q., Zhang, Z., Gao, Y., Shi, J. & Li, Y. Intracellular localization and cytotoxicity of spherical mesoporous silica nano- and microparticles. *Small* **5**, 2722-2729, doi:10.1002/smll.200900923 (2009).
165 Nel, A., Xia, T., Madler, L. & Li, N. Toxic potential of materials at the nanolevel. *Science* **311**, 622-627, doi:10.1126/science.1114397 (2006).
166 Lee, S., Yun, H. S. & Kim, S. H. The comparative effects of mesoporous silica nanoparticles and colloidal silica on inflammation and apoptosis. *Biomaterials* **32**, 9434-9443, doi:10.1016/j.biomaterials.2011.08.042 (2011).
167 Chung, T. H. *et al.* The effect of surface charge on the uptake and biological function of mesoporous silica nanoparticles in 3T3-L1 cells and human mesenchymal stem cells. *Biomaterials* **28**, 2959-2966, doi:10.1016/j.biomaterials.2007.03.006 (2007).
168 Yu, T., Malugin, A. & Ghandehari, H. Impact of Silica Nanoparticle Design on Cellular Toxicity and Hemolytic Activity *Acs Nano* **5**, 5717-5728 (2011).
169 Vasconcelos, T., Sarmento, B. & Costa, P. Solid dispersions as strategy to improve oral bioavailability of poor water soluble drugs. *Drug Discov. Today* **12**, 1068-1075 (2007).
170 Evans, D. F., Pye, G., Brambley, R., Clark, A. G., Dyson, T. J., Hardcaslte, J. D. Measurement of gastrointestinal pH profiles in normal ambulant human subjects. *Gut* **29**, 1035-1041 (1988).
171 Jaganathan, H. & Godin, B. Biocompatibility assessment of Si-based nano- and micro-particles. *Adv. Drug Deliv. Rev* **64**, 1800-1819 (2012).
172 Chu, Z., Huang, Y., Tao, Q. & Li, Q. Cellular uptake, evolution, and excretion of silica nanoparticles in human cells. *Nanoscale* **3**, 3291-3299 (2011).
173 Yuan, H. *et al.* Study on controllable preparation of silica nanoparticles with multi-sizes and their size-dependent cytotoxicity in pheochromocytoma cells and human embryonic kidney cells. *J. Health Sci.* **56**, 632-640 (2010).
174 Lin, Y. H., C. L. . Impacts of Mesoporous Silica Nanoparticle Size, Pore Ordering, and Pore Integrity on Hemolytic Activity. *J. Am. Chem. Soc* **132**, 4834-4842 (2010).
175 Lin, Y. S. & Haynes, C. L. Impacts of Mesoporous Silica Nanoparticle Size, Pore Ordering, and Pore Integrity on Hemolytic Activity. *Journal Of The American Chemical Society* **132**, 4834-4842 (2010).
176 Maurer-Jones, M. A., Lin, Y.-S. & Haynes, C. L. Functional assessment of metal oxide nanoparticle toxicity in immune cells. *ACS nano* **4**, 3363-3373 (2010).
177 Mortera, R., Fiorilli, S., Garrone, E., Verné, E. & Onida, B. Pores occlusion in MCM-41 spheres immersed in SBF and the effect on ibuprofen delivery kinetics: A quantitative model. *Chem. Eng. J.* **156**, 184-192 (2010).
178 Huang, X. *et al.* The shape effect of mesoporous silica nanoparticles on biodistribution, clearance, and biocompatibility in vivo. *ACS nano* **5**, 5390-5399 (2011).
179 Xie, G., Sun, J., Zhong, G., Shi, L. & Zhang, D. Biodistribution and toxicity of intravenously administered silica nanoparticles in mice. *Arch. Toxicol.* **84**, 183-190 (2010).
180 Jiang, B., Hu, L., Gao, C. & Shen, J. Ibuprofen-loaded nanoparticles prepared by a co-precipitation method and their release properties. *International journal of pharmaceutics* **304**, 220-230 (2005).
181 Iervolino, M., Cappello, B., Raghavan, S. & Hadgraft, J. Penetration enhancement of ibuprofen from supersaturated solutions through human skin. *International journal of pharmaceutics* **212**, 131-141 (2001).

182 Coradin, T., Roux, C. & Livage, J. Biomimetic self-activated formation of multi-scale porous silica in the presence of arginine-based surfactants. *J. Mater. Chem.* **12**, 1242-1244 (2002).
183 Sun, Q. *et al.* PEG-mediated silica pore formation monitored in situ by USAXS and SAXS: systems with properties resembling diatomaceous silica. *J. Phys. Chem. B* **106**, 11539-11548 (2002).
184 Ellin, R. I. & Wills, J. H. Oximes antagonistic to inhibitors of cholinesterase part I. *J. Pharm. Sci.* **53**, 995-1007 (1964).
185 Allen Jr, L. V. *pH and Solubility, Stability, and Absorption, Part II*, <https://compoundingtoday.com/Newsletter/Science_and_Tech_1112.cfm> (2011).
186 Yamana, T. & Tsuji, A. Comparative stability of cephalosporins in aqueous solution: kinetics and mechanisms of degradation. *J. Pharm. Sci.* **65**, 1563-1574 (1976).
187 He, Q., Zhang, Z., Gao, F., Li, Y. & Shi, J. In vivo biodistribution and urinary excretion of mesoporous silica nanoparticles: effects of particle size and PEGylation. *small* **7**, 271-280 (2011).
188 NHS. *Clinical trials and medical research - Phases of trials* <http://www.nhs.uk/Conditions/clinical-trials/Pages/phasesoftrials.aspx> (2015).
189 Agency, T. M. a. H. p. R. *Medicines & Medical Devices Regulation: What you need to know*, <http://www.mhra.gov.uk/home/groups/comms-ic/documents/websiteresources/con2031677.pdf> (2008).

Appendix

Appendix 1 – Nitrogen adsoption theory

Adsorption Isotherms

Both the BET and BJH methods rely on data from adsorption isotherms. This is the relationship between the amount of adsorbate gas (in this case nitrogen) adsorbed on the surface of a sample (in this case silica) and the pressure of the system [98]. Adsorption isotherms rely on Le-Chatelier's principle of equilibrium. So, in the case of gas adsorption, when pressure is increased in the system the equilibrium, adsorbate + adsorbent ⇌ adsorption, will shift to release stress in the system (i.e. decrease the number of molecules in the system) and so the forward direction is favoured and gas molecules adsorb to the surface of a material. By observing the shape of the adsorption isotherms curves one can deduce some information about the samples surface characteristics [97]. The majority of these isotherms can be grouped into 6 types (as shown in Figure A1.1). Table A1.1 gives a brief description of what each type of adsorption isotherms suggests about the samples surface characteristics.

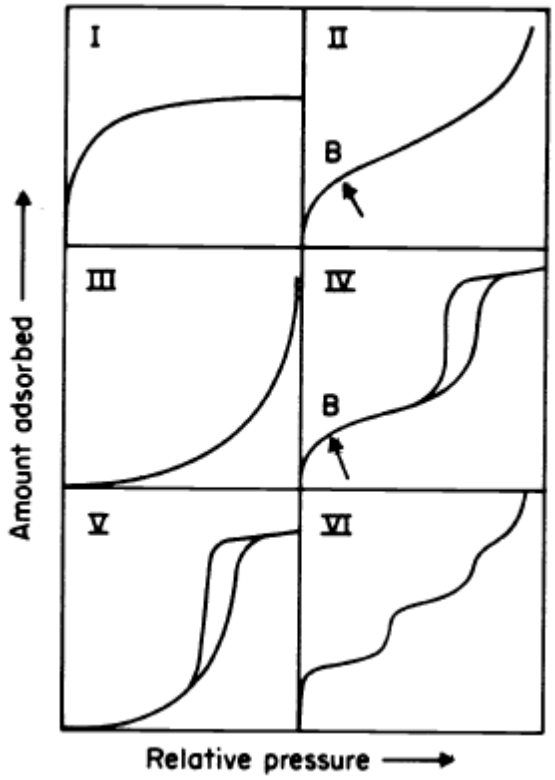

Figure A1.1 - 6 main types of adsorption isotherms, Figure reproduced from ref [97]

Table A1-1 - Description of adsorption isotherms (Figure 2.3) [97]

Isotherm Type	Description
Type I	Suggests a microporous solid with a relatively small external surface. Adsorption is controlled by the micropore volume rather than internal surface area.
Type II	Normal isotherm for non-porous or macroporous materials. Here there is unrestricted monolayer to multilayer adsorption.
Type III	Uncommon isotherm. Suggests a role of adsorbate-adsorbate interactions
Type IV	This isotherm has a characteristic hysteresis loop. This occurs when adsorption occurs in mesopores first and limits the uptake at higher pressures. This type of isotherm is characteristic of mesoporous materials.
Type V	Another uncommon isotherm. The adsorbent-adsorbate interaction is weak when this type of isotherm is observed.
Type VI	This isotherm shows a stepwise multilayer adsorption on a uniform non-porous surface.

BET theory

The BET method, originally proposed by Brunauer, Emmett and Teller in 1938 [98], is a model used to describe the specific surface area of porous materials [97].

There are two main equations used to plot a BET isotherm; one for the low pressure section and one for the high pressure section.

The low pressure section of the isotherm is calculated first, as some units calculated in this equation are used in plotting the high pressure isotherm. The equation for the low pressure section is shown and described in equation A1.1.

$$\frac{p}{v(p_0 - p)} = \frac{c - 1}{v_m c}\left(\frac{p}{p_0}\right) + \frac{1}{v_m c}$$

Equation A1.1 - BET equation to fit the low pressure section of the isotherm. Where p is the partial pressure, v is the total volume of the gas, P_0 is the reference pressure, V_m is the volume of gas required to from a complete uni-molecular adsorbed layer and c is a constant which is roughly equal to $e^{[(E1-EL)/RT)}$ (where E_1 is the heat of monolayer adsorption, E_L is the heat of liquefaction of adsorbate) [98].

This equation is ultimately the equation of a straight line and the linear graph produced suggests the formation of a monolayer. Values V_m and c (used for calculating the higher pressure isotherm) are calculated here; the gradient is $\frac{c-1}{v_m c}$and the y intercept is $\frac{1}{v_m c}$. It was found that when pressures rose above 0.35 , then equation 1 no longer accurately fits the experimental data [98]. As such a second equation was developed to plot the high pressure section of the BET isotherm (equation A1.2).

$$v = \frac{v_m c x}{1 - x}\left(\frac{1 - (n+1)x^n + nx^{n+1}}{1 + (c-1)x - cx^{n+1}}\right)$$

Equation A1.2 - BET equation to fit the high pressure section of the isotherm. Where V_m and c have the same meaning as in equation 2.2 and n is the number of layers adsorbed [98].

Knowing the volume of the monolayer (V_m) the surface area of a sample can be determined. This is achieved by first determining the number of adsorbate

molecules on the surface (equation A1.3), and secondly calculating the surface area by using equation A1.4.

$$\frac{\text{volume of the monolayer}}{\text{volume of one molecule of adsorbate}} = \text{number of adsorbate molecules}$$

Equation A1.3 - Equation to calculate the number of adsorbed molecules using the BET method

$$(\text{average area of one molec.}) \text{x} (\text{number of adsorbate molecules}) = \text{absolute adsorbent surface area}$$

Equation A1.4- Equation to calculate the specific area of a sample using the BET method

BJH theory

Based on a 1951 paper by Barrett, Joymer and Halenda, the BJH method is utilised to calculate the pore size, volume and pore size distribution using the desorption curve (calculated as described above [99]. By applying a vacuum to the system, the partial pressure of the adsorbate gas (in this case nitrogen) is reduced and so small volumes of the adsorbate can be removed from the surface of the adsorbent in a controlled and sequential manner. The largest pores empty first and so it can be said that the n^{th} desorption corresponds with the emptying of the n^{th} largest pore and a thinning of the remaining adsorbate layer within the n-1 largest pore.

As each layer of the adsorbate (N_2) evaporates as the partial pressure decreases, the volume of gas removed is plotted and can be related to pore size. This is then used to create a plot of the pore size distribution. The volumes of the pores are also calculated in the BJH method using equation A1.5.

$$V_{pn} = \left(\frac{r_{pn}}{r_{kn} + \left\{ \frac{\Delta t_n}{2} \right\}} \right)^2 \left(\Delta V_n - \Delta t_n \sum_{j=1}^{n-1} C_j A_{pj} \right)$$

Equation A1.5 - Equation used in the BJH method to calculate the pore volume distributions with respect to the pore width. Where V_{pn} is the pore volume of the n^{th} desorption, Δt_n is the change in thickness of the adsorbed layer, r_{pn} is the pore radius, r_{kn} is the Kelvin capillary radius, A_c is the average area from which the adsorbed gas is evaporated, and A_p is the area of pores which is a constant equalling $\frac{2V_p}{r_p}$ [99].

This equation makes two fundamental assumptions. Firstly, it assumes that all the pores have a cylindrical shape and, secondly, it assumes that the gas is retained in/on the adsorbent via physical adsorption on the pore walls and no chemical bonding occurs [99].

Using the Bet and BJH theory information regarding a material's surface area, porosity and pore size distribution can be determined, making it a useful tool for surface characterisation.

Appendix 2 – Example adsorption isotherms

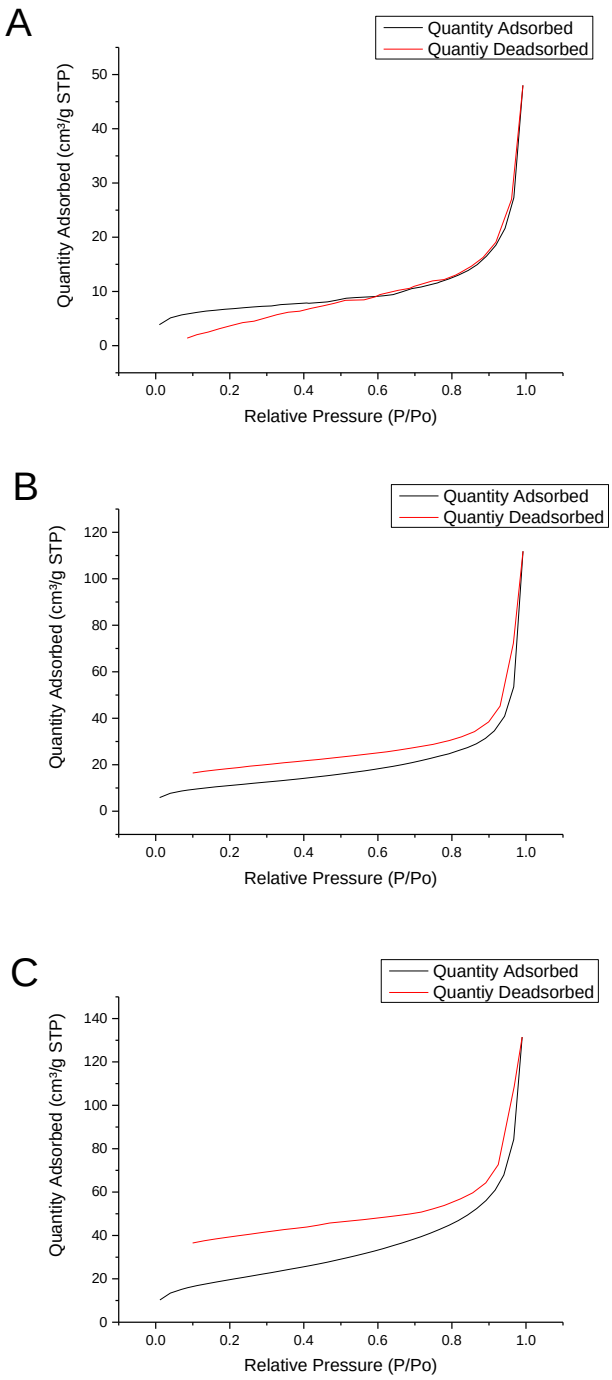

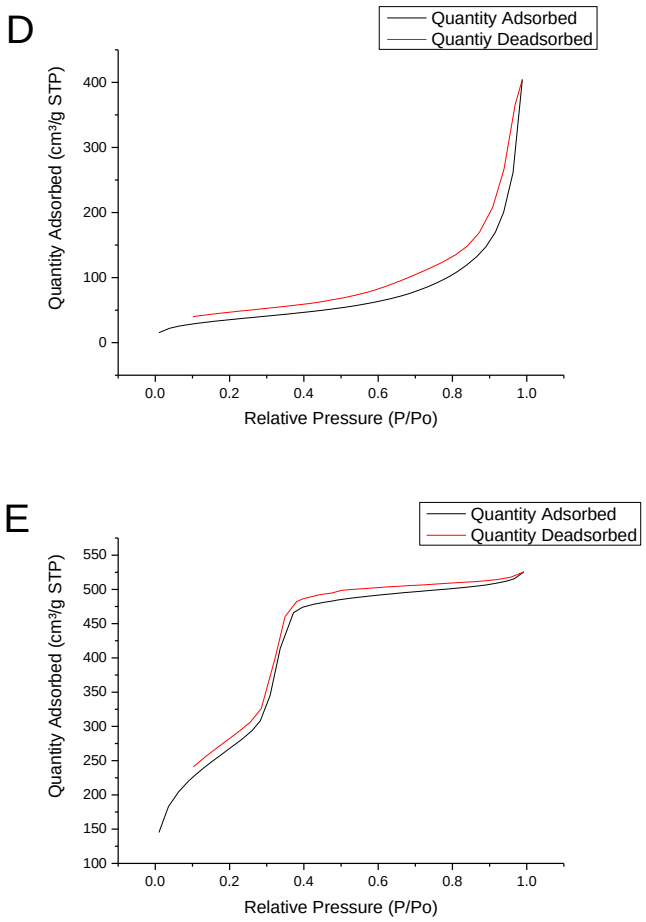

Figure A2.1 :- Adsprotion isotherms for (A) BIS-DETA, (B) BIS-TEPA, (C) BIS-PEHA, (D) BIS-PAH and (E) MCM-41

Appendix 3 - HPLC traces of hydrocortisone

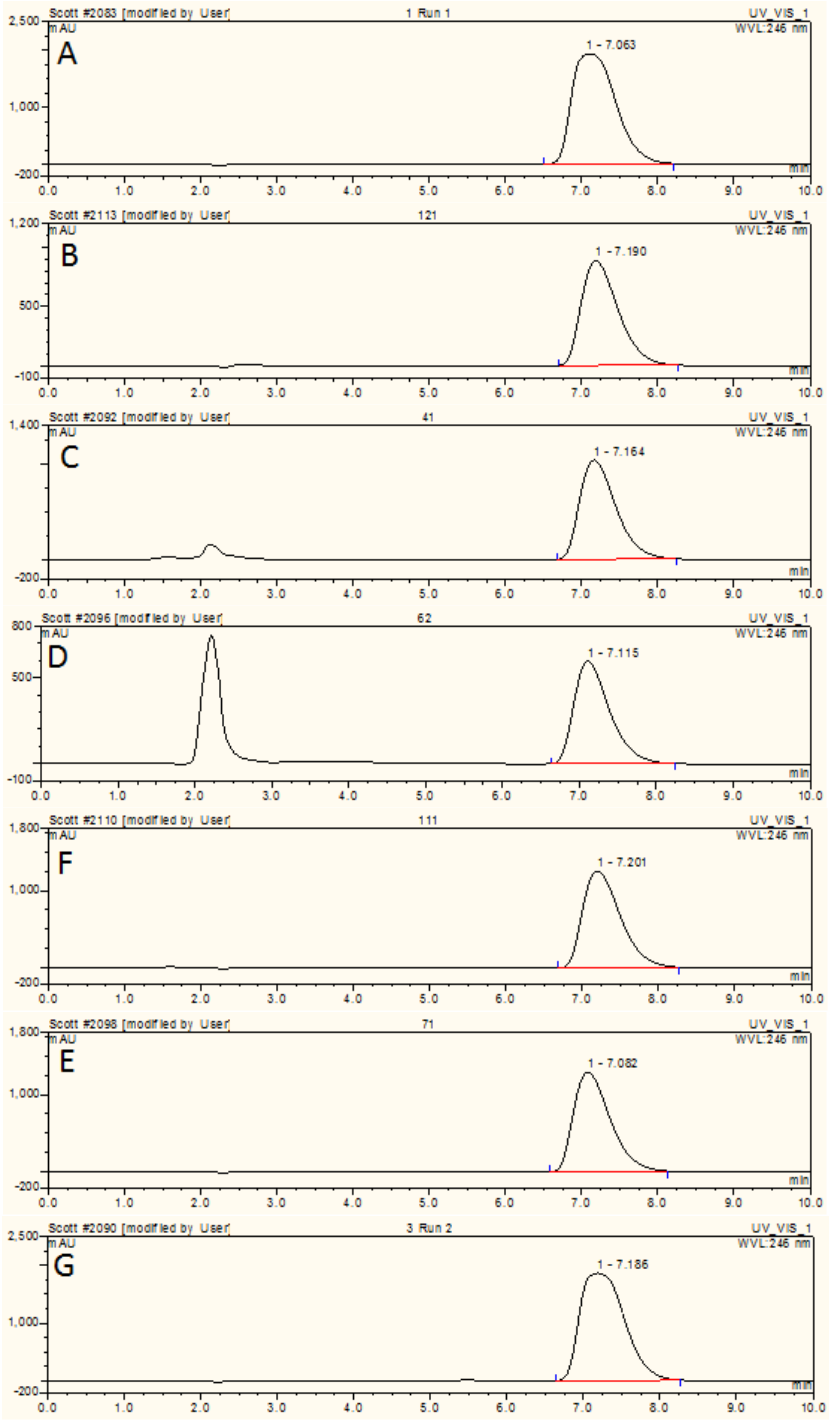

Figure A3.1 :- –. HPLC traces of hydrocortisone when exposed to various conditions (A) 70:30 - EtOH:H2O (pH 7.4), (B) 70:30 - EtOH:PBS (pH 7.2), (C) 1M HCl (pH1) (D) 30mM Sodium metasilicate (pH 12), (E) 30mM Sodium metasilicate (pH 7), (F) 1mg/ml PAH (pH5), (G) 1M NaOH (pH 17), (H) Heated at 85oC for 1 hour. Hydrocortisone detected using an isocratic reverse phase HPLC method, with 40 µl injection volume , mobile phase of acetonitrile: water (7:3), flow rate of 1ml min^{-1}, ACE 5 C-18 column (150X4.6 nm with 5 µm particle size).

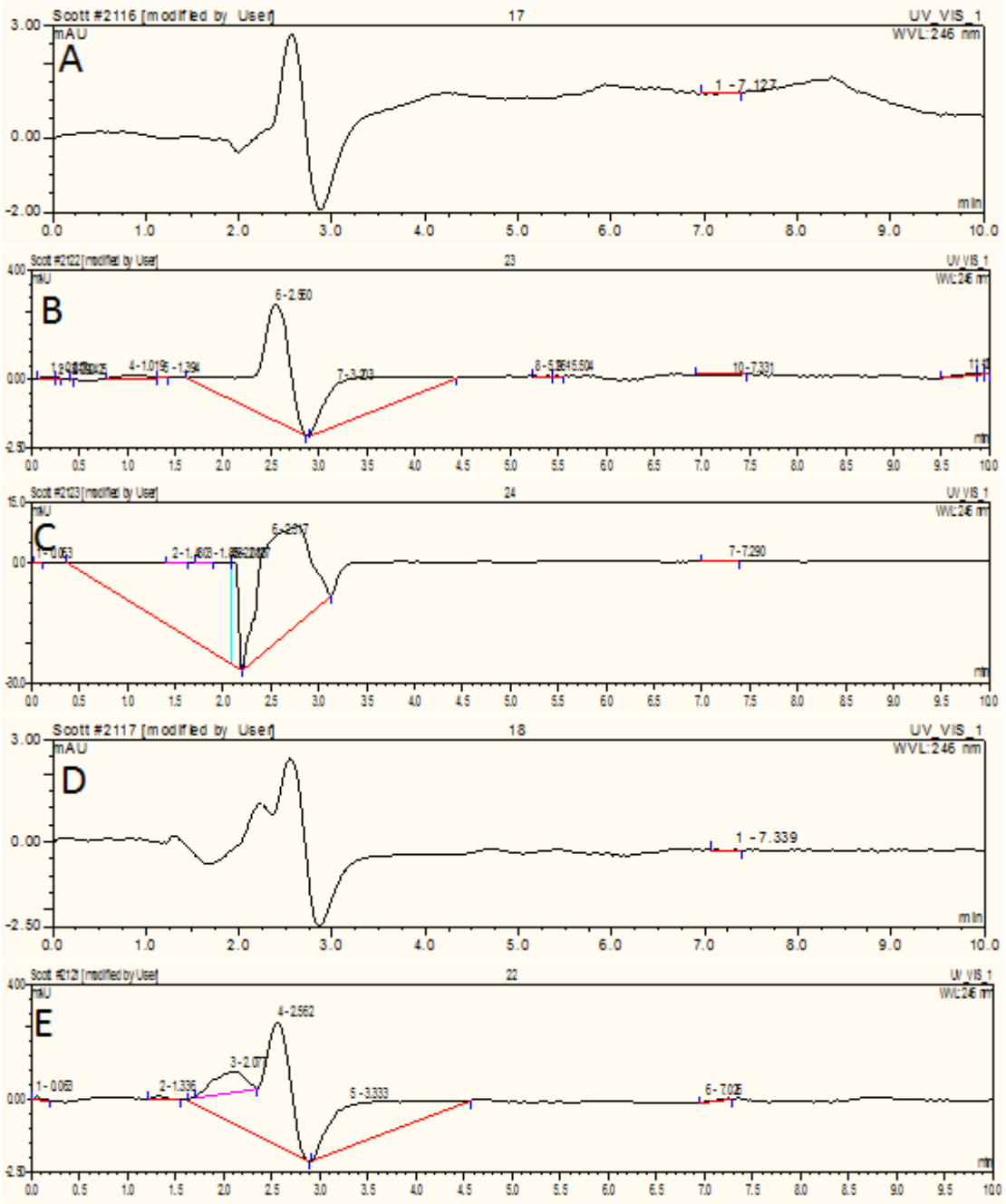

Figure A3.2 :- HPLC traces negative controls (A) 70:30 - EtOH:H2O (pH 7.4), (B) 70:30 - EtOH:PBS (pH 7.2), (C) 30mM Sodium metasilicate (pH 12), (D) 30mM Sodium metasilicate (pH 7), (E) 1mg/ml PAH (pH5). Hydrocortisone detected using an isocratic reverse phase HPLC method, with 40 µl injection volume , mobile phase of acetonitrile: water (7:3), flow rate of 1ml min^{-1}, ACE 5 C-18 column (150X4.6 nm with 5 µm particle size).